

Design of Fuel Flow Controller for Efficient and Stable Solid Ducted Ramjet Propulsion System for Air-to-Air Missile Applications

Thesis

Submitted in partial fulfilment of the requirements
for the award of the degree of

Doctor of Philosophy
in
Electrical Engineering

by

Srikant Srivastava
(Roll No. : 716120)

Under the supervision of

Dr. D.M. Vinod Kumar
Professor (HAG), N.I.T. Warangal
and
Dr. Prasiddha Nath Dwivedi
Sc'F', RCI, DRDO, Hyderabad



Department of Electrical Engineering
National Institute of Technology Warangal
(An Institute of National Importance)
Warangal – 506 004, Telangana State, India

June-2022

Approval Sheet

This Thesis entitled "**Design of Fuel Flow Controller for Efficient and Stable Solid Ducted Ramjet Propulsion System for Air-to-Air Missile Applications**" by **Srikant Srivastava, Roll No. 716120** is approved for the degree of Doctor Philosophy in Electrical Engineering.

Examiners

Supervisor(s)


Dr. P. N. Dwivedi
Scientist-F
RCI (DRDO), Hyderabad

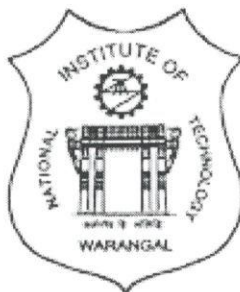
Dr. D.M. Vinod Kumar
Professor (HAG), EED
NIT Warangal

Chairman

Dr. Sailaja Kumari M.
Professor & Head
EED, NIT Warangal
Date: _____

Department of Electrical Engineering
National Institute of Technology Warangal
Warangal – 506 004, Telangana State, India

DEPARTMENT OF ELECTRICAL ENGINEERING
NATIONAL INSTITUTE OF TECHNOLOGY WARANGAL
WARANGAL - 506004, INDIA



CERTIFICATE

This is to certify that the thesis entitled "**Design of Fuel Flow Controller for Efficient and Stable Solid Ducted Ramjet Propulsion System for Air-to-Air Missile Applications**" which is being submitted by **Mr. Srikant Srivastava (Roll No. 716120)**, is a bonafide work submitted to National Institute of Technology Warangal in partial fulfilment of the requirements for the award of the degree of **Doctor of Philosophy** in Electrical Engineering. To the best of our knowledge, the work incorporated in this thesis has not been submitted elsewhere for the award of any degree.


Dr. P. N. Dwivedi
(Co-Supervisor)
Scientist-F & Project Director
Research Centre Imarat
Hyderabad - 500005, India

Dr. D.M. Vinod Kumar
(Supervisor)
Professor (HAG), EED
NIT Warangal
Warangal - 506004, India

DECLARATION

This is to certify that the work presented in the thesis entitled "**Design of Fuel Flow Controller for Efficient and Stable Solid Ducted Ramjet Propulsion System for Air-to-Air Missile Applications**" is a bonafide work done by me under the supervision of **Dr. D. M. Vinod Kumar, Professor (HAG)**, Department of Electrical Engineering, National Institute of Technology Warangal and **Dr. P. N. Dwivedi, Scientist-F**, Research Centre Imarat (RCI), DRDO, Hyderabad and was not submitted elsewhere for the award of any degree.

I declare that this written submission represents my ideas in my own words and where others ideas or words have been included; I have adequately cited and referenced the original sources. I also declare that I have adhered to all principles of academic honesty and integrity and have not misrepresented or fabricated or falsified any idea / data / fact / source in my submission. I understand that any violation of the above will be cause for disciplinary action by the Institute and can also evoke penal action from the sources which have thus not been properly cited or from whom proper permission has not been taken when needed.



(Srikant Srivastava)

(Roll No. 716120)

Date: 10-08-2022

Place: Warangal

*I would like to dedicate the thesis to my Mother Late **Smt. Devanti Devi**.*

ACKNOWLEDGEMENTS

It gives me immense pleasure to convey my deep sense of gratitude and sincere thanks to my supervisors **Dr. D.M. Vinod Kumar**, Professor (HAG), Department of Electrical Engineering, NIT Warangal, and **Dr. P.N. Dwivedi, Scientist-F & Project Director**, RCI-DRDO, Hyderabad, for their perpetual encouragement, guidance, and supervision. Their steady influence throughout my Ph.D. career has oriented me in a proper direction and supported me. They not only gave me the required knowledge to pursue my research work, but also the required moral support during hard times. I truly appreciate their logical and thought provoking advice both technically and morally which I will follow for the rest of my life.

Also, I take this privilege to thank all my Doctoral Scrutiny Committee members, **Dr. T. Kishore Kumar**, Professor, Department of ECE, **Dr. Ch. Venkaiah**, Associate Professor, Department of Electrical Engineering and **Dr. B.L. Narasimharaju**, Associate Professor, Department of Electrical Engineering for their detailed review, constructive suggestions, and excellent advice during the progress of this research work.

I express my heartfelt gratitude to **Dr. M. Sailaja Kumari**, Professor & Head, Department of Electrical Engineering, for her valuable suggestions, cooperation, help, and moral support towards the completion of the research work. Also, I extend my thanks to senior Professors of EED for their continuous support and motivation. I thank all the **faculty and non-teaching staff of EED at NIT Warangal** who helped me during the tenure of my research work.

I am grateful to **Director, DRDL, Sri Ankathi Raju, Outstanding Scientist & Sc-H, Project Director** and **Head HRD & Members of the HRD** for granting me permission for the research work while working at DRDL.

I am also grateful to all my colleagues, scholars, friends, and well-wishers who helped me to write my thesis with their support. Also, especially I would like to thank **Dr. Subhas Chandran, Distinguish Scientist (Retd.), DRDL, Mr. Abhishek Richharia, Scientist & Head, DRDL, Mr. R. Vivek, Scientist, DRDL** for their help and support during my Ph.D. I also

acknowledge my gratitude to **Mr. G. Shivanand, Scientist, DRDL, and Mr. Shambhav Kumar Jain, Scientist & PD, DRDL** for their support during my research work.

Finally, I am very grateful to my father Mr. **Y. N. Srivastava**, my wife Ms. **Shivangni Srivastava**, my son **Yayin Srivastava**, and my daughter **Yashavani Srivastava** for their sincere prayers, blessing, constant encouragement, moral support, understanding and sacrifice during my research work. Last but not the least, I wish to express my sincere thanks to all those who helped me directly or indirectly at various stage of my work.

Above all, I express my deepest regards and gratitude to 'ALMIGHTY' whose divine light and warmth showered upon me the perseverance, inspiration, faith and enough strength to keep the momentum of work high at trying moments of research work.

Srikant Srivastava

ABSTRACT

The ramjet engine is a supersonic air-breathing engine, which has no moving parts. The ramjet engine carries only fuel, where the required oxygen can be obtained from atmosphere while it is flying. In the ramjet engine, air entering into the intake gets compressed due to the formation of terminal shock waves called ‘ram effect’. The compressed air mixes with fuel in combustion chamber, fuel burns and hot gases are generated which exit through convergent divergent nozzle, resulting in forward thrust to accelerate the missile. However the ramjet engine is not effective at lower speeds (less than Mach number 2) due to the fact that at low speed, terminal shock waves are not formed in the intake and hence air does not get compressed. The fuel will not burn at lower temperature and pressurised air and hence the required thrust will not be generated. An additional booster is required to accelerate the vehicle to a certain high Mach number which guarantees the required speed (more than Mach number 2) for stable operation of ramjet based propulsion systems.

The applications of ramjet engines are increasing day by day especially in various missile applications because of the engine’s ability to generate thrust with high specific impulse (more than 1000 sec). Ramjet engines deliver more thrust with relatively lesser weight in comparison with rocket engines. Since rocket engines carry both fuel and oxidizer, they are relatively heavier than ramjet engines but less sensitive to flight conditions. Variable thrust during the operation of a rocket provides tremendous advantages during snap up/snap down scenario or when chasing down a target.

According to the type of fuel used, ramjet engines are classified in two types: 1) Liquid fuel ramjet engine and 2) Solid fuel ramjet engine. In this work, the solid fuel based ducted ramjet engine has been considered for air-to-air missile application. It is more compatible for design for high manoeuvre tactical missile.

To fly the missile at a desired Mach number, the engine has to produce adequate thrust which can generate the desired thrust to ensure the desired Mach number. The thrust generated by the engine, is controlled by varying the mass flow rate of fuel rich gas which is released into the combustion chamber. Since the fuel mass flow rate cannot be measured in flight directly, hence it cannot be controlled. However the gas generator pressure that directly affects the fuel mass flow rate can be controlled by varying the throttle valve area of gas generator. The gas generator pressure decides the fuel mass flow rate and corresponding thrust delivered by the engine.

In this thesis, two types of design problems of solid fuel ramjet based propulsion system have been worked out for efficient operation of an air-to-air tactical missile. First, Design objectives of fuel flow controller have been brought out from Proportional Navigation (PN) based guidance loop for air-to-air target engagement. Two loop non-linear dynamic inversion (NDI) based controller design have been proposed to track the commanded thrust and to meet the time constant requirement as a function of altitude, Mach number and angle of attack. The outer thrust loop is meant to control the required thrust and to generate demand for gas generator pressure loop. The inner pressure loop is meant to meet outer loop demand by controlling throttle valve area. The solid propellant based ramjet engine mathematical model has been carried out keeping in mind angle of attack. Throttle valve actuator specification requirements were also brought out to meet the operational fuel rate requirement at different altitudes and Mach number. Second, various factors such as combustion-intake interaction, atmospheric disturbance and other flight conditions have a significant impact on air intake operation to compress atmospheric air, which can impact engine performance. Due to the above phenomena, intake un-start and buzzing phenomena can occur due to back pressure fluctuation and it adversely affects intake air mass flow rate. Most of the missiles use nozzle throat area control or bleed movement at upstream pressure control with the support of extra hardware for controlling un-start and buzz phenomena. So, in a three loop structure based fuel flow controller design the extra loop of back pressure is introduced in two loop fuel flow controller design such that the required thrust is achieved by ramjet engine without endangering engine stability and performance. Here, third loop exercise tight control on back pressure margin for smooth and stable operation of air intake without the necessity of extra hardware.

Finally, the fuel flow controller design has been evaluated to ensure overall missile performance in six-degrees-of-freedom simulation platform with guidance and autopilot at different engagement scenarios along with aerial target from 0.5km altitude to 15km altitude and varying from Mach number 2.2 to Mach number 3.2.

CONTENTS

Acknowledgements.....	(vi)
Abstract.....	(viii)
List of Figures.....	(xiv)
List of Tables.....	(xxi)
List of Abbreviations.....	(xxii)
List of Symbols.....	(xxiii)
Chapter 1: Introduction.....	2
1.1 Introduction	2
1.2 Solid Fuel Ducted Ramjet Propulsion System.....	5
1.2.1 Air Intake Operation of Ramjet.....	7
1.3 Importance of Fuel Flow Controller Role of Solid Propellant Ramjet for Air-to-Air Missile.....	8
1.3.1 Missile Aerodynamics.....	8
1.3.2 Missile Guidance System.....	9
1.3.2.1 Pre-Guidance Phase.....	10
1.3.2.2 Mid-Course Guidance Phase.....	10
1.3.2.3 Homing Guidance Phase.....	10
1.3.3 Missile Autopilot.....	11
1.4 Role of Fuel Flow Controller.....	12
Chapter 2: Literature Review.....	14
2.1 Introduction.....	14
2.2 History of Ramjet Engine Development.....	14
2.3 Solid Ramjet Engine Design and Concept of Operation.....	15
2.4 Air Intake Design and Operation.....	16
2.5 Variable Throat Design and Operation.....	16
2.6 Fuel Flow Controller Design to meet Thrust Requirements.....	17
2.7 Intake Instability Analysis and its Control Techniques.....	18
2.8 Controller: Dynamic Inversion.....	19
2.9 Motivation.....	20
2.10 Contributions.....	21
2.11 Thesis organisation.....	23

2.12	Summary.....	25
Chapter 3: Mathematical Model of Solid Ramjet Engine, Air-to-Air Missile and Aerial Target.....		27
3.1	Introduction.....	27
3.2	Mathematical Modelling of Ducted Ramjet.....	27
3.3	Intake Buzz Modelling.....	31
3.4	Six-DOF Model of Solid Ducted Ramjet Air-to-Air Missile.....	34
3.5	Point Mass Model of Aerial Target.....	36
3.6	Summary.....	38
Chapter 4: Two Loop Fuel Flow Controller Design for Efficient operation of Solid Fuel Ducted Ramjet Engine.....		40
4.1	Introduction.....	40
4.2	Fuel Flow Controller Design Specification for Air-to-Air Missile.....	40
4.3	Non-linear Dynamic Inversion based Control.....	44
4.4	Two Loop Fuel Flow Controller using Non-linear Dynamic Inversion.....	45
4.5	Scheduling of Controller Gains.....	47
4.6	Standalone simulation results and analysis of two loop NDI fuel flow controller.....	48
4.6.1	Fixed Vs Scheduled Gains Comparison.....	52
4.7	Proportional-Integral Vs Non-linear Dynamic Inversion Fuel Flow controller.....	53
4.8	Summary.....	55
Chapter 5: Three Loop Fuel Flow Controller Design for Stable Operation of Ramjet Engine.....		57
5.1	Introduction.....	57
5.2	Air Intake Operation and Characteristic.....	57
5.3	Third Loop Control Requirement.....	59
5.4	Three Loop Structure based Fuel Flow Controller Design.....	60
5.5	Three Loop Fuel Flow Controller Results and Analysis with Air Intake Disturbance.....	64
5.6	Three Loop Structure based Fuel Flow Controller performance with and without Disturbance.....	67
5.6.1	Low Altitude Scenario.....	67
5.6.2	High Altitude Scenario.....	69
5.7	Summary.....	71
Chapter 6: Fuel Flow Controller Performance Validation on Six-Degrees-of-Freedom Simulation Platform of Air-to-Air Missile.....		73

6.1	Introduction.....	73
6.2	Air-to-Air Missile Engagement.....	73
6.3	Operational Sequence of Fuel Flow Controller.....	75
6.4	Description of 6-DOF model and its interaction with FFC for Air-to-Air missile...	76
6.5	Air-to-Air missile performance with FFC at Different Engagement Scenario.....	79
6.5.1	Missile-Target Engagement at 0.5km Altitude	79
6.5.2	Missile-Target Engagement at 5.0km Altitude	84
6.5.3	Missile-Target Engagement at 10.0km Altitude	88
6.5.4	Missile-Target Engagement at 15.0km Altitude	96
6.5.5	Missile-Target Engagement at Varying Altitude (Snap down condition).....	100
6.6	Fuel Flow Controller Robustness (Stability) studies in Closed Loop...	104
6.7	Monte-Carlo Simulation Result and Analysis.....	106
6.8	Summary.....	107
Chapter 7: Conclusions.....	109	
7.2	Introduction.....	109
7.2	Conclusion.....	109
7.3	Scope of Future Research	112
References.....	113	
Appendix	126	
List of Publications.....	131	
Curriculum-Vitae.....	132	

List of Figures

Figure 1.1:	Schematic diagram of solid rocket missile.....	3
Figure 1.2:	Thrust and velocity profile of solid rocket missile.....	3
Figure 1.3:	Thrust and velocity profile of ramjet missile.....	4
Figure 1.4:	Schematic diagram of ducted ramjet.....	6
Figure 1.5:	Schematic diagram of throttle valve.....	6
Figure 1.6:	Schematic diagram of Air Intake.....	7
Figure 1.7:	Diagram of the longitudinal Forces.....	8
Figure 1.8:	Closed loop Block diagram of missile Sub-system.....	10
Figure 1.9:	Missile Autopilot functional Block diagram.....	11
Figure 1.10:	Block diagram of back pressure loop.....	12
Figure 3.1:	Schematic diagram of ramjet engine.....	28
Figure-3.2:	Representation of missile forces and orientation diagram.....	30
Figure-3.3:	Representation of 3-moment (body rate) and 3-force (acceleration).....	34
Figure-3.4:	Representation of point mass motion of aerial target.....	37
Figure-4.1:	Schematic diagram of guidance loop.....	41
Figure-4.2:	Simulation model of guidance loop.....	42
Figure-4.3:	Normalized homing time requirement for miss distance at different altitude....	43
Figure-4.4:	Block diagram of two loop fuel flow controller.....	46
Figure-4.5:	Block diagram of scheduling two loop fuel flow controller gain.....	48
Figure-4.6:	Mach number performance of two loop NDI fuel flow controller at low and high Altitude.....	49
Figure-4.7:	Gas generator demand Vs feedback performance of two loop NDI fuel flow controller at low altitude.....	50
Figure-4.8:	Gas generator demand Vs feedback performance of two loop NDI fuel flow	

controller at high altitude.....	50
Figure-4.9: Throttle valve area and fuel mass rate demand Vs feedback performance of two loop NDI fuel flow controller at low altitude.....	51
Figure-4.10: Throttle valve area and fuel flow rate demand Vs feedback performance of two Loop NDI fuel flow controller at high altitude.....	51
Figure-4.11: Mach number performance of two loop NDI fuel flow controller for Scheduled gains Vs fixed gains.....	52
Figure-4.12: Nonlinear Dynamic Inversion fuel flow controller Vs proportional-integral fuel flow controller performance at same altitude for Mach number.....	53
Figure-4.13: Nonlinear Dynamic Inversion fuel flow controller Vs proportional-integral fuel flow controller performance at same altitude for throttle valve area.....	54
Figure-4.14: Nonlinear Dynamic Inversion fuel flow controller Vs proportional-integral fuel flow controller performance at same altitude for gas generator pressure.....	54
Figure-5.1: Schematic Diagram of the Intake Duct.....	58
Figure 5.2: Buzzing effect on back pressure under disturbance.....	59
Figure 5.3: Buzzing effect on air mass rate under disturbance.....	59
Figure 5.4: Block diagram of two loop fuel flow controller.....	61
Figure 5.5: Representation of feed-forward control for back pressure loop.....	61
Figure 5.6: Block diagram of three loop structure of fuel flow controller.....	62
Figure 5.7: Sense back Pressure profile with intake disturbance.....	64
Figure 5.8: Throttle Area computed by Fuel flow controller against the disturbance.....	65
Figure 5.9: Fuel mass rate with corresponding throttle area for controlling back pressure.	65
Figure 5.10: Air intake buzz instability effect on thrust produce by ramjet engine.....	66
Figure 5.11: Fuel flow controller response on Mach number with and without air intake disturbance at low altitude.....	67
Figure 5.12: Fuel flow controller response on throttle area with and without air intake disturbance at low altitude.....	68

Figure 5.13:	Fuel flow controller response on gas generator pressure with and without air intake disturbance at low altitude.....	68
Figure 5.11:	Fuel flow controller response on Mach number with and without air intake disturbance at high altitude.....	69
Figure 5.12:	Fuel flow controller response on throttle area with and without air intake disturbance at high altitude.....	70
Figure 5.13:	Fuel flow controller response on gas generator pressure with and without air intake disturbance at high altitude.....	70
Figure-6.1:	Air-to-Air missile engagement for non-manoeuvring, manoeuvring and varying altitude against the aerial target.....	74
Figure-6.2:	Operational requirements and different phases of air-to-air missile engagement scenario	75
Figure-6.3:	Block diagram of complete 6-DOF model.....	76
Figure-6.4:	Representation of missile-target engagement.....	77
Figure-6.5:	Block diagram representation of PN guidance representation.....	78
Figure-6.6:	Block diagram of missile autopilot representation.....	78
Figure-6.7:	6-DOF simulation result of missile-target engagement scenario at 0.5km altitude with manoeuvring target in pitch up plane.....	80
Figure-6.8:	Requirement of angle of attack in different phase of trajectory at 0.5km engagement scenario.....	80
Figure-6.9:	Missile Mach number (velocity) at different phase of trajectory at 0.5km altitude engagement by solid ramjet engine propulsion through fuel flow controller....	81
Figure-6.10:	Requirement of throttle valve deflection generated by fuel flow controller for different phase of trajectory at 0.5km engagement scenario.....	81
Figure-6.11:	Throttle valve area profile of solid ramjet engine by changing deflection angle through fuel flow actuator for different phase of trajectory at 0.5km engagement scenario.....	82

Figure-6.12:	Gas generator pressure profile of solid ramjet engine by changing throttle valve area for different phase of trajectory at 0.5km engagement scenario.....	82
Figure-6.13:	Achieved fuel mass rate profile of solid ramjet engine by changing gas Generator pressure to produce thrust meeting missile velocity for different phase of trajectory at 0.5km engagement scenario.....	83
Figure-6.14:	6-DOF simulation result of missile-target engagement scenario at 5.0km altitude with manoeuvring target in pitch up plane.....	84
Figure-6.15:	Requirement of angle of attack in different phase of trajectory at 5.0km engagement scenario.....	85
Figure-6.16:	Missile Mach number (velocity) at different phases of trajectory at 5.0km Altitude engagement by solid ramjet engine propulsion through fuel flow Controller.....	85
Figure-6.17:	Requirement of throttle valve deflection generated by fuel flow controller for different phases of trajectory at 5.0km engagement scenario.....	86
Figure-6.18:	Throttle valve area profile of solid ramjet engine by changing deflection angle through fuel flow actuator for different phases of trajectory at 5.0km engagement scenario.....	86
Figure-6.19:	Gas generator pressure profile of solid ramjet engine by changing throttle valve area for different phases of trajectory at 5.0km engagement scenario.....	87
Figure-6.20:	Achieved fuel mass rate profile of solid ramjet engine by changing gas Generator pressure to produce thrust meeting missile velocity for different phases of trajectory at 5.0km engagement scenario.....	87
Figure-6.21:	6-DOF simulation result of missile-target engagement scenario at 10.0km altitude with non-manoeuvring target.....	88
Figure-6.22:	Requirement of angle of attack in different phases of trajectory at 10.0km engagement scenario.....	89
Figure-6.23:	Missile Mach number (velocity) at different phases of trajectory at 10.0km	

Altitude engagement by solid ramjet engine propulsion through fuel flow Controller.....	89
Figure-6.24: Requirement of throttle valve deflection generated by fuel flow controller for different phases of trajectory at 10.0km engagement scenario.....	90
Figure-6.25: Throttle valve area profile of solid ramjet engine by changing deflection angle through fuel flow actuator for different phases of trajectory at 10.0km engagement scenario.....	90
Figure-6.26: Gas generator pressure profile of solid ramjet engine by changing throttle valve area for different phases of trajectory at 10.0km engagement scenario.....	91
Figure-6.27: Achieved fuel mass rate profile of solid ramjet engine by changing gas Generator pressure to produce thrust meeting missile velocity for different phases of trajectory at 10.0km engagement scenario.....	91
Figure-6.28: 6-DOF simulation result of missile-target engagement scenario at 10.0km altitude with manoeuvring target in pitch up plane.....	92
Figure-6.29: Requirement of angle of attack in different phases of trajectory at 10.0km engagement scenario.....	92
Figure-6.30: Missile Mach number (velocity) at different phases of trajectory at 10.0km Altitude engagement by solid ramjet engine propulsion through fuel flow Controller.....	93
Figure-6.31: Requirement of throttle valve deflection generated by fuel flow controller for different phases of trajectory at 10.0km engagement scenario.....	93
Figure-6.32: Throttle valve area profile of solid ramjet engine by changing deflection angle through fuel flow actuator for different phases of trajectory at 10.0km engagement scenario.....	94
Figure-6.33: Gas generator pressure profile of solid ramjet engine by changing throttle valve area for different phases of trajectory at 10.0km engagement scenario.....	94
Figure-6.34: Achieved fuel mass rate profile of solid ramjet engine by changing gas	

generator pressure to produce thrust meeting missile velocity for different phases of trajectory at 10.0km engagement scenario.....	95
Figure-6.35: 6-DOF simulation result of missile-target engagement scenario at 15.0km altitude with manoeuvring target in pitch up plane.....	96
Figure-6.36: Requirement of angle of attack in different phases of trajectory at 15.0km engagement scenario.....	97
Figure-6.37: Missile Mach number (velocity) at different phases of trajectory at 15.0km altitude engagement by solid ramjet engine propulsion through fuel flow controller	97
Figure-6.38: Requirement of throttle valve deflection generated by fuel flow controller for different phases of trajectory at 15.0km engagement scenario.....	98
Figure-6.39: Throttle valve area profile of solid ramjet engine by changing deflection angle through fuel flow actuator for different phases of trajectory at 15.0km engagement scenario.....	98
Figure-6.40: Gas generator pressure profile of solid ramjet engine by changing throttle valve area for different phase of trajectory at 15.0km engagement scenario..	99
Figure-6.41: Achieved fuel mass rate profile of solid ramjet engine by changing gas Generator pressure to produce thrust meeting missile velocity for different phases of trajectory at 15.0km engagement scenario.....	99
Figure-6.42: 6-DOF simulation result of missile-target varying altitude engagement scenario (Snap down condition) from 10.0km to 0.5km altitude with non-manoeuvring Target.....	100
Figure-6.43: Requirement of angle of attack in different phases of trajectory at varying altitude engagement scenario (Snap down condition) from 10.0km to 0.5km altitude.....	101
Figure-6.44: Missile Mach number (velocity) at different phases of trajectory at varying altitude engagement scenario (Snap down condition) from 10.0km to 0.5km	

altitude by solid ramjet engine propulsion through fuel flow controller.....	101
Figure-6.45: Requirement of throttle valve deflection generated by fuel flow controller for different phases of trajectory at varying altitude engagement scenario (Snap down condition) from 10.0km to 0.5km altitude.....	102
Figure-6.46: Throttle valve area profile of solid ramjet engine by changing deflection angle through fuel flow actuator for different phases of trajectory at varying altitude engagement scenario (Snap down condition) from 10.0km to 0.5km altitude.....	102
Figure-6.47: Gas generator pressure profile of solid ramjet engine by changing throttle valve area for different phases of trajectory at varying altitude engagement scenario (Snap down condition) from 10.0km to 0.5km altitude.....	103
Figure-6.48: Achieved fuel mass rate profile of solid ramjet engine by changing gas generator pressure to produce thrust meeting missile velocity for different phases of trajectory at varying altitude engagement scenario (Snap down condition) from 10.0km to 0.5km altitude.....	103
Figure-6.49: Gain-phase offset for loop criteria with plant perturbation.....	105
Figure-6.50: Angle-of-attack at each runs of 6-DOF simulation for different missile perturbations and parameters uncertainties in Monte-Carlo simulation with manoeuvring aerial target	106
Figure-6.51: Miss-distance performance at each runs of 6-DOF simulation along with fuel Flow controller for different missile perturbations and parameters uncertainties in Monte-Carlo simulation with manoeuvring aerial target.....	107

List of Tables

Table 4.1	Guidance loop time constant as a function of altitude and Mach number.....	41
Table 4.2	Fuel flow controller time constant as a function of altitude and Mach number....	43
Table 5.1	Buzz frequency as a function of altitude and Mach number.....	60

Lists of Abbreviations

AAM	Air-to-Air missile
CC	Combustion Chamber
CFD	Computational Fluid Dynamics
CG	Centre of Gravity
CP	Centre of Pressure
DCM	Direction Cosine Matrix
DI	Dynamic Inversion
DOF	Degree-of-Freedom
FFC	Fuel Flow Controller
GG	Gas Generator
INS	Inertial Navigation Sensor
LOS	Line-of-Sight
MC	Monte-Carlo
NDI	Nonlinear Dynamic Inversion
NED	North, East and Down
NHT	Normalized Homing Time
PN	Proportional Navigation
SAM	Surface-to-Air Missile

List of Symbols

V_M	Missile Velocity (m/s)
T_{ap}	Autopilot time constant (sec)
ω_{ap}	Autopilot bandwidth (rad/sec)
T_{seeker}	Seeker time constant (sec)
$T_{estimator}$	Estimator time constant (sec)
γ	Flight path angle (deg)
θ	Missile orientation angle (deg)
ρ_a	Air density (kg/m ³)
P_g	Gas generator pressure (N/m ²)
R_g	Specific gas constant (J/kg-K)
T_g	Gas generator temperature (K)
α	Angle of attack (deg)
V_a	Sound of Air (m/s)
C_D	Drag force coefficient
C_L	Induce drag force coefficient
A_v	Area of throttle valve (m ²)
P_c	Combustion chamber pressure (bar)
P_{cs}	Sensed combustion chamber pressure (bar)
M_s	Sensed Mach number

M_d	Demanded Mach number
C_g	Characteristic velocity of gas (m/s)
P_{g0}	Gas generator initial pressure (bar)
A_{tr0}	Initial area of throttle valve (m^2)
δ_{Ar}	Deflection of FFC actuator (deg)
ρ_g	Density of gas in gas generator (kg/m^3)
m_f	Fuel mass rate (kg/s)
m_a	Air mass rate (kg/s)
H	Representation of altitude (km)
ω_{outer}	Gain of Mach number loop (Outer loop)
ω_{inner}	Gain of gas generator pressure loop (Inner loop)
ω_{third}	Gain of feed forward control of back pressure loop
T_{ffc}	Fuel flow controller time constant (sec)
T_g	Guidance time constant (sec)
R_{TM}	Relative missile to target distance (m)
F_y, F_z	Lateral acceleration in pitch and yaw plane of missile (m/s^2)
F_{ys}, F_{zs}	Sense lateral acceleration in pitch and yaw plane of missile (m/s^2)
F_{\max}	Maximum lateral acceleration capability (m/s^2)
P, Q, R	Missile body rate in X, Y and Z axis (deg/sec)
X_t, Y_t, Z_t	Aerial target position in X, Y and Z (m)
X_m, Y_m, Z_m	Missile position in X, Y and Z axis (m)
V_{xt}, V_{yt}, V_{zt}	Aerial target velocity in X, Y and Z axis (m/s)

V_{mx}, V_{my}, V_{mz}	Missile velocity in X, Y and Z axis (m/s)
$\omega_{INS}, \zeta_{INS}$	Inertial navigation sensor bandwidth and damping factor
$\omega_{ACT}, \zeta_{ACT}$	Fuel flow actuator bandwidth and damping factor
$\omega_{PRE}, \zeta_{PRE}$	Pressure sensor bandwidth and damping factor

Chapter 1

Introduction

Chapter 1

Introduction

1.1 Introduction

Scientists and those in academia have invested efforts in innovative methods to develop the state-of-the-art technology for developing advanced weapons for their country. The air defense force is constantly seeking new approaches to improve the performance of existing air-to-air missiles. There is a constant striving to reach new levels of missile technology regarding maneuverability and performance in all aspects. One way of improving capabilities is to develop a new missile technology over existing ones and solid ramjet propulsion system based air-to-air missile is developing, which provides enhanced range and capability against aerial target by improving the total specific impulse (thrust force) and has a POWER-ON interception. The specific impulse, which is the total impulse (thrust force) that the ramjet engine can produce per unit propellant mass burnt, is very high for ramjet engine systems since it does not carry oxidizers as well, which makes them highly preferable for long range flight.

There are broadly two types of propulsion systems which define the range and speed capability of air-to-air tactical missiles. These are:

1. Rocket (Solid) propulsion system and
2. Ramjet propulsion system

Tactical air-to-air missile has a dimensional limitation due to the launch platform constraints of fighter aircraft. The missile configuration design is different for both types of propulsion systems; it is carried out at the beginning phase of project for aerial target. Rocket propulsion system based missiles operate at finite time (T) and have a high velocity at the beginning and then missile velocity decreasing up to the required velocity for target interception, as shown in figure 1.1 and 1.2.

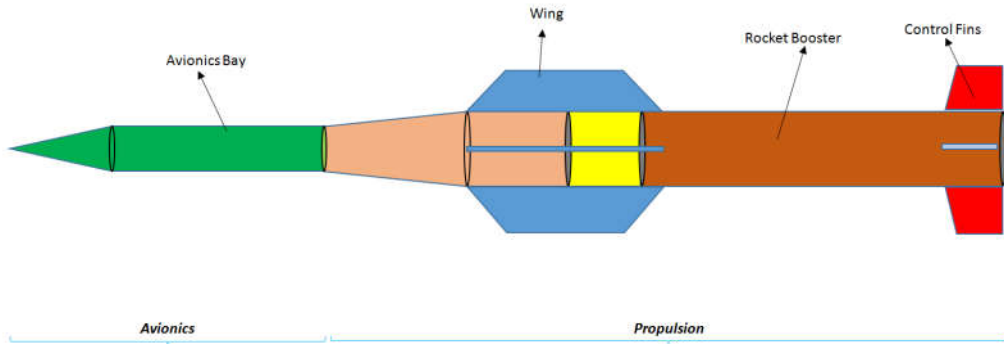


Figure-1.1: Schematic diagram of solid rocket missile

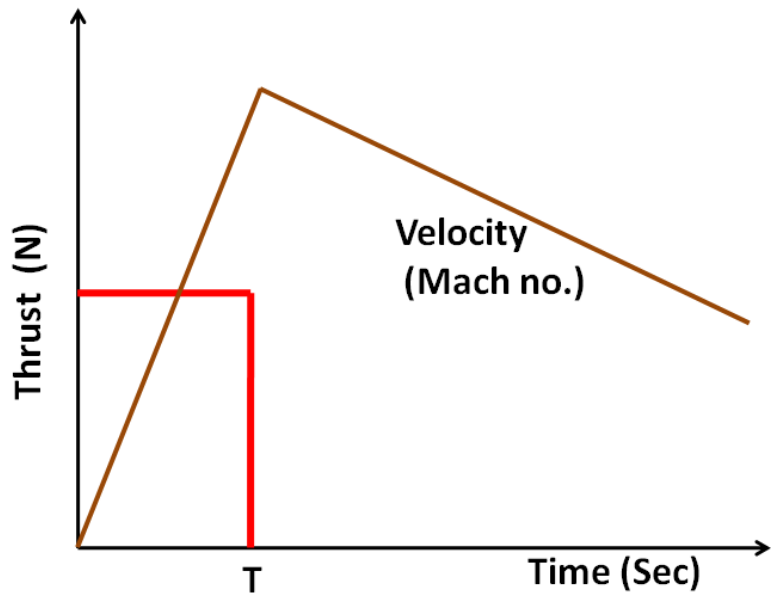


Figure-1.2: Thrust and velocity profile of solid rocket missile

So, the manoeuvring capability of missiles, which is a function of configuration and velocity, needs a large size wing on the missile to intercept the target. Large wing on the missile increases the drag force. So within the dimensional limitations of a missile, the trade off rocket propulsion and configuration design is carried out to meet range and speed requirement of the missile. Once the design of rocket propulsion based missile is finalized, the missile range capability gets affected for non-manoeuvring target to manoeuvring target. The reason is that the missile velocity is reduced by additional drag generated due to increase of angle of attack for intercepting

the manoeuvring target. This is the biggest drawback of missile performance of rocket propulsion system. Another drawback is that the rocket propulsion system propellant grain mixed with both oxygen and chemical grain together which constrains the design of huge propulsion system to enhance the range [1-4].

The above drawbacks have been overcome with technological advancements in ramjet propulsion system design. Ramjet technology uses oxygen from the atmosphere to burn fuel stored in the missile. So, given the dimensional limitations on missile, it can carry more fuel and have better range superiority than similar dimension rocket propulsion based missile. Atmospheric air can be compressed by air intake before using it to burn with fuel in the combustion chamber. The compression of air is possible by air intake only if the speed of the missile is more than Mach number 2.0 (Mach number is the ratio of the speed of missile to the speed of sound). Hence, the operation of ramjet propulsion system is applicable at supersonic speed of missile which may vary from Mach number 2.0 to Mach number 4.5. This is the reason ramjet system depends on rocket booster or some other means to accelerate missile nearly or at more than Mach number 2.0 as shown in figure-1.3 [6-9].

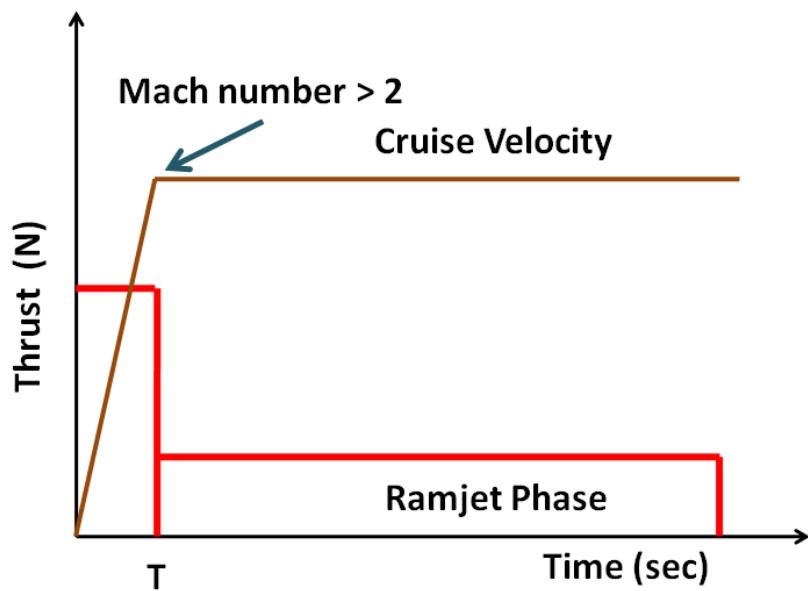


Figure-1.3: Thrust and velocity profile of ramjet missile

The significant advantage of ramjet propulsion based missile is that the speed of missile can be changed depending on the trajectory requirement through injecting incremental fuel in combustion chamber. The reason is that the additional induce drag force generated by angle of

attack, can be compensated through extra thrust produced by injecting extra fuel on combustion chamber. So, the missile range capability will be same for a non-manoeuvring target as for manoeuvring target [1][3].

There are two types of ramjet propulsion systems:

1. Liquid fuel based ramjet propulsion system and
2. Solid fuel based ramjet propulsion system.

Liquid fuel is injected into the combustion chamber to burn with compressed air in liquid fuel based ramjet propulsion system. Thrust level of the ramjet engine is produced by controlling liquid fuel flow rate. However, injection of fuel in liquid fuel based ramjet propulsion requires complex and expensive systems. Also, air breathing engines suffer from flameout problem, which is the dying out of the flame in combustion chamber. Liquid fuel based ramjet, as a member of air-breathing engine, needs a flame stabilizer in order to avoid this problem, which increases the complexity of design further. Solid fuel based ramjet propulsion, on the other hand, is simple and contains solid fuel on the outer part of the ramjet engine with a throat hole in middle to get mixed with compressed air flow from air intake [5].

Presently, realizing solid fuel based ramjet propulsion system for air-to-air tactical missile application is simpler and more advantageous then liquid fuel based ramjet propulsion system to obtain more range and intercept manoeuvring aerial targets.

1.2 Solid Fuel Ducted Ramjet Propulsion System

Ramjet engine is a potential source of power supply, especially for high speed supersonic long range air-to-air missile. A ramjet engine is an air-breathing combustion system consisting of a gas generator housing the solid propellant, a throttle valve which regulates fuel flow rate into the secondary combustion chamber, an air intake system, an exit nozzle and an integrated booster to start the ramjet engine, as shown in figure 1.4. The function of a gas generator is to provide oxidizer deficient fuel in appropriate form to combustion chamber, where the main combustion process occurs by a mixture of compressed air which then generates thrust [6-8] [36-38].

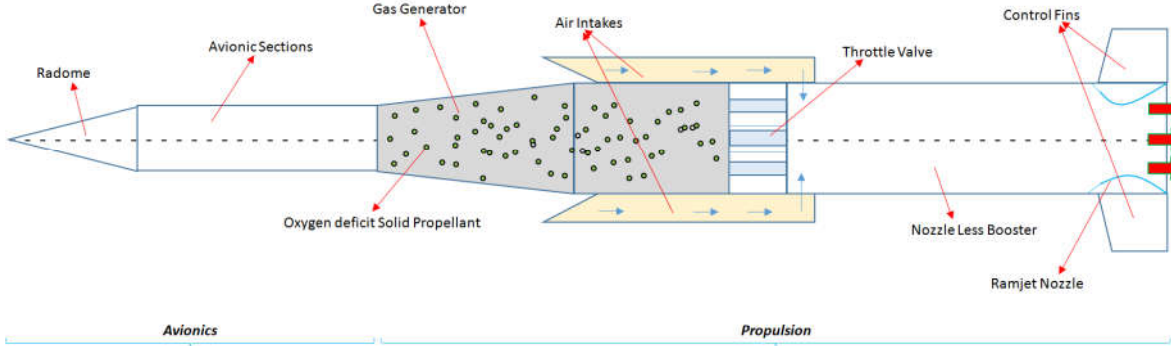


Figure-1.4: Schematic diagram of ducted ramjet

In the gas generator, solid propellant is converted into fuel by a pre-burn process and sent through a throat valve between gas generator and combustion chamber by means of pressure difference. The important aspect of solid based ramjet engine is the possibility to control fuel injection supplied through gas generator. So, the required fuel flow rate is injected into the combustion chamber in a controlled manner. The simplicity of solid rocket engines is that it doesn't need a flame stabilizer for the flameout problem, because hot gas from the gas generator is able to maintain and sustain combustion.

It is desirable that changing the burning area of the propellant in the gas generator is done in a controlled manner, assuming the solid propellant burns with uniform cross sectional area (so-called cigarette type burning). A smaller burning area of solid propellant generates less fuel in combustion chamber and then generates less thrust. It is known that the burning rate of a solid propellant is affected by the pressure of the gas generator. This property is called pressure sensitivity of propellant. Burning rate of the solid propellant can be controlled by means of controlling the pressure at the gas generator chamber by introducing a fuel flow controller [7-9] [36].

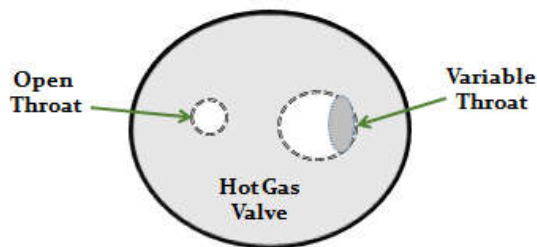


Figure-1.5: Schematic diagram of throttle valve

Injected fuel flow rate from gas generator to combustion chamber is directly dependent on the effective throat area between the two as shown in figure 1.5. Therefore, changing the effective throat area can be carried out to change fuel flow rate. Fuel flow actuator is used for throat area control and it would receive command from fuel flow controller. The functions of fuel flow controller are:

- 1- Achieve the desired thrust.
- 2- Maintain fuel flow regulation within the safe operation air intake margin and
- 3- Prevention of reduction of flight Mach number below the minimum Mach number.

1.2.1 Air Intake Operation of Ramjet

The ramjet engine carries only fuel and the required oxygen for burning, it can be supplied from atmosphere while the missile is flying at more than Mach number 2.0. The air which carries oxygen gets compressed into the intake due to the formation of terminal shock inside it. The terminal shock location is a dynamic function of downstream pressure (Atmospheric pressure) and upstream back pressure (Combustion chamber) as shown in figure 1.6.

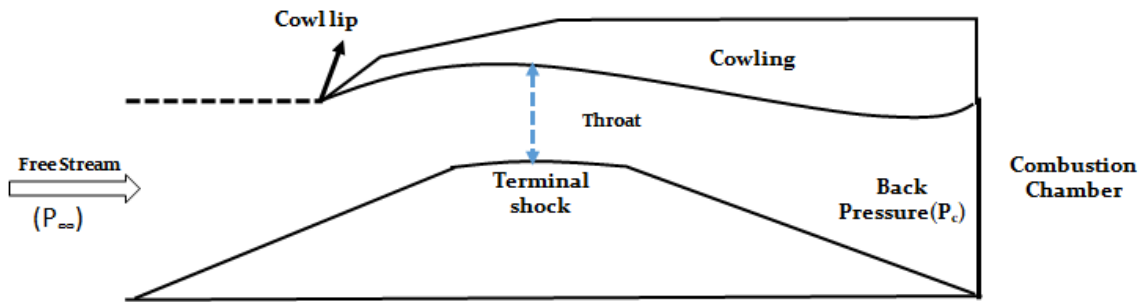


Figure-1.6: Schematic diagram of Air Intake

The reason could be terminal shock location and it would lead either to un-start or buzz oscillatory phenomena.

1. Atmospheric disturbance like gust can suddenly change downstream pressure, leading to un-start.
2. Combustion-intake interaction in which under a certain dynamic condition, the combustion pressure increases beyond back pressure margin, leading to intake buzz.

Air intake buzz is a phenomenon of self-sustained shock oscillations, which result in high-amplitude variations of inlet air mass flow and pressure. It generally arises when the mass flow entering is reduced below a given value. Air intake buzz can lead to thrust loss and engine surge, or even cause structural damages to the missile; this violent and dangerous phenomenon is therefore highly undesirable. So, in order to maintain high performance without crossing the buzz margin of intake, buzz protection controller is necessary [61-72].

1.3 Importance of Fuel Flow Controller Role of Solid Propellant Ramjet for Air-to-Air Missile

Air-to-Air tactical missiles act in a closed loop interaction of the systems shown in figure 1.8 to ensure effective overall performance of a missile. These are:

1. Missile Aerodynamics
2. Missile Guidance system and
3. Missile Autopilot

1.3.1 Missile Aerodynamics

The flow of air around a missile produces pressure variations, which is the basic cause of aerodynamic forces and moments. The magnitude of the forces and moments that act on missile depend on different factors. These factors are: [3-4]

1. Configuration of missile
2. Angle of attack
3. Dimension/ size of missile
4. Free-stream velocity
5. Density of air

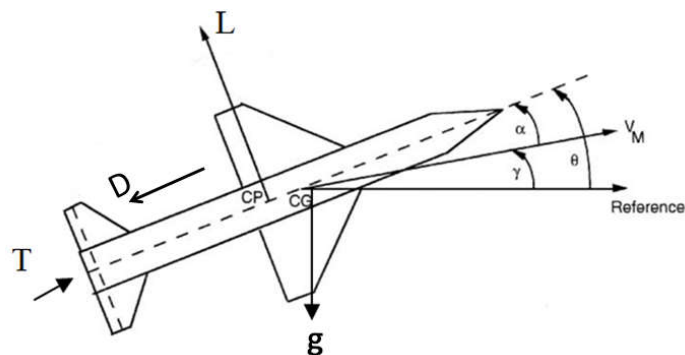


Figure-1.7: Diagram of the longitudinal Forces

These forces are thrust force (T), lift force (L) and drag force (D). The relation of lift and drag forces to reference velocity is shown in figure 1.7.

Lift force is the resultant aerodynamic force that is perpendicular to the direction of reference velocity. The aerodynamic lift force is generated by pressure forces acting on the missile surface. Also, the lift force is perpendicular to the missile's velocity vector in the vertical plane.

$$\text{Lift(Force)} = Q * S * C_n(\alpha) \quad (1.1)$$

Where, $Q = 1/2 * \rho * V_m^2$ is dynamic pressure and which is function of air density (ρ) and velocity of missile (V_m). $C_n(\alpha)$ is aerodynamics force coefficient is a function of angle of attack and S is the surface area of missile.

Drag force is the resultant aerodynamic force that acts opposite to the direction of flight motion. The aerodynamic drag is produced by pressure forces and by skin friction forces that act on the missile surface. The drag force is measured along the velocity vector, but in opposite direction.

$$\text{Drag(Force)} = Q * S * C_T \quad (1.2)$$

$$\text{Where, } C_T = C_{d0} + C_d(\alpha)$$

C_T is the total aerodynamics drag coefficient of missile, C_{d0} is the aerodynamics drag coefficient due to skin friction and $C_d(\alpha)$ is the aerodynamics induce drag coefficient due to angle of attack and S is the surface area of missile. $Q = 1/2 * \rho * V_m^2$ is dynamic pressure and it is function of air density (ρ) and velocity of missile (V_m).

1.3.2 Missile Guidance System

Ramjet based propulsion system needs three phases of guidance for air-to-air missile application.

- Pre-guidance phase,
- Mid-course guidance phase,
- Homing guidance phase.

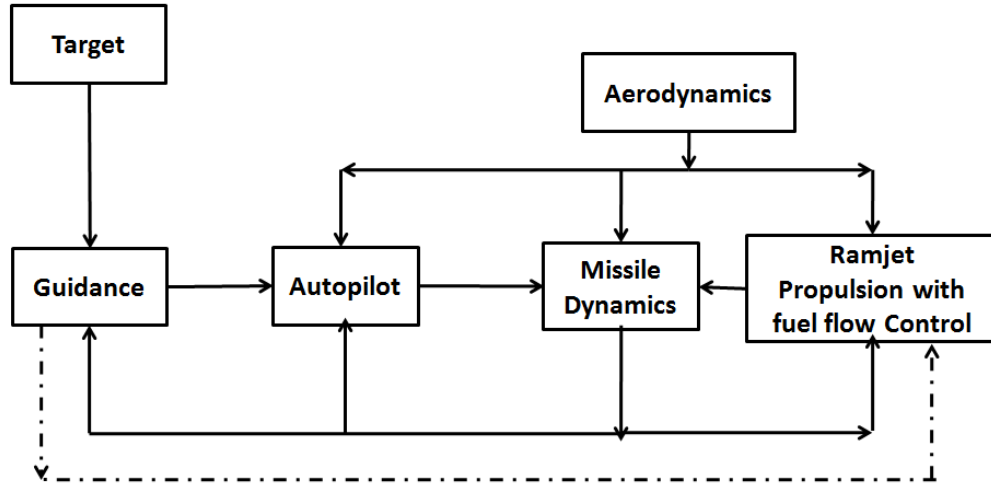


Figure: 1.8 - Closed loop Block diagram of missile sub-systems

1.3.2.1 Pre-Guidance Phase

This type of guidance needs computation before launch of missile from the aircraft. In this phase, the guidance law will decide the trajectory as well as Mach number based on target distance and altitude.

1.3.2.2 Mid-course Guidance Phase

In this phase, guidance law generates lateral acceleration demand for Autopilot to maintain the cruise Mach number for a level flight based on missile-target kinematics. Generally, the angle of attack of missile is low in this phase. If the target altitude is different from the missile altitude, the mid-course guidance generates the thrust demand to achieve corresponding Mach number. The Mach number of ramjet operation is a function of altitude.

1.3.2.3 Homing Guidance Phase

In this phase, guidance law generates lateral acceleration demand for autopilot based on seeker (In borne radar into the missile) tracking to target. This is a most critical phase of guidance in which target carry out evasive manoeuvre to escape the missile. The generated guidance demand will be high for autopilot and it will lead to higher angle of attack. High angle of attack will increase the total drag and then Mach number starts decreasing; therefore, to retain the Mach number, fuel flow control is

executed to close throat area further and it will increase fuel flow rate and the ramjet engine produces more thrust for hitting the target.

1.3.3 Missile Autopilot

Missile autopilot is a flight control system inside the guidance loop that ensures meeting missile acceleration demand in pitch and yaw plane through a guidance algorithm and this has to be executed while maintaining missile stability. It will generate corresponding fin deflection for missile actuator. Missile actuator executes it to change the dynamics of missile to achieve new position [3].

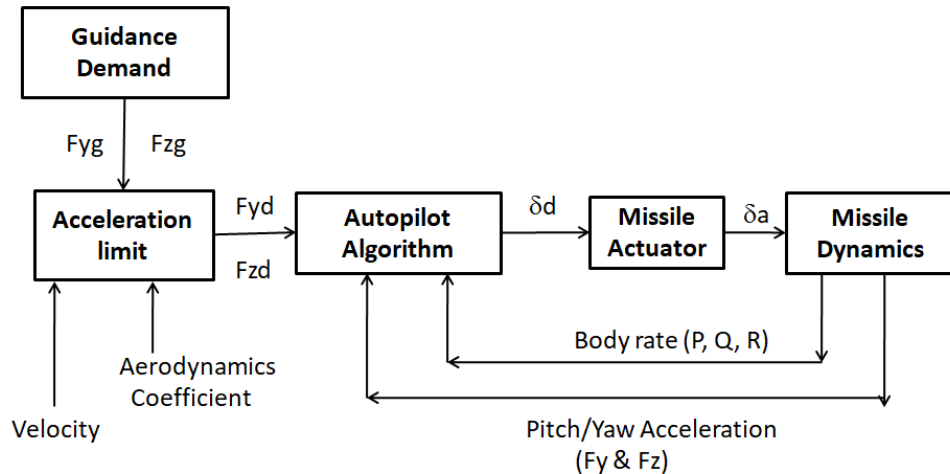


Figure-1.9: Missile Autopilot functional Block diagram

The aerodynamic capability of acceleration demand (Pitch and Yaw channel) by guidance algorithm needs to be checked before bypassing to autopilot as shown in figure-1.9. If it is not checked and the guidance demand is higher for the missile aerodynamics capability, an autopilot algorithm may destabilize the missile. So, aerodynamics capability of acceleration is given by

$$Acceleration = \frac{Q * S * C_n(\alpha)}{Mass} \quad (1.3)$$

Where, $Q = 1/2 * \rho * V_m^2$ is dynamic pressure and a function of air density (ρ) and velocity of missile (V_m). $C_n(\alpha)$ is aerodynamics force coefficient, which is a function of angle of attack and S is the surface area of missile.

So, for a given missile configuration, the acceleration capability in pitch and yaw plane depends mostly on the velocity of missile. If the missile velocity is not able to ensure missile trajectory, the guidance cannot follow the exact path to engage the target.

1.4 Role of Fuel Flow Controller

Performance of ramjet engine depends heavily on flight operating conditions like altitude, Mach number and angle of attack. Stable and efficient operation of ramjet in the presence of operating flight conditions and effective fuel flow control is required. The function of fuel flow controller is to open throttle valve area for primary burning of propellant into gas generator, often which the solid propellant is converted to fuel gas. The fuel gas will further bypass into combustion chamber to produce thrust. The roles of fuel flow controller are as follows:

1. It computes initial presetting of deflection angle of throat area at pre-guidance phase to ensure supply of required gas generator pressure for fuel mass rate at the time of gas generator ignition.
2. It computes and provides incremental deflection to change gas generator pressure for increasing, decreasing or maintaining the Mach number during mid-course guidance phase and homing guidance phase.
3. In this work, an innovative way to use fuel flow controller to maintain back pressure margin within buzzing limit without the need of extra hardware, has been proposed and validated. So, the fuel flow controller performs a supervisory control on back pressure for stable operation of air intake throughout the flight, as shown in figure-1.10.

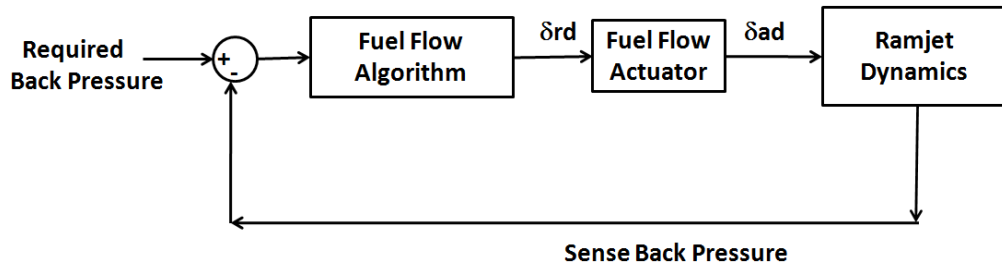


Figure: 1.10: Block diagram of back pressure loop

Chapter 2

Literature Review

Chapter 2

Literature Review

2.1 Introduction

Ramjet engine is a potential source of power supply especially for high speed supersonic long range missile. Solid fuel ramjet propulsion is the latest development in the area of missile propulsion. It has been mostly used till today for surface-to-air missiles with fixed throat and validated as potential propulsion system to enhance the range and capability of missiles. Presently, this technology is made attractive for air-to-air missile development. The operational flight trajectory of air-to-air missile may vary from low altitude to high altitude based on fighter aircraft position for launching with respect to aerial target position. So, thrust requirement from the solid fuel ramjet needs to be used effectively. To achieve variable thrust for different altitude of the missile, an efficient fuel flow controller is required for controlling the flow of fuel mass rate. Performance of ramjet engine is highly dependent on flight operating conditions. Hence, development of ramjet engine dynamics, role of intake and its impact on engine performance, types of variable throat and techniques for designing fuel flow controller need to be understood. This chapter consists of the details of critical appraisal of previous work published in the literature pertaining to the topic of investigation.

2.2 History of Ramjet Engine Development

Ronald [6] clearly brought out the history of ramjet evolution as well as the concept and technology, which was initiated around 1913. Actual construction and testing of variable ramjet engine did not occur until mid-1930s. The ramjet propulsion system works began during this phase with the objective to achieve high speed and a long range for missiles. It began to receive attention in the second half of 1940 and reached a relative peak during in 1950. The solid

propellant ramjet received attention beginning 1980s and this continues till today. The key technology and components that have had significant impact on the maturation of ramjet were brought to light during 1980s and these include air induction system, missile aerodynamics, combustion design and material, fuels, injection and mixing, ejectable and non-ejectable components, thermodynamics and engine modeling and ground testing. During this era, no choked throat was available between the gas generator and combustion chamber. The gas generator solid propellant burning rate depended on combustion chamber pressure. In [6-8], the actual development of solid propellant ramjet for missile took place between 1980 and 2000.

2.3 Solid Ramjet Engine Design and Concept of Operation

In the field of tactical supersonic missile development, for air-to-air missile, an increasing interest in ramjet propulsion has been shown because of its contribution to improved missile performance in terms of range, sustained speed and manoeuvrability compared to missiles using solid rocket propulsion. Solid based ramjet engine has few or no moving parts and thus they are simple, reliable and provide efficient operation over a wide range of supersonic Mach numbers and altitudes for air-to-air missiles. It needs a rocket booster to be integrated for accelerating missile while launched them from a jet fighter to ensure supersonic speed. In general, rocket booster has a nozzle and it should be ejected at the transition phase between boost and ramjet phase. So, it is preferable to have a nozzle-less booster to avoid ejection. During the integrated booster operation phase, the air intake and gas generator to combustion chamber throat need to be closed and it needs to be opened for a very short time at the transition between boost and ramjet phase. Once the nozzle-less booster burns out the ramjet propulsion takes over for producing the thrust for sustaining the supersonic speed of the missile [7-9].

A special characteristic of solid propellant burn rate depends on the pressure variation in gas generator. So, the fuel flow rate of gas generator is controllable for active thrust variation which allows the missile speed to be a function of altitude and Mach number in a controlled manner. Further, extra thrust can be generated during the high manoeuvre requirement at the end phase of target engagement by controlling fuel mass rate. The solid propellant in gas generator has high density and volumetric heating value. It has an advantage over other propellants which allows auto-ignition of the propellant and is not sensitive to flameout on combustion instability [7-10].

2.4 Air intake Design and Operation

Air intake provides oxygen for combustion with fuel mass to produce thrust. The intake must provide the engine with sufficient air mass flow and the required pressure recovery in all flight conditions for stable combustion in ramjet missile. The intake system mainly consists of two parts, the first part in which external compression is accomplished when air flow arrives at the initial portion of intake called cowl lip. The second part is when internal compression is accomplished at the intake throat by terminal shock. An optimal design for intake is required to meet the maximum gain of pressure recovery and corresponding air mass flow. [11-13] brought out the intake design with multiple shock provision to ensure reasonable pressure recovery for a different Mach number. [14-17] carried out research on optimal location of intake on missile considering the operations at different orientations and angle of attack and also brought out that the internal bleed system ensures the functions of air-intake even at off-design conditions (below and above the designed Mach number).

2.5 Variable Throat Design and Operation

The beginning phase of solid propellant based ramjet missile is used for surface to air missile where fixed throat is used to control the flow of fuel mass rate from gas generator to combustion chamber. It was found that the optimal use of ramjet propulsion system for range enhancement was not adequate with fixed throat method. Further, the fixed throat concept ramjet technology is difficult to apply for air-to-air missile. So, changing the throat area based concept was essential to vary the thrust based on altitude and Mach number. The fuel flow rate generation and flow to combustion chamber in a controlled manner were the main concerns in solid propellant ramjet since it directly affects the thrust of the missile. It can be realized by several different methods listed below [18-23].

1. Introducing secondary injection to gas generator to control the burning rate of solid propellant
2. Introducing a swirl in vortex valve to fuel flow rate in order to control the effective throat area between gas generator to combustion chamber
3. Changing the throat area using a control valve. This can be done by :

- a. The needle-type (or pintle-type) valve
- b. Pressure-balanced gas regulating systems
- c. Electromechanical actuation for changing the throat area

2.6 Fuel Flow Controller Design to meet Thrust Requirement

For control design, the first step is the modelling of plant. [7][25-32][36-38] discussed propulsion modelling of ducted rocket and components like gas generator, throttle valve and combustion chamber. The researchers presented the relation between throttle area, burning rate of gas generator propellant, gas generator pressure and fuel flow rate to combustion chamber. The modelling of ramjet engine was done and the fuel flow controller design of ramjet using throat area as control input was considered. In [36], the controller designed a model considering gas generator pressure as first order lag dynamics and gain scheduled using P and PI controller. There are many studies available which talk about controller for ramjet ducted rocket in [42-44] [50-52]. PID based single set of controller gain for fuel flow controller was designed to meet the objectives. However these gains are inadequate to provide the desired performance for a wide range of operations. In [32-35][52], fuel flow controller design was done using variable throttle valve and variable gas generator pressure through pneumatic pressure (pressure balance mode) with the help of PID controller. However, this needs extra hardware which leads to complexities in small missile design. Further work was done in [32][38][53], where two loop based thrust controller was proposed (Outer loop as thrust control loop and inner loop as pressure control loop). Mathematical models of both loops were obtained in state space equation. In [29-31], a new fusion feedback input from gas generator pressure and combustion pressure was discussed to ensure stability. [38-40][44][53] presented PID controller gain scheduling based on look-up table and it also showed comparison with PI controller vs. adaptive controller and concluded that both controller performances were satisfactory.

2.7 Intake Instability Analysis and its Control Techniques

The position of air intake terminal shock is affected by perturbation of the propagation upstream from combustion chamber and from disturbance in the free-stream. Due to propagation phenomena, two types of instability, un-start and Buzz occur in intake. In general, when combustion chamber pressure (back pressure) rises and the terminal shock emerges, the position outside the intake duct is usually called un-start and when the terminal shock position oscillates in the duct, it is called air intake Buzz [60][63][72]. Buzz can lead to thrust loss, engine surge or even structural damages. There is also heightened risk of intake un-start or buzz for ramjet powered missile during manoeuvre such as acceleration, snap up and snap down conditions, where fuel rate requirement may increase or decrease with altitude.

These phenomena have been the subject of research while developing ramjet engine. Intake instability was experimentally established and presented [65-69][79-80]. In [81-83], theoretical model of buzz phenomena was presented. However, it has been impossible to model the buzz with accurate precision over the years. In [70-73], although some attempts have been made to model the buzz, it was found that in the supercritical region, the terminal shock is inside the intake duct and the acoustic waves travelling back and forth between intake and combustion chamber can affect shock location while the total pressure recovery of intake hardly changes. In contrast, shock is outside intake duct in the subcritical regime. The total pressure recovery is not much affected. So, obtaining a dynamic model of buzz is a challenge. [67] presented the experimental study with two types of shock oscillations, little buzz and big buzz that exist inside the intake duct. The little buzz is due to acoustic phenomena and has high frequency, whereas big buzz is due to boundary layer separation and has low frequency.

Simon Trapier et al. [57] presented low-order model for un-start and buzz need to control engine stable operation. So, controlling air intake un-start and buzzing for stable ramjet engine operation is a very important part. [51-52][64] presented the active control design to establish the position of terminal shock inside the intake duct through ensuring back pressure margin within the intake. It is possible through bleed control or exit nozzle throat area control by including extra hardware. However, the control design measures are successful, provided the terminal shock is maintained inside the intake duct. But once full-fledged buzz has occurred, it needs pro-

active control to avoid it. [67][84-87] proposed the variable ramp technique to effectively nullify the occurrence of buzz, which also demand complex hardware.

2.8 Controller: Dynamic Inversion

To accomplish effective fuel flow controller for solid based ramjet air-to-air missile, it should be designed for optimal thrust to meet the maximum range and high manoeuvrability. Traditional controllers are based on classical control theory with linearized equations of plant dynamics. These controllers require substantial tuning and gain-scheduling techniques [93]. For a missile, with increased angle of attack, variation of pressure as a function of altitude and Mach number and enlarged range of operation, nonlinear terms are much more significant and cannot be ignored [94]. Thus, geometric nonlinear control theory, which has provided systematic design tools for nonlinear feedback systems, has excited the interest of control engineers [95]. Among these methods, exact linearization techniques have been applied to aircrafts and missiles. Recently, control researchers have developed an advanced flight control design called nonlinear dynamic inversion (NDI) based on feedback linearization [96-102]. Conventional controller designs assume that plant dynamics are linear and time invariant for nominal flight condition and they feature stability and command augmentation systems to meet the required flying/handling qualities, with gains scheduled as functions of nominal flight conditions. In extreme flight conditions, the performance of these systems begins to deteriorate because of the un-modeled effects of strong nonlinearities inherent in flight dynamics. The main advantage of NDI methodology is that, it avoids gain-scheduling process of other methods, which is rather time consuming, expensive, iterative and labor intensive. NDI technique offers greater reusability across different batches of propellants and greater flexibility for handling changed models. Control laws based on NDI offer potential for providing improved levels of performance over conventional flight control designs in extreme flight conditions. This is due to NDI controllers being more accurate representation of forces and moments that arise in response to large state and control perturbations. These control laws also allow specific state variables to be commanded directly [98-100]. Because of the superior performance of NDI methodology, many designs of modern, advanced aerospace vehicles are based on this technique.

Successful flight control designs using nonlinear dynamic inversions have been developed. A two-time scale, or two-stage dynamic inversion approach has been widely applied for highly manoeuvrable fighter aircrafts [95-111] and missiles [112].

Dynamic inversion, or equivalent feedback linearization, is one of the most popular control design methodologies for nonlinear systems that are defined by control variables [116-117]. However, many practical applications give rise to non-affine nonlinear systems, for which an explicit inversion is not possible. Hovakimyan [118-119] presents a new method for approximate dynamic inversion for non-affine cases in control systems via time-scale separation. The control signal is sought as a solution to fast dynamics and is shown to asymptotically stabilize the original non-affine system. Additionally, different types of desired dynamics will respond differently to uncertainties and it is important that the desired dynamics has robustness. The choice of desired dynamics and its effects have been discussed in [98][108-110][130-140].

Time-scale separation exists in many dynamical systems. Using natural separation between 'fast' and 'slow' variables to reduce the complexity of a dynamic system can greatly simplify the control design and analysis problem. There are natural timescale separations in many flight control problems, both in the design of attitude control autopilots and Fuel flow controller design. Examples of dynamic inversion flight control using time-scale separation can be found in [141-146].

In this method, fast dynamics is assumed to go on a steady state, and the stability of the simplified system is studied. Based on the above discussion, it can be concluded that dynamic inversion is a very powerful controller for design of fuel controller of ramjet propulsion system. Battacharya et al. [147] presented two and three loop structure based design using dynamic Inversion controller.

2.9 Motivation

Tactical air-to-air missile manoeuvre while engaging aerial target at different altitudes from 0.5km to 15.0km that would lead to high angle of attack, which tends to affect missile velocity due to induced drag and reduce overall capability of the missile. So, missile velocity dropping

can be avoided by injecting more fuel into the combustion chamber for producing extra thrust. Hence, fuel flow controller is a very important algorithm to use in ramjet propulsion system. The thesis presents an extensive review of the research topic and found that the existing design has focused on different control techniques in standalone situations to produce thrust and control/ avoid intake instability through nozzle throat area or bleed movement, which need extra hardware to implement in a missile. Therefore, the following gaps along with space constraints have been worked out for designing an efficient and stable fuel flow controller to meet the objectives of air-to-air missile.

1. Bring out the design objectives of fuel flow controller for achieving overall performance of a missile.
2. Effect of angle of attack on mathematical model of ramjet engine has not been considered and this can deteriorate the performance of controller in the presence of missile manoeuvre and impact missile performance.
3. Generic fuel flow controller design as a function of altitude and Mach number has not been formulated and this can affect the performance at operating conditions from 0.5km to 15km altitude.
4. Air intake instability problem has not been addressed as there appears to be no hardware for solid ramjet propulsion system.

The thesis in general addresses all the above aspects and constraints to design a fuel flow controller for effective performance of air-to-air tactical missile.

2.10 Contributions

The work undertaken aims at designing a fuel flow controller for efficient and stable operation of solid based ramjet propulsion systems as a function of varying altitude and Mach number. The following are the contributions of the proposed work:

1. The existing literature discuss controller design with respect to solid fuel ramjet functionality to produce thrust with different control techniques. Ramjet system is a dynamic system and its performance depends on aerodynamic configuration and operating condition like altitude,

Mach number and angle of attack of missile. The existing mathematical models of the ramjet engine have been made without considering angle of attack that plays a crucial role to cruise Mach number in the presence of a manoeuvring missile. While the existing design is important for testing and stabilizing the ramjet technology on ground, in flight, the design may not be useful, specially for realizing air-to-air missile which can be launched from different altitude from 0.5km to 15km against an aerial target. In this work, keeping in mind angle of attack the mathematical model of the ramjet engine was improved.

2. Not a single piece of literature has talked design specification in terms of speed of response (Bandwidth) of fuel flow controller and its applicability for missile performance as a function of altitude, Mach number and angle of attack. To bring out the specification of fuel flow controller design, it is assumed that missile velocity (Mach number) is a crucial parameter for designing an efficient and optimal guidance and autopilot of the missile. So, velocity of missile is to be a function of altitude for effective use of aerodynamic manoeuvring capability. So fuel flow controller specifications have been generated to nullify the effect of total drag force as a function of angle of attack. To meet the design specifications, the actuator specification was generated based on loop separation theory.
3. A generic two loop fuel flow controller was designed to meet the specification as a function of altitude, Mach number and angle of attack. Step by step design relation was brought out from outer loop (Thrust/Mach number) to inner loop (gas generator pressure). To meet the guidance requirement and design specification, the outer loop design relation generates the requirement of inner loop and to meet the outer loop requirement; the inner loop generates the requirement of actuator deflection to rotate the throat valve for changing gas generator pressure. The dynamics of gas generator along with aerodynamics are nonlinear in nature. Hence, dynamic inversion based control methodology was adopted for the design.
4. The above two loop design of fuel flow controller was carried out assuming ideal performance of air intake which provides compressed air flow. In practice, the performance of air intake plays a crucial role to provide adequate air mass flow rate in the combustion chamber for producing the thrust. In the presence of disturbance in upstream flow (combustion chamber) or downstream flow (gust in atmosphere), back pressure margin is affected and ramjet engine performance deteriorates due to intake instability. The behavior of

intake instability is characterized for air-to-air missile to control it. An innovative provision using feed forward dynamic inversion has been proposed to protect pressure margin of intake without the use of extra hardware. Feed forward based back pressure control loop needs to act very fast to capture the fast dynamics of buzz oscillation. So, the three loop structure based fuel flow controller was designed for meeting two objectives for stable operation of the ramjet engine.

- i. To keep back pressure margin within the design margin for avoiding intake instability and
- ii. To control air intake buzz oscillation when set in motion.
5. Six-Degree-of-Freedom (6-DOF) simulation platform of missile was carried out in which complete dynamics of missile was simulated along with Guidance & Control algorithm, Fuel flow controller and ramjet model. Fuel flow controller design was evaluated at different engagement scenarios along with aerial target from 0.5km altitude to 15km altitude with missile velocity varying from 2.2 Mach number to 3.2 Mach number under nominal and off-nominal conditions. The design stability was evaluated against ramjet engine uncertainties and missile perturbations.
6. Fuel flow controller design implementation and coding has been carried out using MATLAB software. However, the design validation of fuel flow controller for different engagements scenario in six-degrees-of-freedom are carried out using FORTRON software.

2.11 Thesis Organization

The thesis is organized in seven chapters. The following is a brief description of each chapter.

Chapter 1: Introduces the basic concept and requirements of solid based ramjet propulsion systems for development of air-to-air missile and it also describes the importance and necessity of fuel flow controller design.

Chapter 2: Presents a detailed literature review on the research topic focussing on past and present research. The literature reviewed various methods or techniques used for fuel flow controller design to meet thrust requirement. The literature review also reveals the intake instability and various techniques used to control it using external hardware. Later, the literature on dynamic inversion control techniques is also presented with relevant applications.

Following an extensive literature survey on the topic, the motivation for the proposed research work is presented and then the objective, contribution and organization of the thesis.

Chapter 3: The ramjet engine mathematical model is presented keeping in mind angle of attack. This model is used to design fuel flow controller for generating the required thrust. Buzz mathematical model of air intake is presented to evaluate the performance of ramjet systems in the presence of disturbance and this model is used to design an extra loop controller to avoid it. The air-to-air missile and aerial target mathematical model is also presented to provide suitable simulation platform to evaluate the ramjet performance at different engagement scenarios.

Chapter 4: The design specifications of fuel flow controller are specified based on guidance loop design of missile. Fuel flow controller design using Dynamic Inversion technique has been discussed. Design principles of all the loops have been explained and step by step design relation presented. Standalone performance of fuel flow controller results are presented for different Mach number (thrust) and the corresponding results of gas generator pressure, actuator deflection, throat area and mass flow rate have been discussed.

Chapter 5: The oscillatory behaviour of intake buzz has been analyzed for air-to-air missile configuration. Based on this analysis, requirement of back pressure loop design is discussed. Feed forward gain based dynamic inversion design is presented for fast control ensuring the stable operation of ramjet engine. Further, Standalone performance results are evaluated for different Mach numbers and the corresponding deviation in tracking performance is brought out. Apart from this, three loop designs which also keeps track of back pressure margin to avoid intake instability, is discussed in the chapter.

Chapter 6: The complete fuel flow controller design results have been evaluated in six-degrees-of-freedom simulation platform at different engagement scenarios along with aerial target from 0.5km altitude to 15km altitude and Mach number varying from Mach number 2.2 to Mach number 3.2. The design stability is evaluated against ramjet engine uncertainties and missile perturbation. The performance of guidance and autopilot results are also presented to bring out overall missile performance in the presence of fuel flow controller output.

Finally, the thesis concludes in **Chapter 7**. The chapter summarizes research contribution, findings and observations of the present work. Then it presents scope for future research based on the limitations of the present study.

2.12 Summary

In this chapter a general discussion on existing work relevant to the fuel flow controller for solid fuel ramjet propulsion system is presented. Controlling the fuel flow from gas generator to combustion chamber for producing desired thrust is the main area of interest. Existing research proposes various techniques and methods for fuel flow controller and has mostly focused on development of solid fuel ramjet propulsion for the purpose of ground testing. This chapter has included various research discussions on air intake instability like buzz, which needs extra control hardware to handle it. However, designing fuel flow controller for air-to-air missile applications is comparatively a new area of research due to varying operational scenarios and manoeuvrability constraints. Putting extra control hardware in air-to-air missile is difficult due to space constraint. So, handling intake instability through fuel flow controller for air-to-air missile makes the design further challenging. The typical challenges and the relevant literature on the development of solid fuel ramjet propulsion system have been presented in this chapter. Furthermore, the motivation, contribution and organization of the thesis are presented in this chapter.

Chapter 3

Mathematical Model of Solid Ramjet Engine, Air-to-Air Missile and Aerial Target

Chapter 3

Mathematical Model of Solid Ramjet Engine, Air-to-Air Missile and Aerial Target

3.1 Introduction

In order to realise an efficient and stable fuel flow controller, the behaviour of the complete ramjet engine under these operating conditions, especially the very tight interdependencies between actual flight variable, fuel mass flow, air intake stability and the missile dynamics, has to be understood and modelled. Moreover, the performance of ramjet propulsion system has to validate air-to-air engagement scenario. This chapter proposes a mathematical modelling of ramjet engine including intake, six-degrees-of-freedom (6-DOF) missile modelling and point mass modelling of aerial target. The objectives of mathematical modelling are, (i) It helps to characterize the ramjet engine at different operating condition, (ii) find out the algebraic relation between throttle valve area, gas generator and fuel flow rate and (iii) find out the relation between missile parameters and engine dynamics. The outer loop Mach number dynamic and inner loop gas generator dynamic have been formulated for designing an efficient fuel flow controller. Moreover, the scheduling of controller gain and desired response for air-to-air missile application has become feasible after characterisation of ramjet engine variable along with missile variables. Fuel flow controller for solid fuel ramjet propulsion requires validation in air-to-air missile against the aerial target. So, six-degrees-of-freedom (6-DOF) modelling of ramjet missile and point mass modelling of aerial target have been also presented to provide an interacting platform for fuel flow controller validation.

3.2 Mathematical Modelling of Ramjet Engine

The basic design objective of ramjet engine is to meet the thrust requirement as a function of altitude and Mach number for a high speed supersonic long range air-to-air missile. A ramjet engine is an air-breathing combustion system consisting of a gas generator housing the solid

propellant, a throttle valve which regulates fuel flow rate into the secondary combustion chamber and an air intake system. The function of a gas generator is to provide oxidizer deficient fuel in appropriate form to combustion chamber, where the main combustion process occurs by a mixture of the compressed air, which then generates thrust. So the modelling of ramjet engine components as shown in figure 3.1 is done. Combustion engine dynamics provides thrust based on fuel flow rate, static pressure and temperature.

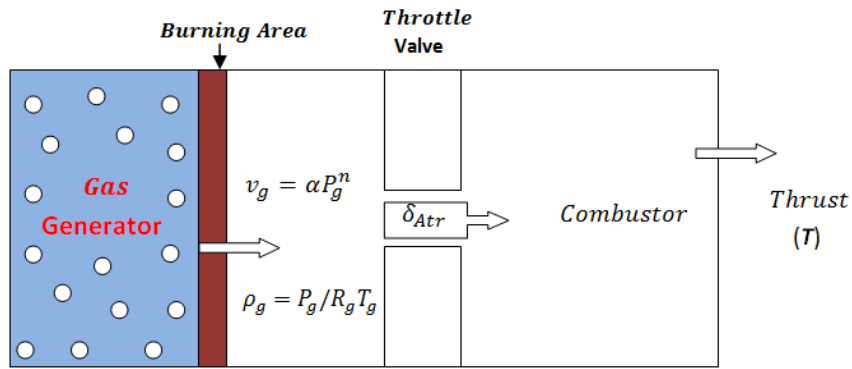


Figure-3.1: Schematic diagram of ramjet engine

Basically, throttle valve opens through the fuel flow actuator based on the error generated by Mach number control loop to release fuel flow rate. Generation of fuel flow rate depends on dynamic condition of gas generator [25-26, 36]. The working principle of fuel flow rate control depends on the following conditions

1. When the throttle area reduces, it will increase the gas generator pressure and the fuel flow rate of gas increases.
2. Burning rate of solid propellant in gas generator is proportional to the chamber pressure of gas generator.
3. So, reduction of throttle valve area through actuator will generate more gas burning and produce more fuel flow rate.

The gas generator propellant designed as a cigarette burning with a constant area (A_g) has:

$$\dot{m}_g = \rho_g A_g v_g \quad (3.1)$$

Where, $\rho_g = P_g / R_g T_g$ is the density of gases propellant and $\nu_g = \alpha_g P_g^n$ is the burn rate of the propellant.

The variation of gas generator volume is:

$$\dot{V}_g = A_g \nu_g \quad (3.2)$$

In gas generator burning progress of the propellant vacant free volume of gas generator and it will be filled with hot gases. Then the gas starts flowing from the gas generator to the combustion area through the throttle valve.

Now, the flow fuel rate of gas through the throttle valve is:

$$\dot{m}_{flow} = \frac{p_g A_{tr}}{C_g} \quad (3.3)$$

Where, C_g is characteristic velocity of solid propellant. Then, Incremental change in fuel flow rate is

$$\Delta \dot{m}_{flow} = \frac{p_{g0} \Delta A_{tr}}{C_g} + \frac{A_{tr0} \Delta p_g}{C_g} \quad (3.4)$$

Where, A_{tr} is a function of throttle valve opening area.

The gas generator dynamics is given by,

$$\dot{P}_g = \frac{R_g T_g}{V_g} (\dot{m}_g - \dot{m}_{flow}) \quad (3.5)$$

Incremental relation can be obtained from the above relation

$$\dot{P}_g = \frac{R_g T_g}{V_g} (\rho_g A_g \alpha p_{g0}^{n-1} \Delta P_g - \frac{p_{g0} \Delta A_{tr}}{C_g} - \frac{A_{tr0} \Delta p_g}{C_g}) \quad (3.6)$$

Gas generator propellant is designed as cigarette burning, so the characteristic velocity of solid propellant C_g is constant. And from the above equation, gas flow rate capacity can be written as:

$$\frac{\dot{m}_{max}}{\dot{m}_{min}} = \left(\frac{A_{tr_max}}{A_{tr_min}} \right)^{\frac{n}{n-1}} \quad (3.7)$$

From the above equation, it may be included that the gas flow capacity depends on the propellant characteristic regardless of the throttle area ratio.

Now, gas generator dynamics is:

$$\dot{P}_g = \frac{R_g T_g}{V_g} (\rho_g A_g \alpha p_{g0}^{n-1} \Delta P_g - \frac{p_{g0} \Delta A_{tr}}{C_g} - \frac{A_{tr0} \Delta p_g}{C_g}) \quad (3.8)$$

$$\Delta \dot{m}_{flow} = \frac{p_{g0} \Delta A_{tr}}{C_g} + \frac{A_{tr0} \Delta p_g}{C_g} \quad (3.9)$$

Longitudinal equation of missile motion is defined by Newton's law

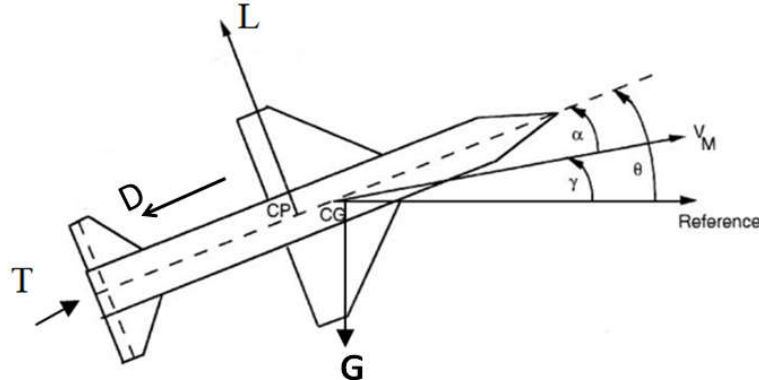


Figure-3.2: Representation of missile forces and orientation diagram

$$m \frac{dV}{dt} = T + L + D + G \quad (3.10)$$

Where 'm' is mass of missile, V_M is the missile velocity, T is the thrust force, G is gravity force, L and D is the lift and drag force of missile as a function of Mach and angle of attack. Gravity is a minor factor and can be ignored.

The equation can be re-written as;

$$mV_a \Delta M = \Delta T - \frac{n}{2} P_s (C_D \cos \alpha + C_L \sin \alpha) \Delta M \quad (3.11)$$

Induce Drag and Drag force are:

$$L = \frac{n}{2} P_s C_L \Delta M \quad \text{and} \quad D = \frac{n}{2} P_s C_D \Delta M \quad (3.12)$$

For an isentropic fluid,

$$V_a = \sqrt{n \frac{P_s}{\rho}} \quad (3.13)$$

Thrust generated by engine

$$T = f(P_s, T_s, M, \alpha, m_{flow}) \quad (3.14)$$

Where, P_s and T_s are static pressure and temperature respectively.

Linearization of a thrust equation can be written as

$$\Delta T = \frac{\partial T}{\partial \dot{m}_g} \cdot \Delta \dot{m}_g + \frac{\partial T}{\partial M} \cdot \Delta M \quad (3.15)$$

After solving the above equation, the thrust model is:

$$\Delta \dot{M} = \frac{A_{tro}}{V_a m C^*} \frac{\partial T}{\partial \dot{m}_g} \Delta p_g + \frac{p_{ro}}{V_a m C^*} \frac{\partial T}{\partial \dot{m}_g} \Delta A_{tr} + \frac{1}{m \cdot V_a} \left(\frac{\partial T}{\partial M} - \frac{n}{2} p_s S (C_D \cos \alpha + C_L \sin \alpha) \right) \Delta M \quad (3.16)$$

3.3 Intake BUZZ Modelling

Buzz Modelling

The dynamic model of intake is the updating of the combustion chamber/back pressure P_c based on the mass accumulation in the combustion chamber, i.e., the difference between the fuel plus air mass entering the combustion chamber and the gas mass exiting at the choked nozzle throat. This relation follows for compression systems [54,71]:

$$\dot{P}_c = \frac{1}{B_p} (\dot{m}_c - \dot{m}_{th}) \quad (3.17)$$

Where, \dot{m}_c is the mass of the fuel and air entering the combustion chamber, \dot{m}_{th} is the mass of the air exiting from the exit nozzle throat and B_p is the back pressure factor given by:

$$B_p = \int \frac{1}{\gamma R T(x)} A_{cch} \quad (3.18)$$

Where, γ is a specific heat ratio, R is a specific gas constant, $T(x)$ is the static temperature as a function of x which is the distance ranging from the fuel injection point to the exit nozzle throat and A_{cch} is the area of cross section of the combustor.

Using Mass conservation and assuming ideal conditions in between combustor exit and nozzle throat, we recast the equation as:

$$\dot{m}_{th} = \frac{\beta A_{th} P_{oth}}{\sqrt{T_{oth}}} \quad (3.19)$$

Where, A_{th} is the throat area at the exit nozzle,

P_{oth} is the total pressure at the exit nozzle throat and T_{oth} is the total temperature at the exit nozzle throat and β is a constant given by:

$$\beta = \sqrt{\frac{\gamma}{R} \left(\frac{2}{\gamma+1} \right)^{\frac{\gamma+1}{\gamma-1}}} \quad (3.20)$$

T_{oth} is the maximum temperature at the combustor exit which is a constant value and under ideal conditions, the static pressure at the throat is equal to the combustor pressure. Using isentropic relation, the total pressure at the exit nozzle throat ($M = 1$) is given by:

$$\frac{P_{th}}{P_{0th}} = \left(\frac{\gamma+1}{2} \right)^{\frac{\gamma}{\gamma-1}} \quad (3.21)$$

Using (3.21), we can rewrite (3.19) as ,

$$\dot{m}_{th} = \frac{\beta A_{th}}{\sqrt{T_{0th}}} \left(\frac{\gamma+1}{2} \right)^{\frac{\gamma}{\gamma-1}} P_c \quad (3.22)$$

Now, for change in P_c equation (3.17) can be written as,

$$\Delta \dot{P}_c = \frac{1}{B_p} \left[(1+f) \Delta \dot{m}_a - \frac{\beta A_{th}}{\sqrt{T_{0th}}} \left(\frac{\gamma+1}{2} \right)^{\frac{\gamma}{\gamma-1}} \Delta P_c \right] \quad (3.23)$$

Where, f is the ratio of fuel to the intake air mass and \dot{m}_a is the intake air mass.

The difference between the combustion pressure and the intake pressure behind the terminal shock gives rise to spillage in intake air mass. This can be formulated as:

$$\dot{m}_a = \frac{A_i}{L_i} (\Delta P_t - \Delta P_c) \quad (3.24)$$

Where A_i and L_i are the effective intake cross section area and length of the intake duct. P_t is the intake pressure behind the terminal shock. P_∞ is the atmospheric pressure.

The pressure behind the terminal shock is determined by the incoming Mach number and free stream static pressure. Using the normal shock relation P_t can be written as,

$$P_t = P_\infty \frac{2\gamma M^2 - (\gamma-1)}{\gamma+1} \quad (3.25)$$

Using this relation, the change in the back pressure can be written as:

$$\Delta P_t = P_\infty \frac{4\gamma M}{\gamma+1} \Delta M \quad (3.26)$$

Using (3.25), equation (3.24) can be written as:

$$\Delta \ddot{m}_a = \frac{A_i}{L_i} \left(P_\infty \frac{4\gamma M}{\gamma+1} \Delta M_t - \Delta P_c \right) \quad (3.27)$$

Combining (3.26) and (3.27) the equations can be written in matrix form as follows,

$$\begin{bmatrix} \Delta \dot{P}_c \\ \Delta \ddot{m}_a \end{bmatrix} = \begin{bmatrix} \frac{\beta A_{th}}{B \sqrt{T_{0th}}} \left(\frac{\gamma+1}{2} \right)^{\frac{\gamma}{\gamma-1}} & \frac{1+f}{B} \\ -\frac{A_i}{L_i} & 0 \end{bmatrix} \begin{bmatrix} \Delta P_c \\ \Delta \dot{m}_a \end{bmatrix} + \begin{bmatrix} 0 \\ \frac{A_i}{L_i} P_\infty \frac{4\gamma M}{\gamma+1} \end{bmatrix} \Delta M \quad (3.28)$$

3.4 Six-DOF Model of Solid Ducted Ramjet Air-to-Air Missile

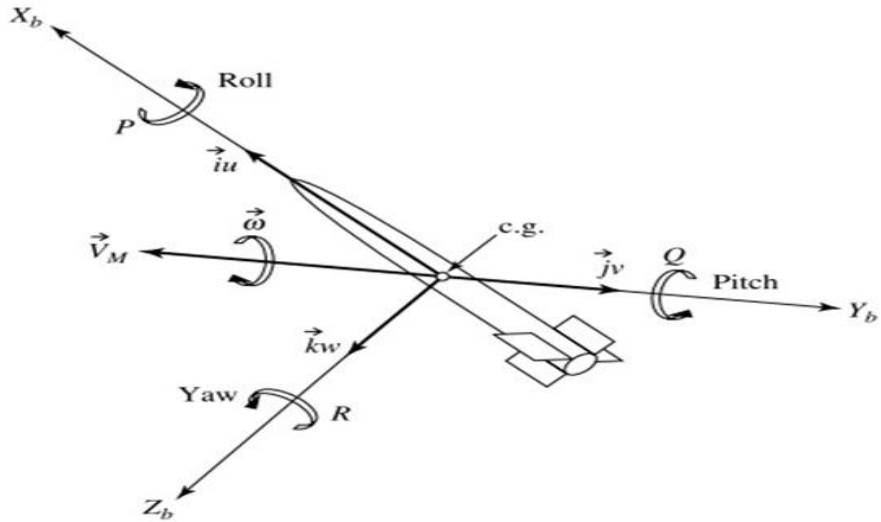


Figure-3.3: Representation of 3-moment (body rate) and 3-force (acceleration)

The missile has six degrees of freedom motions in which three translations and three rotations, along and about the missile (X_b, Y_b, Z_b) axes. These motions of missile are shown in figure 3.3.

The total velocity of missile (V_m) has components U, V, and W along the missile (X_b, Y_b, Z_b) respectively. The missile's angular velocity vector ω has components P, Q and R about (X_b, Y_b, Z_b) axes, respectively [1, 3]. The translations acceleration of the missile in three axis are given below:

$$\begin{bmatrix} \dot{U} \\ \dot{V} \\ \dot{W} \end{bmatrix} = \begin{bmatrix} \frac{(T_x - F_{xaero})}{mass} + g_x + QW - RV \\ \frac{(T_y - F_{yaero})}{mass} + g_y + RV - PW \\ \frac{(T_z - F_{zaero})}{mass} + g_z + PV - QU \end{bmatrix} \quad (3.29)$$

Where, $\begin{bmatrix} T_x & T_y & T_z \end{bmatrix}$ and $\begin{bmatrix} F_{xaero} & F_{yaero} & F_{zaero} \end{bmatrix}$ are thrust and aerodynamics forces along the missile (X_b, Y_b, Z_b) body axes, respectively.

The aerodynamics forces depend on missile dynamic pressure (Q), surface area of missile (S), angle of attack (α) and fin deflection (δ) of missile actuator. The relationship of these force with aerodynamics coefficient is given below.

$$\begin{bmatrix} F_{xaero} \\ F_{yaero} \\ F_{zaero} \end{bmatrix} = QS^* \begin{bmatrix} C_{x0} & C_x(\alpha) & C_x(\delta) \\ C_y(\alpha) & C_y^{dyn} & C_y(\delta) \\ C_z(\alpha) & C_z^{dyn} & C_z(\delta) \end{bmatrix} \quad (3.30)$$

g_x, g_y and g_z are the components of gravity (g) in body axis and given by:

$$\begin{bmatrix} g_x \\ g_y \\ g_z \end{bmatrix} = (C_i^b)_m \begin{bmatrix} -g \\ 0 \\ 0 \end{bmatrix} \quad (3.31)$$

Here, $(C_i^b)_m$ is the DCM matrix from inertial to body frame and given by:

$$(C_i^b)_m = \begin{bmatrix} (q_4^2 + q_1^2 - q_2^2 - q_3^2) & 2(q_1q_2 + q_3q_4) & 2(q_1q_3 - q_2q_4) \\ 2(q_1q_2 - q_3q_4) & (q_4^2 - q_1^2 + q_2^2 - q_3^2) & 2(q_1q_3 + q_1q_4) \\ 2(q_1q_3 + q_2q_4) & 2(q_2q_3 - q_1q_4) & (q_4^2 - q_1^2 - q_2^2 + q_3^2) \end{bmatrix} \quad (3.32)$$

The dynamics of the body frame quaternion components, (q_1, q_2, q_3, q_4) , where (q_1, q_2, q_3) define the principal vector and (q_4) is the magnitude of rotation, are given by the following sets of differential equations.

$$\begin{bmatrix} \dot{q}_1 \\ \dot{q}_2 \\ \dot{q}_3 \\ \dot{q}_4 \end{bmatrix} = \frac{1}{2} \begin{bmatrix} q_4 p + q_3 q + q_2 r \\ q_3 p + q_4 q - q_1 r \\ -q_2 p + q_1 q + q_4 r \\ -q_1 p - q_2 q - q_3 r \end{bmatrix} \quad (3.33)$$

The body rates dynamics in three axis of missile can be written as:

$$\begin{bmatrix} \dot{P} \\ \dot{Q} \\ \dot{R} \end{bmatrix} = \begin{bmatrix} \frac{1}{I_x} \left[l_{aero} - I_x P \right] + \frac{1}{I_x} \left[(I_y - I_z) R Q \right] \\ \frac{1}{I_y} \left[m_{aero} - I_y Q \right] + \frac{1}{I_y} \left[(I_z - I_x) R P \right] \\ \frac{1}{I_z} \left[n_{aero} - I_z R \right] + \frac{1}{I_z} \left[(I_x - I_y) P Q \right] \end{bmatrix} \quad (3.34)$$

Where, $[I_x \ I_y \ I_z]$ and $[l_{aero} \ m_{aero} \ n_{aero}]$ are moment of inertial and aerodynamic moments along the missile (Xb, Yb, Zb) body axes, respectively.

The aerodynamic moment depends on the missile dynamic pressure (Q), surface area of missile (S), angle of attack (α) and fin deflection (δ) of missile actuator.

$$\begin{bmatrix} l_{xaero} \\ m_{yaero} \\ n_{zaero} \end{bmatrix} = QSD * \begin{bmatrix} C_l(\alpha) & C_l dyn & C_l(\delta) \\ C_m(\alpha) & C_m dyn & C_m(\delta) \\ C_n(\alpha) & C_n dyn & C_n(\delta) \end{bmatrix} \quad (3.35)$$

3.5 Point Mass Model of Aerial Target

A point mass model has been considered for target dynamic. X, Y and Z are the target positions in NED frame and V_t is the target velocity. ψ and γ are the heading angle and flight path angle [3]. η_y and η_z are the lateral acceleration in yaw and pitch plane of aerial target as shown in figure 3.4.

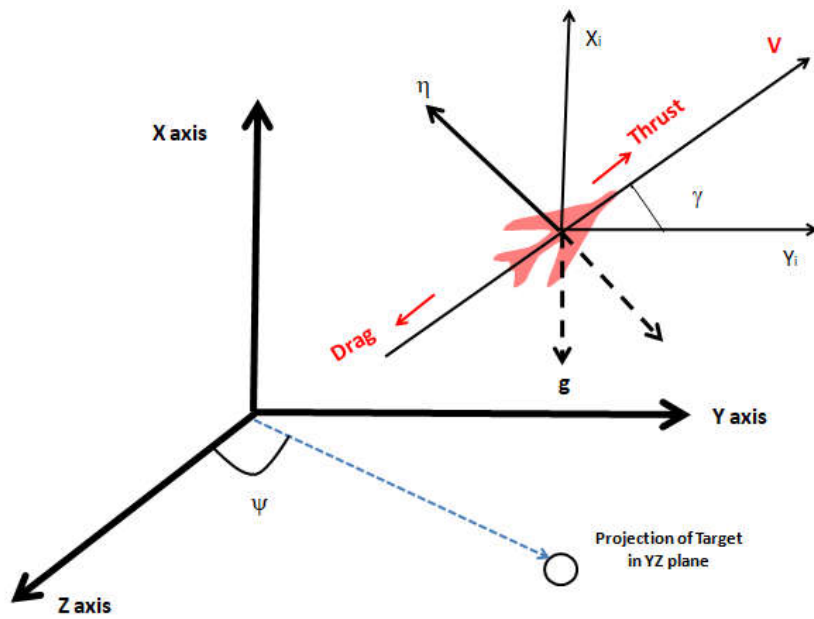


Figure-3.4: Representation of point mass motion of aerial target

$$\dot{V}_t = \frac{(Thrust - Drag)}{m_t} - g \times \sin \gamma \quad (3.36)$$

$$\dot{\gamma} = \frac{\eta_z - g \times \cos \gamma}{V} \quad (3.37)$$

$$\dot{\psi} = \frac{\eta_y}{V \cos \gamma} \quad (3.38)$$

$$\dot{X} = V \times \sin \gamma \quad (3.39)$$

$$\dot{Y} = V \times \sin \psi \times \cos \lambda \quad (3.40)$$

$$\dot{Z} = V \times \cos \psi \times \cos \gamma \quad (3.41)$$

3.6 Summary

This chapter presented the mathematical model of solid fuel ramjet engine, intake, air-to-air missile and aerial target. Solid fuel ramjet engine was proposed keeping in mind angle of attack. It is a very realistic model to design fuel flow controller for air-air missile application. Angle of attack is a prominent missile variable which can affect engine produced thrust to compensate the drag force. This realistic model of ramjet engine is nonlinear in nature and will help design an efficient nonlinear fuel flow controller and gains scheduling technique. Intake model is presented to simulate the instability created by disturbance into the intake duct. Buzz oscillatory instability in intake is very dangerous and it can damage the structure integrity of ramjet engine. This modelling helps to bring out the buzz frequency as a function of altitude and Mach number of air-to-air missile and this information helps to generate fuel flow actuator requirement. Mathematical model of missile and target have been used to validate three loop fuel flow controller design in different engagement of air-to-air missile to ensure miss-distance performance of the missile.

Chapter 4

Two loop Fuel Flow Controller Design for Efficient operation of Solid Fuel Ducted Ramjet Engine

Chapter 4

Two loop Fuel Flow Controller Design for Efficient operation of Solid Fuel Ducted Ramjet Engine

4.1 Introduction

Recently, solid fuel ramjet propulsion system has become a dominant propulsion system for missile application, especially for long range beyond visual range (BVR) air-to-air missile. Fuel flow controller is an algorithm which uses effectively energetic of ramjet propulsion for air-to-air missile application. The following aspects are important to understand while designing fuel flow controller: (i) generation of specification or requirement of controller under missile manoeuvring condition as a function of altitude and Mach number, (ii) the controller technique to be used for nonlinear characteristic of ramjet system and (iii) inherent characteristic of controller meeting design specification as a function of altitude and Mach number. This chapter proposes an efficient nonlinear dynamic inversion technique based fuel flow controller to effectively use ramjet energetic as a function of altitude and Mach number against non-manoeuvring and manoeuvring aerial target. The topic of research is an ongoing project at Defence Research and Development Organisation (DRDO); the results of engine parameter normalized are confidential.

4.2 Fuel Flow Controller Specification for Air-to-Air Missile

Ramjet missile has to engage aerial target from low altitude to high altitude. Based on target manoeuvre capability as a function of altitude and Mach number, proportional navigation (PN) based guidance generates legitimate lateral acceleration demand in presence of autopilot

$(T_{ap} + \frac{2\zeta_{ap}}{\omega_{ap}})$, seeker (T_{seeker}) and estimator ($T_{estimator}$) lag to intercept the target for a given range-to-go as shown in figure 4.1. $R_{min}(H)$ is minimum range-to-go, while $V_T(H)$ and $\eta_T(H)$ are target speed and manoeuvre as a function of altitude. PN guidance collision course works optimally for constant velocity. Autopilot lag (T_{ap}) depends on missile normal force coefficient, altitude, Mach number and angle of attack. In general, configuration of missile design is carried

out to satisfy guidance demand and autopilot time constant. During engagement, air-to-air missile velocity reduces due to the build up of angle of attack (induce drag) while meeting lateral accelerate demand. Reduction in velocity further increases the angle of attack and increased angle of attack again increases the drag forces. So, it would further lead to reduction in missile velocity and manoeuvring capability of the missile. Finally, miss-distance (The distance at which the warhead of a missile can be expected to damage seriously the target) requirement is affected for engaging the target.

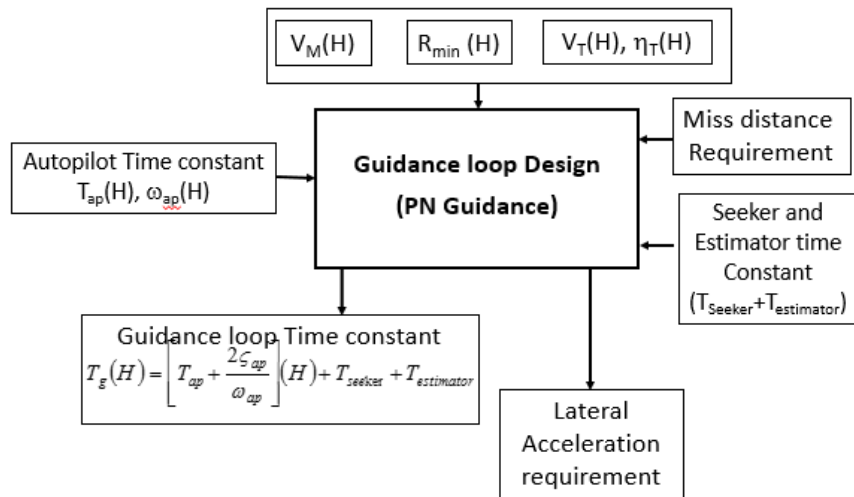


Figure-4.1: Schematic diagram of guidance loop

Guidance loop time constant for constant velocity for engagement trajectory has been worked out as a function of altitude and Mach number as shown in table 4.1 [1, 4].

Guidance loop time constant:

$$T_g = \left[T_{ap} + \frac{2\zeta_{ap}}{\omega_{ap}} \right] + T_{seeker} + T_{estimator} \quad (4.1)$$

Table 4.1: Guidance loop time constant as a function of altitude and Mach number

S. No	Altitude (km)	Mach number (M)	Autopilot time Constant (sec)	Guidance loop time constant (sec)
1.	0.5	2.2	0.1	0.30
2.	5.0	2.4	0.2	0.45
3.	10.0	2.8	0.5	0.70
4.	15.0	3.2	0.8	1.00

Using the parameters given, guidance loop simulation model with seeker lag, estimator lag and autopilot lag as shown in figure 4.2 have been carried out to bring normalized homing time for the desired miss-distance of missile at each altitude.

$$\text{Normalised Homing Time (NHT)} = \frac{T_{to_go}}{T_g} \quad (4.2)$$

Where, T_{to_go} is the total duration when target start manoeuvre.

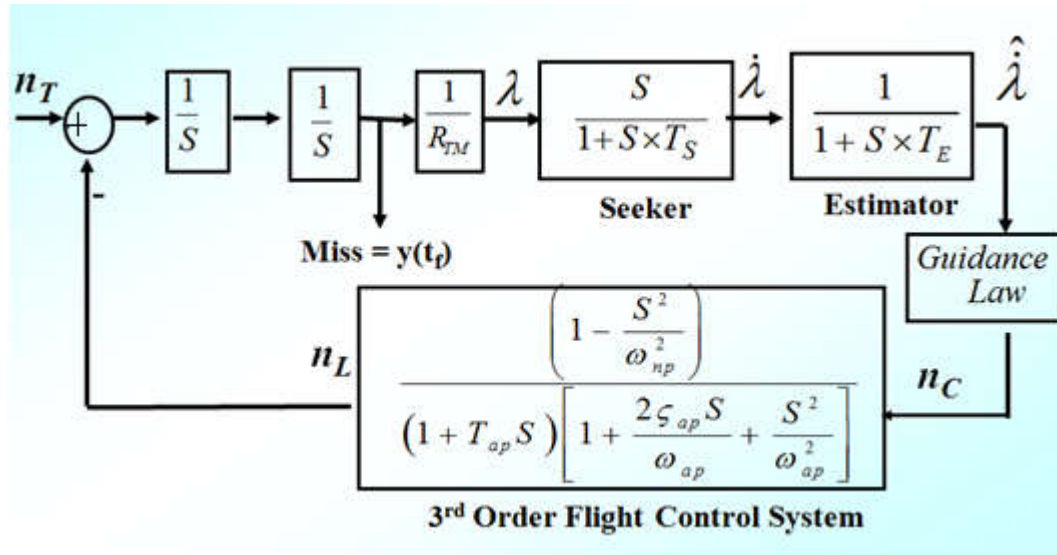


Figure-4.2: Simulation model of guidance loop

A typical scenario is considered with constant missile velocity as a function of altitude and target manoeuvre at the start of guidance loop. The simulation result is shown in figure 4.3. The following conclusions have been reached:

1. It is found that even though the guidance time constant can vary with respect to altitude, if the missile velocity can be constant during the homing phase for PN guidance, the normalised homing time (NHT) is the same for ensuring miss-distance of missile.
2. In terminal/homing guidance phase, if the missile is manoeuvring and the missile velocity can decrease due to the angle of attack, the rate of change of velocity needs to be compensated along with guidance time constant.

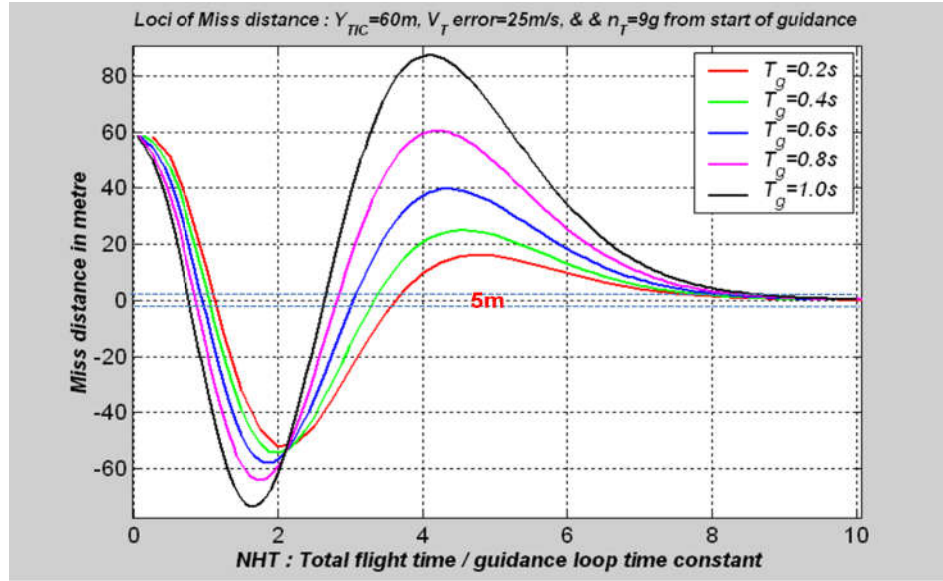


Figure-4.3: Normalized homing time requirement for miss-distance at different altitude

Therefore, Speed of response of fuel flow controller (T_{ffc}) is the same as guidance time constant (T_g) as a function of altitude to maintain constant velocity.

$$T_{ffc}(H) = T_g(H) \quad (4.3)$$

So, the fuel flow controller time constant/ speed of response has been calculated based on the above relation and given in table 4.2.

Table 4.2: Fuel flow controller time constant as a function of altitude and Mach number

S. No	Altitude (km)	Mach number (M)	Autopilot time Constant (sec)	Guidance loop time constant (sec)	Fuel flow controller time constant (sec)
1.	0.5	2.2	0.1	0.30	0.30
2.	5.0	2.4	0.2	0.45	0.45
3.	10.0	2.8	0.5	0.70	0.70
4.	15.0	3.2	0.8	1.00	1.00

To achieve speed of response of fuel flow controller as a function of altitude, actuator bandwidth requirement can be computed based on the minimum time constant of fuel flow controller. Minimum time constant requirement of controller would be computed for low altitude

engagement scenario. Fuel flow controller has two loop based structures for producing velocity. Based on loop separation theory, 4 time separation needs between thrust loops (Outer) to pressure loop (Inner). However;

$$\text{Gas pressure loop bandwidth} = \frac{4}{T_{ffc_min}} \quad (4.4)$$

Where, T_{ffc_min} is fastest time constant requirement at low altitude.

Further, fuel flow actuator situated in the inner loop of pressure loop results in faster dynamics. So 4-5 times separation is to be ensured for actuator for loop separation. Thus:

$$\text{Actuator bandwidth} = \frac{16 - 20}{T_{ffc_min}} \quad (4.5)$$

Generally, outer loop (Mach number loop) bandwidth varies from 1.0Hz to 3.0Hz, so inner loop (gas generator pressure loop) requires bandwidth of around 4Hz to 12Hz and actuator bandwidth requirement of a two loop fuel flow controller will be 20Hz to 45Hz.

4.3 Nonlinear Dynamic Inversion Based Control

The basic concept behind time scale separation NDI controller is to follow commanded input with the desired fastness and accuracy when the original plant can be thought of as one fast dynamic and one slow dynamics. It can be achieved by inverting the governing equations of the individual dynamics based on measured state and input command [111, 118-120, 147].

If the nonlinear system is written as:

$$\dot{x} = F(x, u) \quad (4.6)$$

Using time scale separation, fast state and slow state can be separated as:

$$\dot{x}_s = f_s(x) + g_s(x)x_f \quad (4.7)$$

$$\dot{x}_f = f_f(x) + g_f(x)u \quad (4.8)$$

Where, $x = [x_s, x_f]$, are slow and fast state variables respectively.

The above equation clearly shows that for slow state dynamics, fast state dynamics appears as input. The following equation can be written from out of plant as follows:

$$\dot{Y} = \frac{\partial y}{\partial x_s} \dot{x}_s = \frac{\partial y}{\partial x_s} f_s + \Delta_s x_f \quad (4.9)$$

where, $\Delta_s = \frac{\partial y}{\partial x_s} g_s(x)$

Now based on desired output and sensed output, the desired output dynamics can be designed as;

$$\dot{Y}_d = f(Y_d, Y, \omega_s, \xi_s) \quad (4.10)$$

Where, ω_s and ξ_s are the desired natural frequency and damping of outer loop or slowly varying output control loop. Based on the desired dynamics of slow states, desired input to faster dynamics can be obtained from equation-21 as;

$$x_{fd} = \Delta_s^{-1}(\dot{Y}_d - \frac{\partial Y}{\partial x_s} f_s) \quad (4.11)$$

Here, Δ_s must be invertible. Now the desired fast state is used to design the desired fast state dynamics as:

$$\dot{x}_{fd} = f(x_{fd}, x_f, \omega_f, \xi_f) \quad (4.12)$$

Now fast dynamics is inverted to obtain control input as:

$$u = g_f(x)^{-1}(\dot{x}_{fd} - f_f(x)) \quad (4.13)$$

4.4 Two Loop Fuel Flow Controller Design using Non-linear Dynamic Inversion

Figure 4.4, shows the loop architecture designed of fuel flow controller for ramjet propulsion system. It is having two loop structure an outer loop and an inner loop. The outer loop is called a thrust control loop and having slow dynamics characteristic. Inner loop is called pressure control loop and has fast dynamic characteristic. The dynamic inversion control design approach presented here exploits the time scale separation that inherently exists in ramjet engine dynamics. The outer loop inversion controller uses the states of fast dynamics to control those of slow dynamics, and the inner loop inversion controller uses the control throttle area to control the states of fast dynamics. In this approach, gas generator pressure is identified as fast dynamic response while Mach number is characterized as slow state variable. The gas generator pressure strongly depends on the throttle area of valve. Thus, to start with, a fast state controller for gas generator was designed. Having designed a fast-state controller, a separate, approximate inversion procedure was carried out to design the slow state controller for Mach number. It may be noted that, such a model reduction was possible as there is significant difference in the time scale between the fast and slow state in the open loop dynamic of solid fuel ramjet engine.

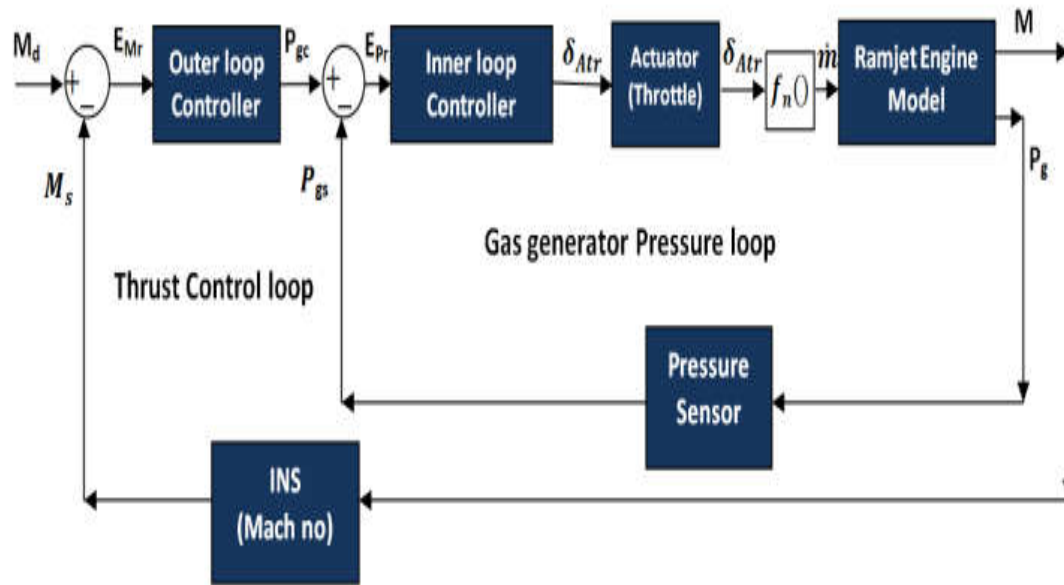


Figure-4.4: Block diagram of two loop fuel flow controller

Outer Loop Design:

The Outer control loop takes the requirement from guidance loop to achieve the velocity and speed of response.

The desired dynamics is:

$$\dot{M}_g = \omega_{outer}(M_d - M_s) \quad (4.14)$$

Where, $\omega_{outer} = 1/T_{ffc}$ time constant of outer loop.

So, the demanded gas generator pressure can be computed as (chapter 3):

$$P_{gc} = \frac{\Delta \dot{M}_g - \frac{1}{m \cdot V_a} \left(\frac{\partial T}{\partial M} - \frac{n}{2} p_s S (C_D \cos \alpha + C_L \sin \alpha) \right) \Delta M_g}{\frac{A_{tro} \frac{\partial T}{\partial m}}{V_a m C^* \partial m_g}} \quad (4.15)$$

Where, $T_{ffc} = f(V_m, H, \text{mass}, C_{n\alpha}, T_f)$, $C_{n\alpha}$ & mass depends on missile configuration and V_m and H (altitude) on trajectory. T_f is tuning factor which depends on guidance phase.

Inner Loop Design:

Gas generator pressure control loop receive the requirement from outer loop. To meet, the desire dynamic condition, the equation can be written as:

$$\dot{P}_{gc} = -2\xi_g \omega_g P_{gs} + \omega_g^2 \int (P_{gs} - P_{gc}) dt \quad (4.16)$$

Where, ξ_g and ω_g ($\sim 3.5\omega_{outer}$) is the required damping ratio and speed of response (natural frequency) of inner loop which is scheduled based on time scale separation between fast loop to slow loop. P_{gc} and P_{gs} are commanded and sense gas generator pressure respectively.

So, from chapter 3, the demanded throttle open area is:

$$\Delta A_{tr} = \frac{\Delta P_g - [\frac{R_g T_g}{V_g} (\rho_g A_g \alpha p_{go}^{n-1}) + \frac{A_{tr0}}{c_g}]}{\frac{p_{go}}{c_g}} \quad (4.17)$$

Throttle area incremental opening ensures the requirement of fuel flow rate to fulfil the desired Mach number or missile velocity.

It should be ensured that ramjet propulsion works reliably with the designed fuel flow controller to ensure time domain performance like steady state (within $\pm 2.0\%$) of all flight engagement conditions.

4.5 Scheduling of Controller Gains

Two loop nonlinear dynamic inversion fuel flow controller has to perform from low altitude to high altitude and at different Mach numbers. The missile aerodynamic behaviour and inertial parameters keep on the changing based on operating condition. To accommodate the dynamic behaviour of missile and the corresponding thrust requirement, the controller gain will be scheduled based on these parameters. So, generic scheduling based on two loop fuel flow controller is designed as shown in figure 4.5. It is difficult to meet this requirement if controller gains are not determined based on these parameters. The comparison of scheduled gain and fixed gain are shown in section 4.6.

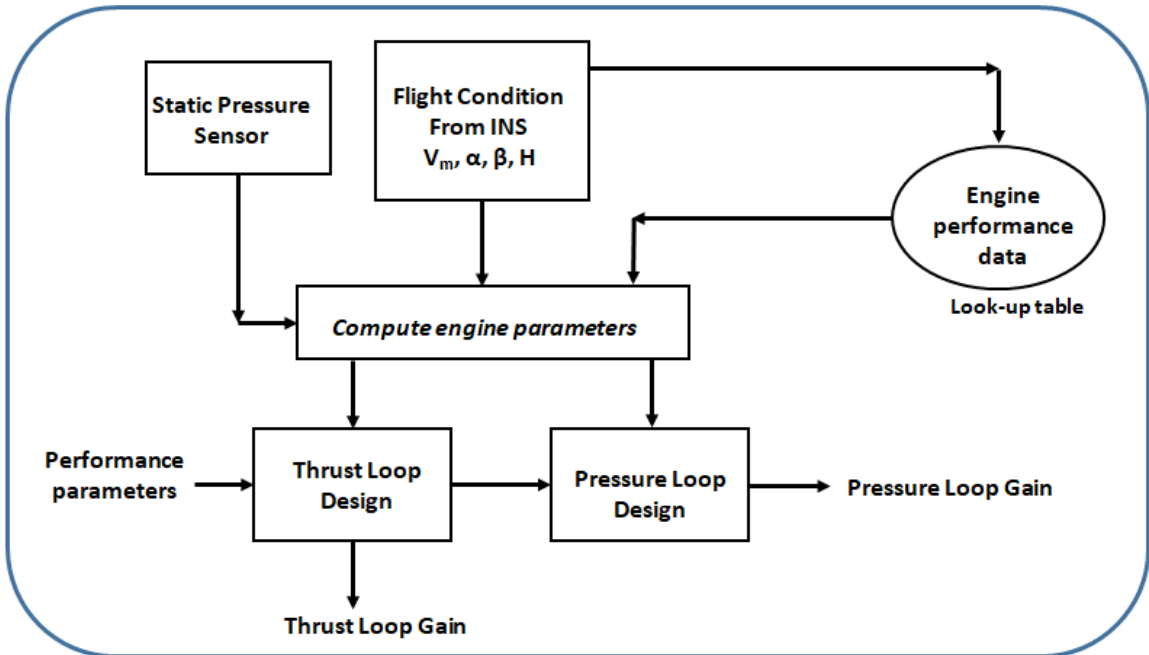


Figure-4.5: Block diagram of scheduling two loop fuel flow controller gain

4.6 Standalone Results and Analysis of Two Loop NDI Fuel Flow Controller

In this section, a two loop non-linear dynamic inversion based fuel flow controller and ramjet engine modeling was carried out in simulation environment in ideal condition (isotropic gas assumption) with actuator model, pressure sensor model and INS model. Simulations were carried out to show the performance of NDI based fuel flow controller for meeting the Mach number demand at low altitude and high altitude scenario. Speed of response (T_{ffc}) was computed based on missile operating conditions as a function of altitude and missile operating Mach number. The dynamic second order models of actuator, INS and pressure sensor are given below, which was used to simulate two loop fuel flow controller. All results like Mach number, gas generator pressure, throttle area and time were normalized.

Actuator Linear Model: Actuator was modelled as a second order equation with an un-damped natural frequency of ω_{ACT} and damping factor of ζ_{ACT} . The differential equation is:

$$\ddot{\delta} = -\omega_{ACT}^2 \dot{\delta} - (2\zeta_{ACT}\omega_{ACT})\delta + \omega_{ACT}^2\delta_0 \quad (4.18)$$

Inertial Navigation Sensor (INS) Model: Inertial Navigation sensor provides missile velocity. INS is modelled as a second order equation with un-damped natural frequency of ω_{INS} and damping factor of ζ_{INS} . The differential equation is:

$$\ddot{\delta} = -\omega_{INS}^2 \delta - (2\zeta_{INS} \omega_{INS})\delta + \omega_{INS}^2 \delta_0 \quad (4.19)$$

Pressure Sensor Model: Pressure sensor provides gas generator pressure of ramjet engine. Pressure sensor is modelled as a second order equation with un-damped natural frequency of ω_{GGP} and damping factor of ζ_{GGP} . The differential equation is:

$$\ddot{\delta} = -\omega_{GGP}^2 \delta - (2\zeta_{GGP} \omega_{GGP})\delta + \omega_{GGP}^2 \delta_0 \quad (4.20)$$

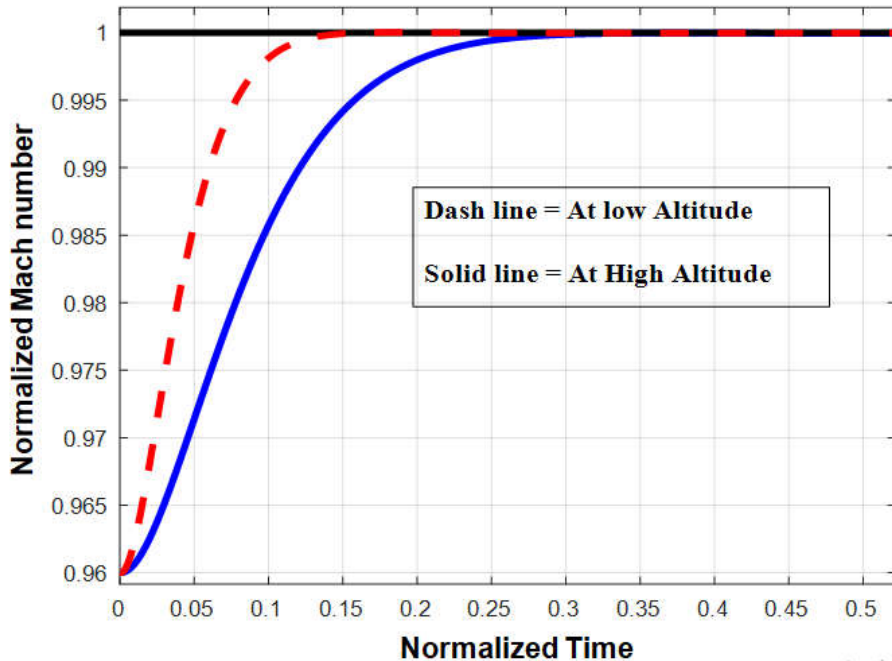


Figure-4.6: Mach number performance of two loop NDI fuel flow controller at low and high altitude

Figure 4.6 shows the performance comparison of two loop fuel flow controller of Mach number. The speed or time constant of response at low altitude is faster than at high altitude for the same parameters. It also shows that the controller gain scheduling has been done as function of altitude to meet the demand. The corresponding gas generator pressure performance is shown in figure 4.7 and 4.8 for low altitude and high altitude. Similarly, throttle valve area and fuel mass rate performance are shown in figure 4.9 and 4.10 for low altitude and high altitude.

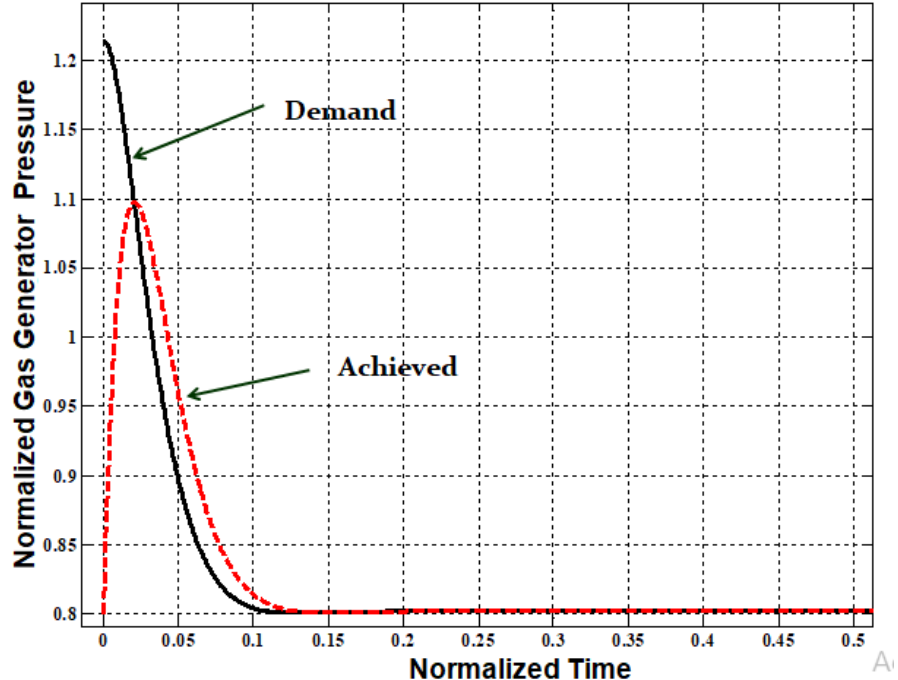


Figure-4.7: Gas generator demand Vs feedback performance of two loop NDI fuel flow controller at low altitude

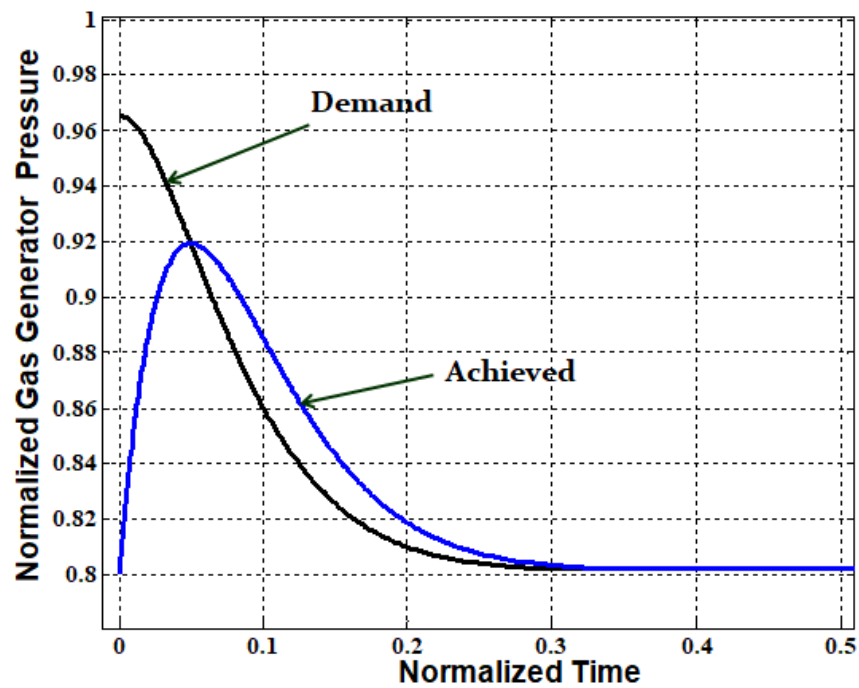


Figure-4.8: Gas generator demand Vs feedback performance of two loop NDI fuel flow controller at high altitude

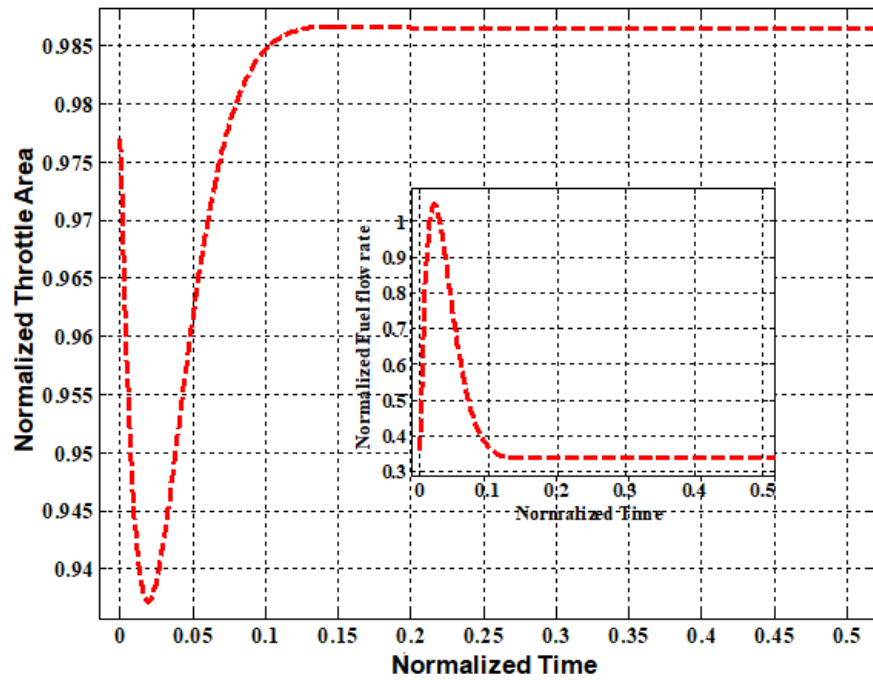


Figure-4.9: Throttle valve area and fuel mass rate demand Vs feedback performance of two loop NDI fuel flow controller at low altitude

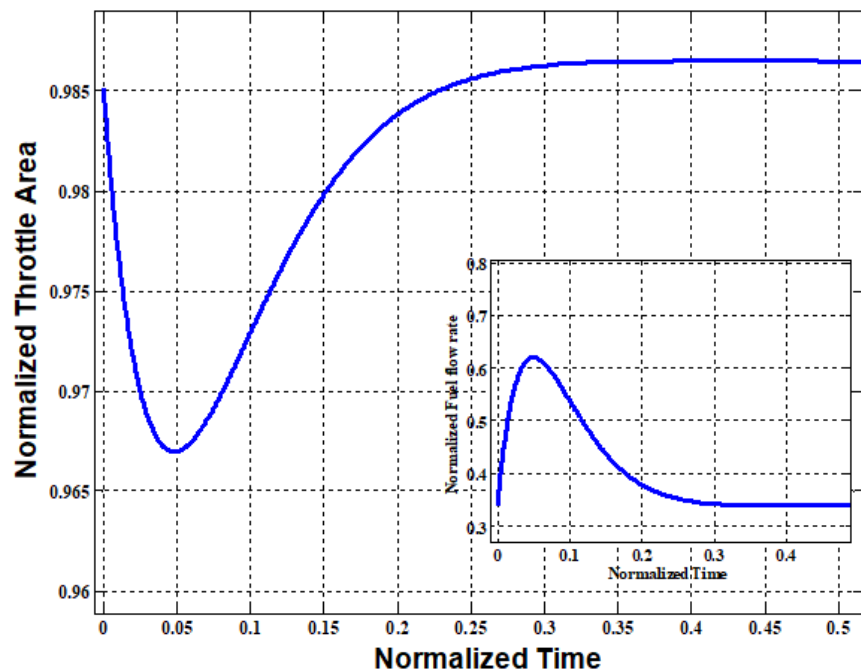


Figure-4.10: Throttle valve area and fuel flow rate demand Vs feedback performance of two loop NDI fuel flow controller at high altitude

To achieve Mach number demand, outer loop design relation generates the demand of gas generator pressure P_{gc} for inner loop. Inner loop design relation computes the rate of change of \dot{P}_{gc} based on time scale separation between slow loop and fast loop. To meet \dot{P}_{gc} , dynamic inversion of inner loop dynamic generates the demand of throttle valve area.

4.6.1 Fixed Vs Scheduled Gains Comparison

Simulation has been carried out to bring out the advantage of nonlinear dynamic inversion (NDI) fuel flow controller gain considered in two different methods.

1. Method 1: This method is called fixed gain. Here the controller gains are designed effectively at a particular altitude and the same gains are considered in different operating scenario.
2. Method 2: This method is called generic scheduling. Here, the controller gains are scheduled based on missile operating conditions.

In general, the objectives of fuel flow controller design are to have low overshoot and better steady state error. The simulation results are presented in figure 4.11.

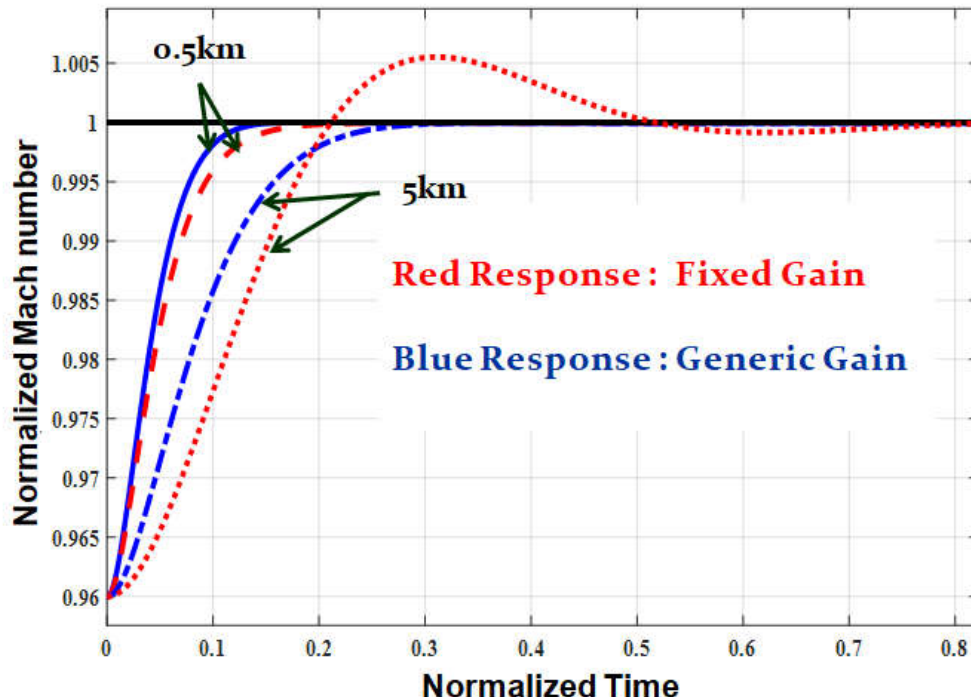


Figure-4.11: Mach number performance of two loop NDI fuel flow controller for Scheduled gains Vs fixed gains

It was found from the simulation results that fixed gains method provides a better performance at 0.5km condition altitude condition but its performance deteriorates at 5km altitude condition. Scheduled gain method provides a better performance at both 0.5km as well as 5km altitude as shown in figure 4.11. Finally generic scheduling which gains computation for fuel flow controller is more efficient for air-to-air missile.

4.7 Proportional-Integral (PI) Vs Non-linear Dynamic Inversion (NDI) Fuel Flow Controller

The dynamic equations of ramjet engine for pressure loop and thrust loop are nonlinear. The performance of two loop NDI fuel flow controller was ensured in above section. It was necessary to come out a comparison analysis between the proposed technique and Proportional-Integral (PI) gain based two loop fuel flow controller design. The nonlinear equation of pressure loop and thrust loop linearization was carried out using Taylor series method. Transfer function based on two loop controller in s-domain was formulated and PI technique based controller was designed. The comparison performance of proportional-integral based controller and NDI based controller was evaluated at same altitude. The Mach number achieved and the corresponding throttle valve area and gas generator pressure are shown in figure 4.12, 4.13 and 4.14.

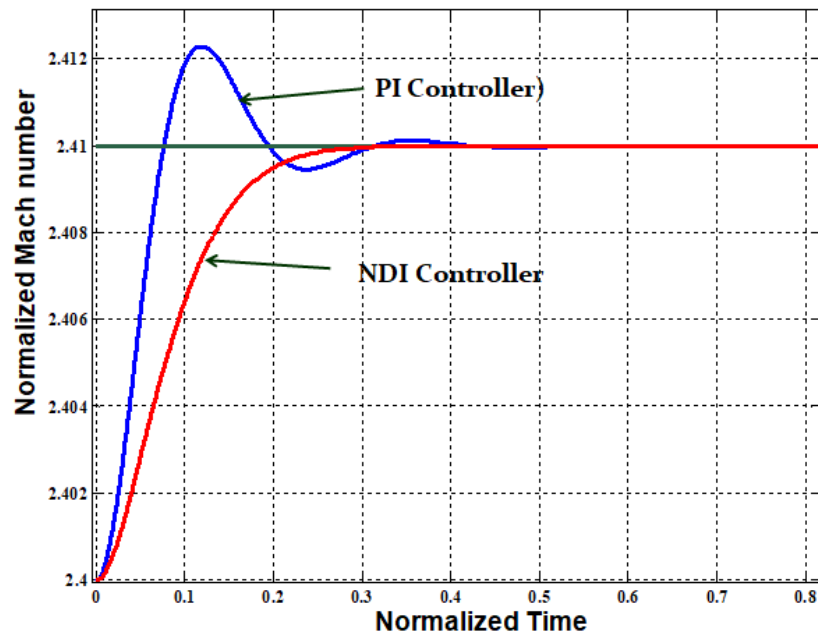


Figure-4.12: Nonlinear Dynamic Inversion fuel flow controller Vs proportional-integral fuel flow controller performance at same altitude for Mach number

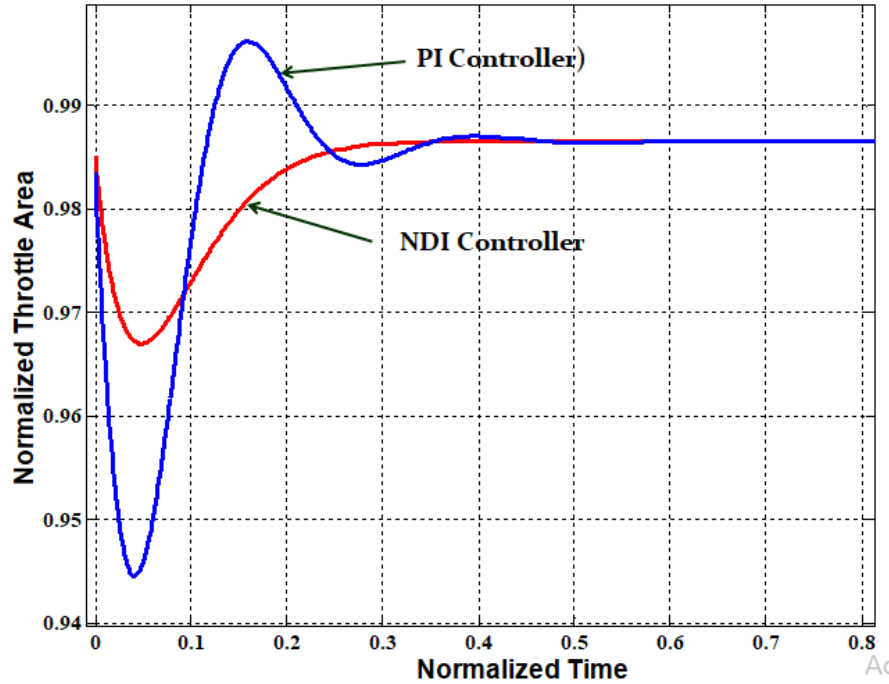


Figure-4.13: Nonlinear Dynamic Inversion fuel flow controller Vs proportional-integral fuel flow controller performance at same altitude for throttle valve area

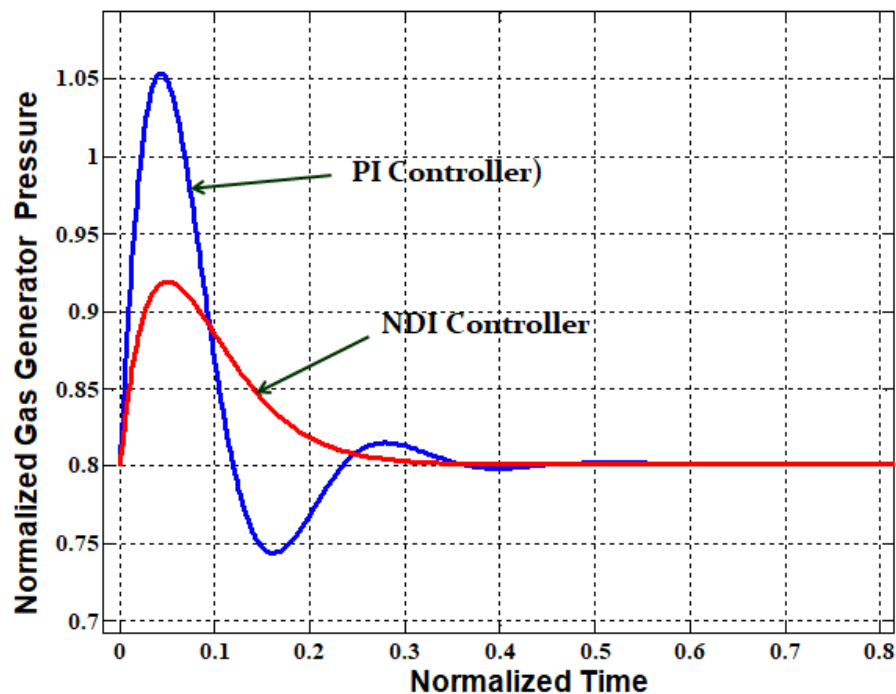


Figure-4.14: Nonlinear Dynamic Inversion fuel flow controller Vs proportional-integral fuel flow controller performance at same altitude for gas generator pressure

The comparison of results show that NDI based fuel flow controller performance is better than Proportional-Integral (PI) based controller with respect to design objective for air-to-air missile trajectory. Proportional-Integral (PI) based controller can be used for ground testing to stabilise the performance of solid fuel ramjet propulsion system.

4.8 Summary

This chapter proposed a nonlinear dynamic inversion fuel flow controller design to use effectively in a solid fuel ramjet propulsion system for air-to-air missile application. Fuel flow controller design specification has been generated from the guidance loop design as a function of altitude and Mach number to meet miss-distance requirement of air-to-air missile against the non-manoeuvring and manoeuvring target. Nonlinear dynamic inversion technique was adopted due to nonlinear characteristic of ramjet engine for gas generator pressure loop (inner loop) and thrust loop (outer loop). The performance between dynamic inversion controller technique and PI controller technique has been evaluated. To meet this design specification of fuel flow controller as a function of altitude and Mach number, a generic scheduling of controller gains methodology has been presented. The performance between fixed gains and generic scheduling gains was presented for different altitudes. It was found that generic scheduling of gain is more suitable to obtain efficient performance of ramjet engine for air-to-air missile. Moreover, simulation results for different altitudes show that the performance of the proposed two loop controller was found to be superior for varying missile characteristics as a function of angle of attack, altitude and Mach number and operational conditions. Hence, the proposed two loop NDI based fuel flow controller is suitable to provide efficient management of ramjet propulsion system for air-to-air missiles.

Chapter 5

Three Loop Fuel Flow Controller Design for Stable Operation of Ramjet Engine

Chapter 5

Three Loop Fuel Flow Controller Design for Stable Operation of Ramjet Engine

5.1 Introduction

The performance of air intake plays a crucial role in providing adequate air mass flow rate in the combustion chamber for producing the thrust. The compression of atmospheric air happens due to terminal shock formation inside the air intake duct. Any disturbance in intake duct creates intake instability like unstart and buzz. In general, other classes of missiles use bleeder control or flex nozzle control to avoid it. These types of control need extra hardware in the missile. The proposed research in air-to-air missile configuration has space constraint to embed extra hardware for handling intake instability. So, this chapter proposes an innovative solution to handle/avoid instability of air intake for stable operation of ramjet engine using fuel flow controller. This topic of research is an ongoing project at Defence Research and Development Organisation (DRDO); therefore, the results of engine parameter have been normalized to ensure secrecy.

5.2 Air Intake Operation and Characteristic

In a mixed compression ramjet, the terminal shock position is determined by the intake back pressure, which is ideally equal to the combustion chamber pressure. In case of any disturbance in the combustion chamber pressure, it pushes the terminal shock outside the intake duct resulting in un-start phenomenon, which can be restarted without much problem. But if the combustion pressure is just sufficient that it pushes the terminal shock just at the cowl lip, then a slight disturbance in the combustion chamber will push the shock just outside the intake duct and intake mass spillage will occur (*Dailey Criterion*) as shown in figure-5.1. This occurs due to the boundary layer separation at the compression ramp.

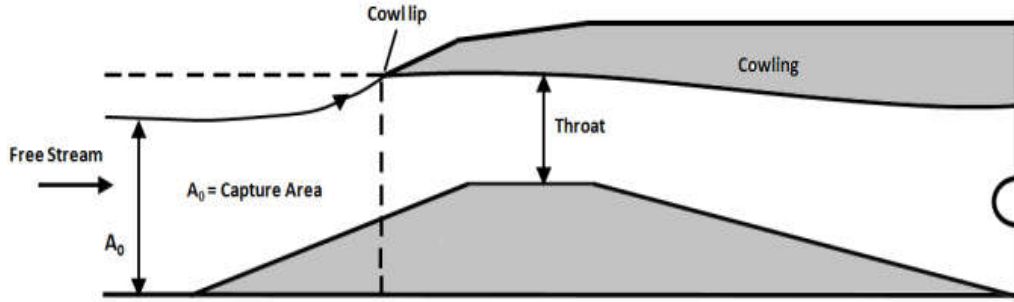


Figure-5.1: Schematic Diagram of the Intake Duct

As the shock moves upstream, the shear layer moves away from the cowl lip thus decreasing the intake air mass. So it'll force the shock to reattach itself to the cowl lip again. And again the high combustor pressure will push the shock just outside the intake duct, because of which an oscillating phenomenon occurs. This phenomenon is termed intake buzz.

In general, intake design for air-to-air missile has been carried out to operate in critical zones with a certain percentage of margin of back pressure for stable operation. If it is taken away by disturbance or uncertainties, then through some control technique, it could be brought out in the critical zone.

Hence, there is a need to control the terminal shock location in intake to operate intake back pressure within intake pressure margin [5].

$$P_{margin} = \frac{P_{critical} - P_{operation}}{P_{critical} - P_{minimum}} \quad (5.1)$$

Where, $P_{critical}$ and $P_{minimum}$ are back pressure forward most limit and rear most limit of terminal shock location in intake duct. P_{margin} is the back pressure operating band to maintain shock location within intake duct. Once intake instability phenomena starts, control action to be initiated to keep back pressure within P_{margin} margin.

So, it is mandatory to characterize intake of all flight operating conditions like Altitude, Mach number and angle of attack to calculate P_{margin} for fuel flow controller design. Data of intake back pressure as a function of Mach, Altitude and angle of attack have been evaluated through CFD or wind tunnel testing.

5.3 Third loop control requirement

Controlling back pressure margin within limit leads to avoiding intake instability. It is also important to bring out the rate of control of intake instability under disturbance. So, the characteristics of buzz oscillation under disturbance have been determined based on previous chapter buzz mathematical model. A typical buzz oscillation condition on back pressure and air mass rate was simulated as shown in figure 5.2 and 5.3.

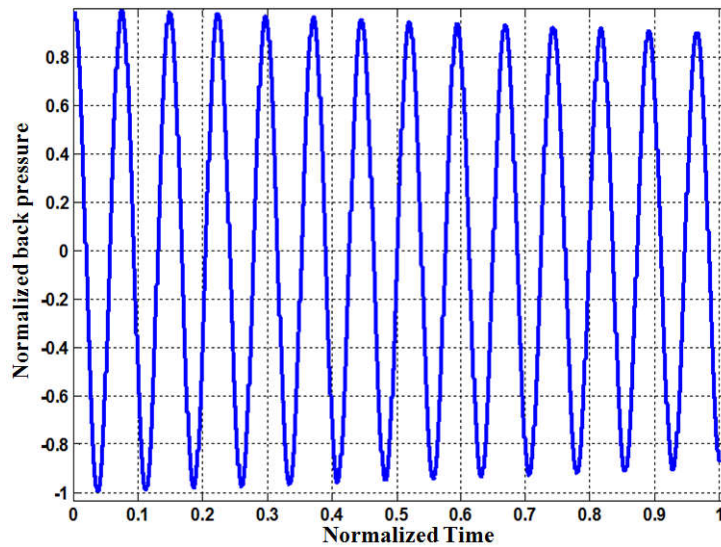


Figure 5.2: Buzzing effect on back pressure under disturbance

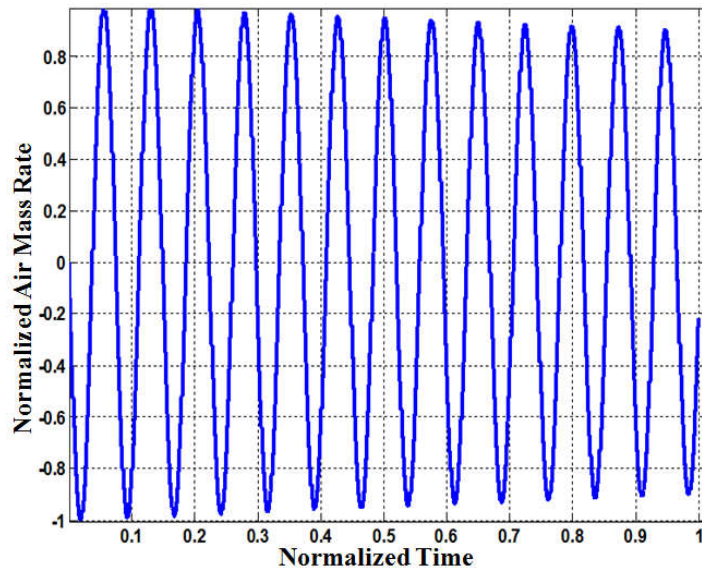


Figure 5.3: Buzzing effect on air mass rate under disturbance

It was also found from the above results that the oscillatory behaviour of buzz varies as a function of altitude and Mach number. So the operational altitude and Mach number range of air-to-air missile and the oscillatory frequency requirements are as shown in table 5.1.

Table 5.1: Buzz frequency range as a function of altitude and Mach number

S. No	Altitude (km)	Mach number Range (M)	Buzz oscillatory Frequency (Hz)
1.	0.5	2.0 – 2.4	16 to 18
2.	5.0	2.2 – 2.8	13 to 16
3.	10.0	2.4 – 3.2	11 to 13
4.	15.0	2.6 – 3.6	11 to 13

So, fastness of fuel flow controller needs to be designed for capturing buzz oscillation dynamics under intake disturbance. Feedback control bandwidth is limited under propagating time delays inherent in the system; therefore, feed forward control requires fast controlling it. The requirement of fuel flow actuator can be estimated based on higher frequency of buzz oscillation and it comes from low altitude of missile operation.

5.4 Three Loop Structure Based Fuel Flow Controller Design

Two loop fuel flow controller was discussed in chapter 4 where the outer loop is the thrust control loop and Inner loop is the pressure control loop. The main task of the two loop controller is to provide needed throttle valve area so that ramjet engine produces the commanded thrust and meets the desired speed of response to satisfy guidance loop requirement as shown in figure 5.4. In addition to the two loop FFC controller, a 3rd loop as a feed forward control is introduced as back pressure loop which is designed to protect intake back pressure margin for all operating conditions of the missile. If, back pressure margin is intact while in operation, this loop will be salient and be on watching mode. Once the back pressure crosses the prescribe limit, this loop get activated and ensures the stable operation of ramjet engine as shown in figure 5.5. Back pressure loop is also called supervisory control. The combustor pressure which is effectively back pressure is given by the chemical properties of the combustion process. The combination of these three loops as shown in figure 5.6 is the three loop structure based fuel flow controller.

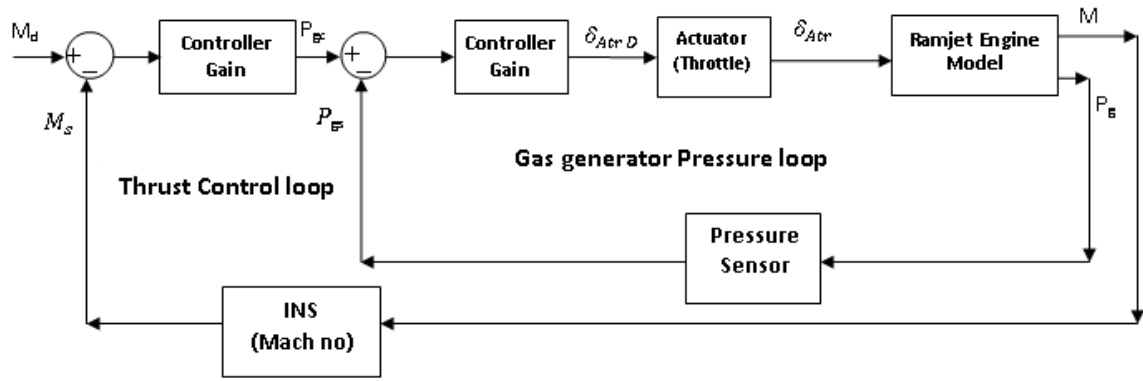


Figure 5.4: Block diagram of two loop fuel flow controller

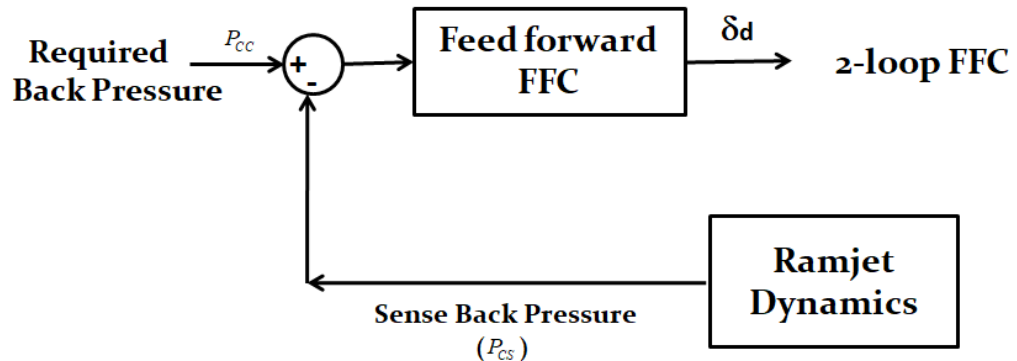


Figure 5.5: Representation of feed-forward control for back pressure loop

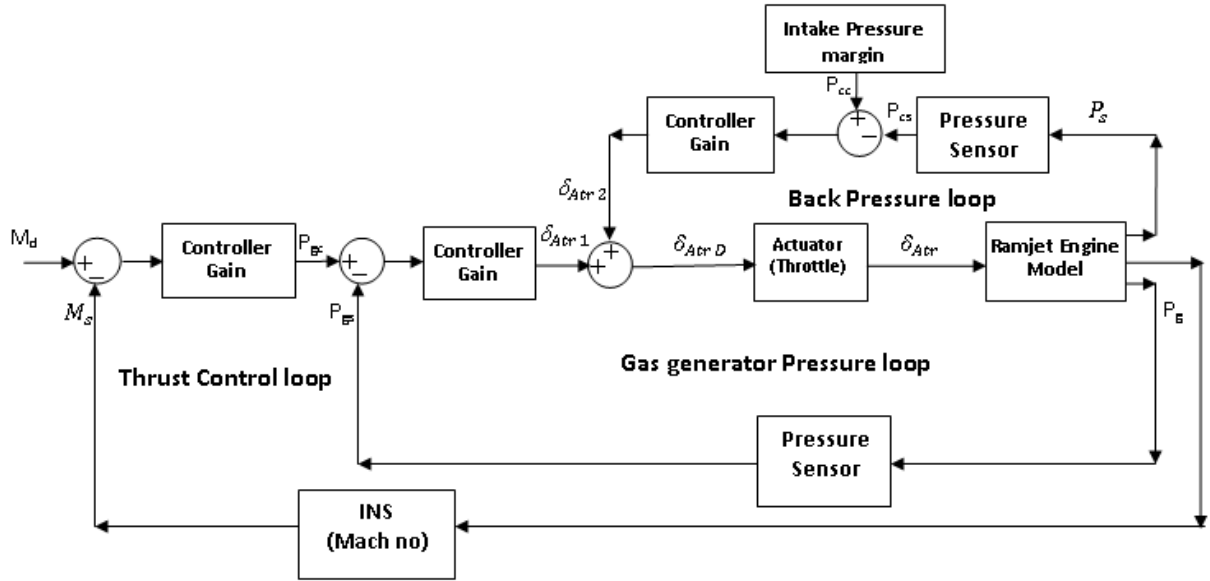


Figure 5.6: Block diagram of three loop structure of fuel flow controller

So, each loop design relation is discussed in below while the required throttle area is generated to meet thrust demand to ensure stable operation of intake at the time of disturbance.

Outer Loop Design:

The outer loop gets the demanded Mach number from the guidance loop and sense Mach number from INS sensor. The desired dynamics for the outer loop is given by:

$$\Delta \dot{M} = \omega_{outer} (\Delta M_d - \Delta M_s) \quad (5.2)$$

Where M_d and M_s stands for demanded and detected Mach number respectively. And ω_{outer} is the time constant of outer loop.

$$\Delta P_{gc} = \frac{\Delta \dot{M} - \frac{1}{m V_a} \left(\frac{\partial T}{\partial M} - \frac{\gamma}{2} P_s (C_D' \cos \alpha - C_L' \sin \alpha) \right) \Delta M_s}{\frac{A_{tr0}}{V_a m C_g} \frac{\partial T}{\partial \dot{m}_f}} \quad (5.3)$$

ii. Inner Loop Design:

The gas generator pressure control loop receives the requirement from outer loop. The demanded throttle valve area is:

$$\Delta A_{tr1} = \frac{\left[\frac{R_g T_g}{V_g} \left(\rho_g A_g \alpha P_{g0}^{n-1} \Delta P_g - \frac{A_{tr0} \Delta P_g}{C_g} \right) \right] \Delta P_{gs} - \Delta \dot{P}_g}{\frac{R_g T_g}{V_g} \frac{P_{g0}}{C_g}} \quad (5.4)$$

Where $\Delta \dot{P}_g = \omega_{inner} (\Delta P_{gc} - \Delta P_{gs})$, P_{gc} and P_{gs} are the commanded and measured gas generator pressure respectively and ω_{inner} is the time constant of the inner loop. This change in throttle valve area ensures the fuel flow rate such that the demanded thrust is achieved.

iii. Feed-forward Back Pressure Loop Design:

The back pressure loop receives the demanded margin. The control logic is designed such that this loop gets activated when back pressure of the margin is specified:

$$\Delta \dot{P}_c = \omega_{third} (\Delta P_{cc} - \Delta P_{cs}) \quad (5.5)$$

Where P_{cc} and P_{cs} are the demanded and measured back pressure (combustor pressure).

From the combustion chamber dynamics in the table, the $\Delta \dot{m}_f$ is computed corresponding to ΔP_c and from the computed value the required throttle valve area is computed:

$$\Delta A_{tr2} = \frac{C_g}{P_{g0}} \left(\Delta \dot{m}_f - \frac{A_{tr0} \Delta P_{gc}}{C_g} \right) \quad (5.6)$$

So the effective throttle valve area is:

$$\Delta A_{tr} = \Delta A_{tr1} \pm \Delta A_{tr2} \quad (5.7)$$

If the back pressure is within the margin, then the throttle valve area computed in equation 5.4 is used in the gas generator for injecting fuel mass rate otherwise taken from equation 5.7. The feed forward gain should be chosen as a function of Mach number and altitude.

5.5 Three Loop FFC Results and Analysis with Air Intake Disturbance

In this section, two loop nonlinear dynamic inversion (NDI) based fuel flow controller with feed forward control for back pressure and ramjet engine modeling with intake dynamics were carried out in simulation environment under ideal condition (isotropic gas assumption).

Simulations were carried out to show the performance of three loop structure based fuel flow controller in presence of disturbance. A typical altitude and Mach number scenario was chosen and applied to a random disturbance in combustion.

Simulation results of three loop structure-based controller are shown in figure 5.7 to 5.9. Figure 5.7 shows that the normalized sense back pressure performance and disturbance occurs at normalized time 0.4. So, total sense pressure can be analyzed in three phases to understand the control action.

Phase-1: Performance of ramjet engine where Normalized time less than 0.4

Phase-2: Performance at normalized time equal to 0.4

Phase-3: Performance of ducted ramjet engine where Normalizes time greater than 0.4

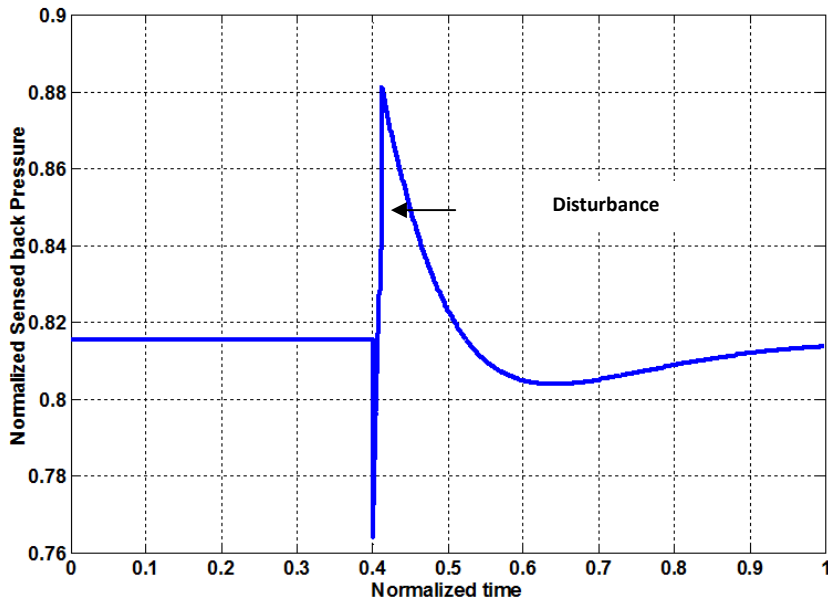


Figure 5.7: Sense back Pressure profile with intake disturbance

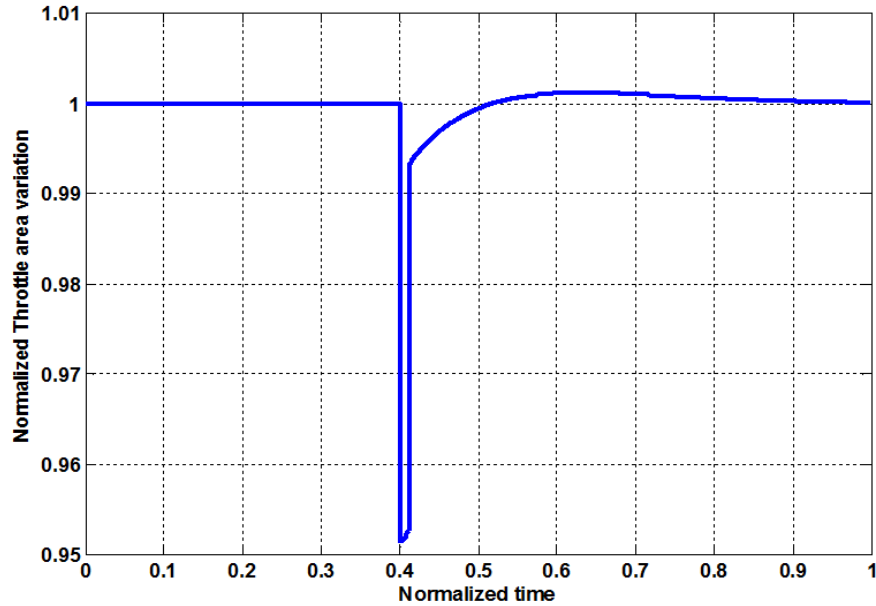


Figure 5.8: Throttle Area computed by Fuel flow controller against the disturbance

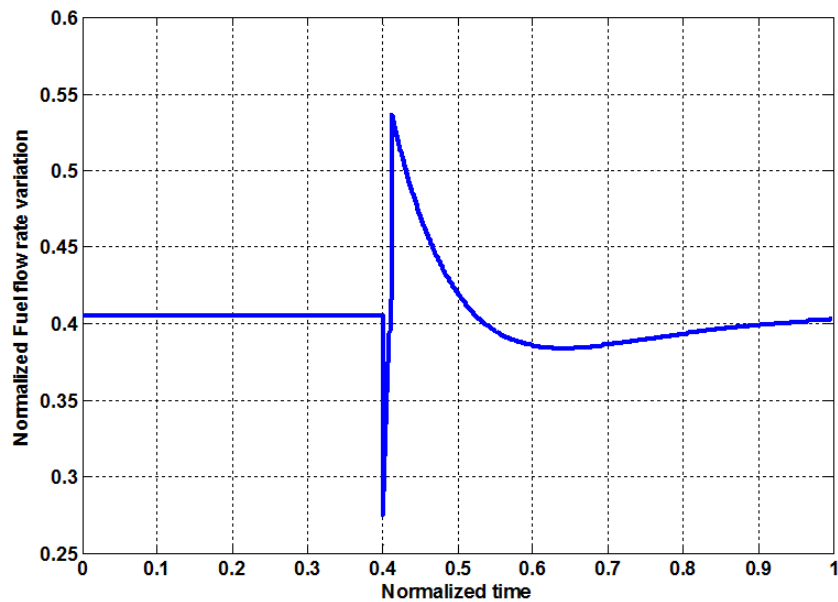


Figure 5.9: Fuel mass rate with corresponding throttle area for controlling back pressure

Phase-1:

The two loop Fuel flow controller sets the throttle valve area in a particular position so that the required fuel mass rate can be injected from the gas generator to the combustion chamber. Injected Fuel mass rate gets mixed with air mass rate which enters through air-intake and burns to produce thrust. During this process, the pressure sensor keeps sensing back pressure and back

pressure margin is computed by back pressure loop. Third loop controller determines that back pressure margin is within band, so no action need be taken and this implies that terminal shock in the intake is in nominal location.

Phase-2:

Back pressure (Combustion chamber pressure) starts deviating due to applied disturbance. If not controlled, it can lead to propulsion instability and impact thrust as shown in figure 5.10. Ramjet engine could have a detrimental effect on the performance of the missile.

Phase-3:

Once buzz oscillation gets started due to disturbance, the feed-forward back pressure loop gets activated before the disturbance digests the entire intake margin. Pressure margin at a given condition is computed and once it crosses the defined value, feed-forward based back pressure loop starts generating extra requirement of throttle valve area to bring back the margin in desire bound. Figure 5.8 shows that how fast the throttle valve area closes and the corresponding mass flow rate of gas generator to vary the back pressure. During this process, the achieved thrust gets affected due to extra fuel flow rate variation which is injected in the combustion chamber. From the above results, it is seen that the controller is successfully bringing down the Combustion chamber pressure / back pressure from the disturbance zone.

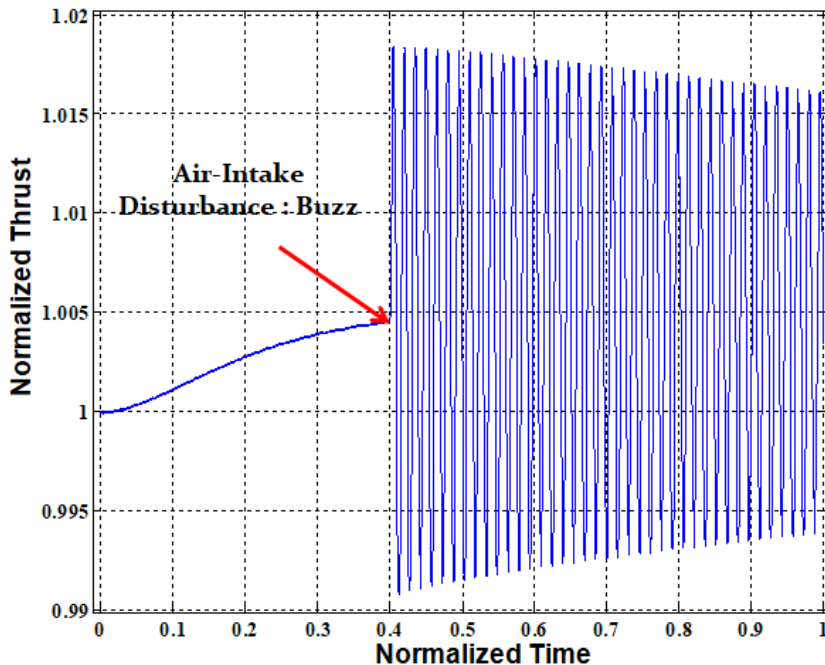


Figure 5.10: Air intake buzz instability effect on thrust produce by ramjet engine

5.6 Three Loop Structure Based FFC Performance With and Without Disturbance

A typical scenario has been simulated at low altitude and high altitude for different Mach number conditions to validate three loop structure based fuel flow controller with and without intake disturbance for air-to-air missile operating range.

5.6.1 Low Altitude Scenario

A constant step Mach number demand is provided to the outer loop of the controller and air intake disturbance has been applied at normalized time 0.4. The performance of the controller was satisfactory except for some deviation in achieved Mach number due to change in throttle area and a corresponding change in gas generator pressure to produce fuel mass rate for controlling the intake disturbance as shown in figure 5.11, 5.12 and 5.13.

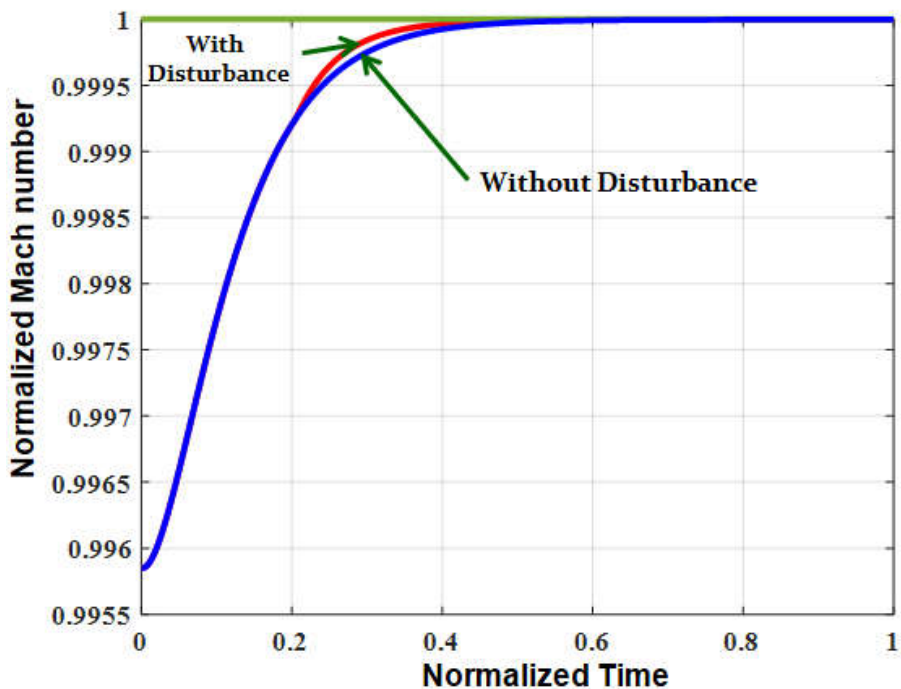


Figure 5.11: Fuel flow controller response on Mach number with and without air intake disturbance at low altitude

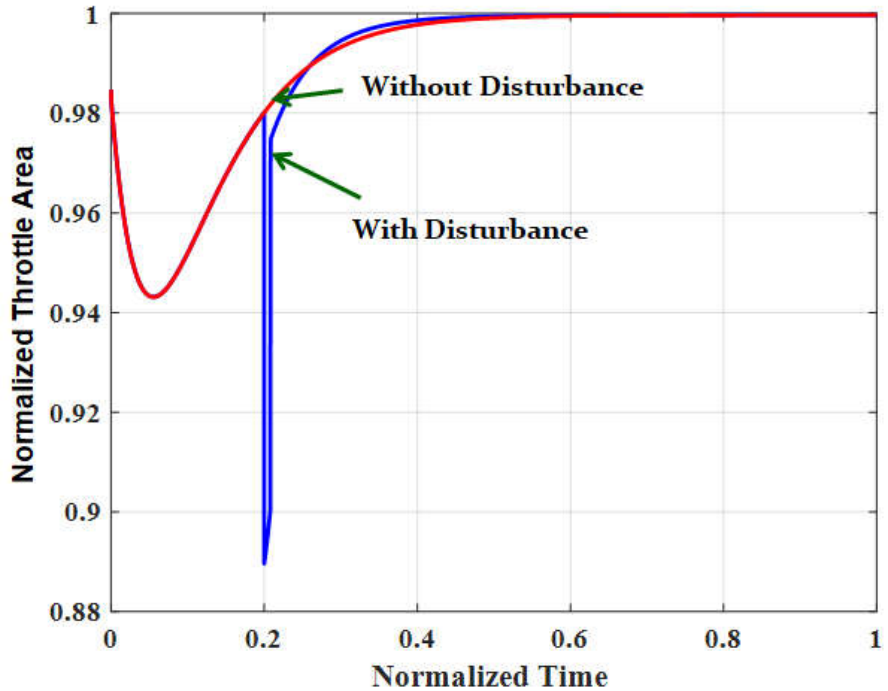


Figure 5.12: Fuel flow controller response on throttle area with and without air intake disturbance at low altitude

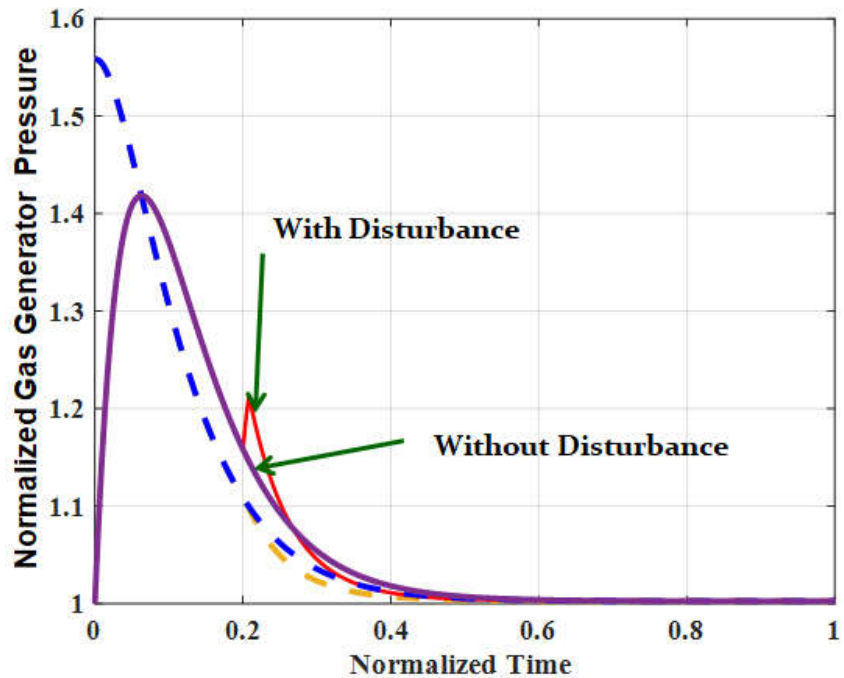


Figure 5.13: Fuel flow controller response on gas generator pressure with and without air intake disturbance at low altitude

5.6.1 High Altitude Scenario

A constant step Mach number demand is provided to the outer loop of controller and air intake disturbance has been applied at normalized time 0.4. The performance of the controller was satisfactory except for some deviation in Mach number achieved due to change in throttle area and a corresponding change in gas generator pressure to produce fuel mass rate for controlling the intake disturbance as shown in figure 5.14, 5.15 and 5.16.

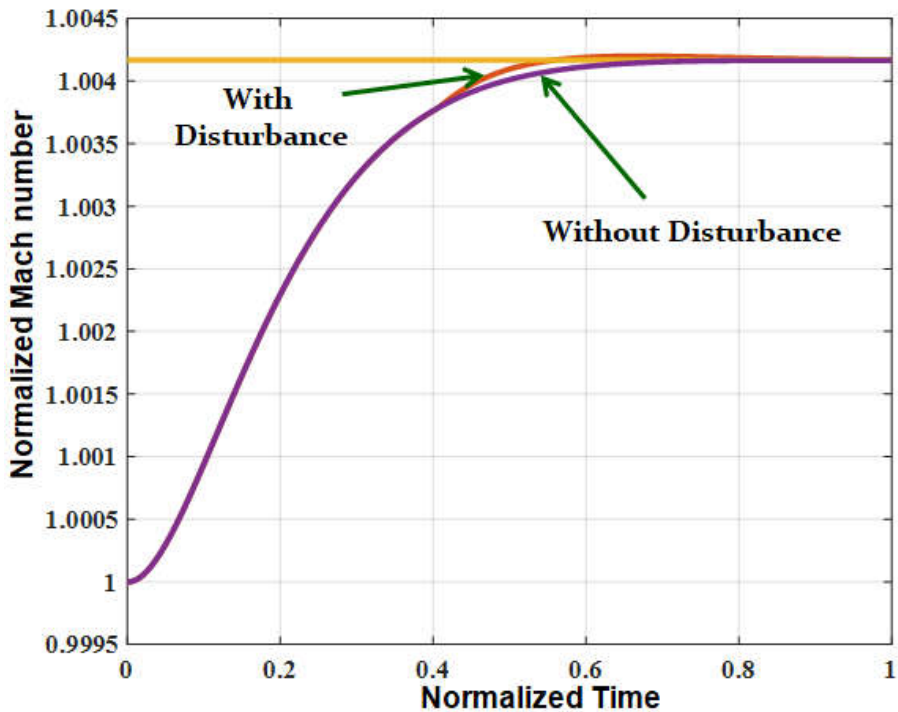


Figure 5.11: Fuel flow controller response on Mach number with and without air intake disturbance at high altitude

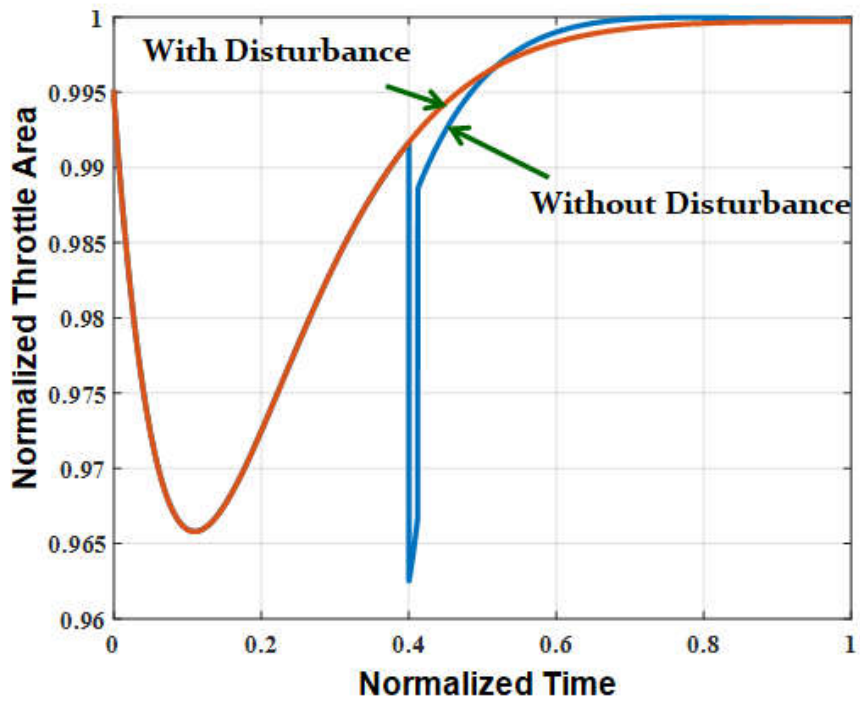


Figure 5.12: Fuel flow controller response on throttle area with and without air intake disturbance at high altitude

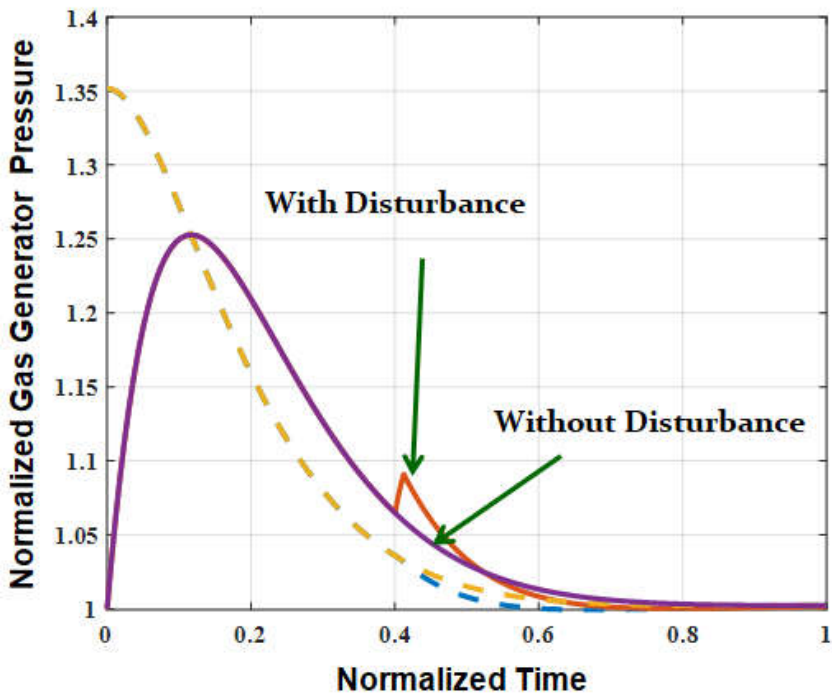


Figure 5.13: Fuel flow controller response on gas generator pressure with and without air intake disturbance at high altitude

5.7 Summary

This chapter proposed an innovative concept of feed-forward back pressure control loop into the two loop fuel flow controller to handle air intake instability under disturbance without the use of extra hardware. Air intake pressure margin has been designed more for air-to-air missile. Any unprecedented disturbance can disturb the terminal shock into the intake duct. This may lead to detrimental effect on engine performance and overall missile performance. It is found that the proposed three loop structure based fuel flow controller is more efficient and stable under various operating conditions and disturbance for a solid fuel ramjet propulsion system. Moreover, the performance of the proposed three loop controller is found to be far superior for air-to-air missile than only two loop fuel flow controller under disturbance, which was discussed in previous chapter. Hence, the proposed controller technique can be used for all types of ramjet propulsion systems which have space constraints to embed in the system hardware oriented control techniques.

Chapter 6

Fuel Flow Controller Performance Validation on Six-Degrees-of-Freedom Simulation Platform of Air-to-Air Missile

Chapter 6

Fuel flow Controller Performance Validation on Six-Degrees-of-Freedom Simulation Platform of Air-to-Air Missile

6.1 Introduction

Air-to-Air missile is a guided flight vehicle and its job is to put warhead (explosive) close to the target so that warhead can destroy the target. The vicinity of warhead is called miss-distance. In this chapter, the performance of fuel flow controller design for solid fuel ramjet propulsion system has been evaluated in closed loop interaction between the missile six-degrees-of-freedom (6-DOF) model, missile aerodynamics force and moment, missile guidance algorithm, missile autopilot algorithm with aerial target model. In the previous chapter, the fuel flow controller design performance was validated under different operational conditions using standalone simulation platform. To get the best validation of fuel flow controller design in real engagement scenario, all mission algorithms and operational parameters are dynamically changing and interacting with each other to ensure the overall missile objectives. Stability Analysis and Monte-Carlo simulations were also carried out with all missile perturbation conditions to show the robustness and miss-distance of missile with fuel flow controller. The topic of research is an ongoing project at Defence Research and Development Organisation (DRDO), so, all the results of engine parameters have been normalized.

6.2 Air-to-Air Missile Engagement Scenario and Mission Sequence

Three cases of engagement trajectory were simulated to evaluate the performance of fuel flow controller as shown in figure 6.1.

1. Case A: In this case, the missile and the target are flying at the same altitude, however, throughout the engagement trajectory, the aerial target does not manoeuvre. Missile guidance

needs to generate fixed path and the autopilot executes it for hitting the target. The requirement of angle of attack for this type of trajectory is low.

2. Case B: In this case, the missile and the target are flying at the same altitude. In mid-course trajectory phase, the aerial target does not manoeuvre. However, at the terminal phase of trajectory, the target does evasive manoeuvring based on the capability as a function of altitude and Mach number, given in table-6.1. Missile guidance needs to generate demand correspondingly and the autopilot executes it for hitting the target. The requirement of angle of attack in terminal phase is high for chasing the target and the rate of building the angle of attack depends on altitude and missile parameters.
3. Case C: In this case, the missile and the target are flying at different altitudes. In mid-course trajectory phase as well as terminal phase of trajectory, the some demand is generated by guidance to shape the missile path towards the target and the autopilot executes it for hitting the target. The requirement of angle of attack in midcourse and terminal phase is moderate and the rate of building angle of attack depends on altitude and missile parameters.

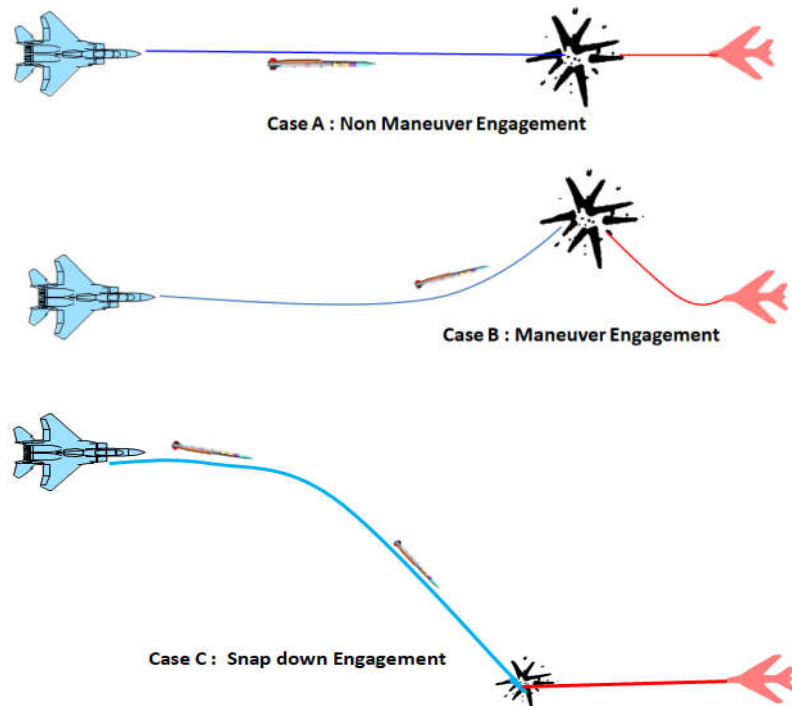


Figure-6.1: Air-to-Air missile engagement for non-manoeuvring, manoeuvring and varying altitude against the aerial target

6.3 Operational Sequence of Fuel flow Controller

There are three phases of operational computation in fuel flow controller which make ramjet propulsion system operation effective, as shown in figure 6.2.

1. Pre-launch phase: In this phase, based on the position like range, altitude and velocity of missile and target aircraft, pre-launch guidance algorithm computes the expected velocity requirement to hit target aircraft. To achieve expected velocity and corresponding thrust requirement from solid ramjet propulsion, fuel flow controller computes the desired throttle valve area and sets the position on throttle valve. So, once ramjet operation is initiated, the pre-fixed throttle valve area ensures gas generator pressure to inject fuel mass rate into the combustion chamber.
2. Mid-course phase: In this phase, Fuel flow controller dynamically computes the position of throttle valve with respect to pre-launch setting, and makes incremental change in valve area to meet the requirements of mid-course guidance velocity. Third loop maintains the back pressure margin under intake disturbance for stable operation of engine.

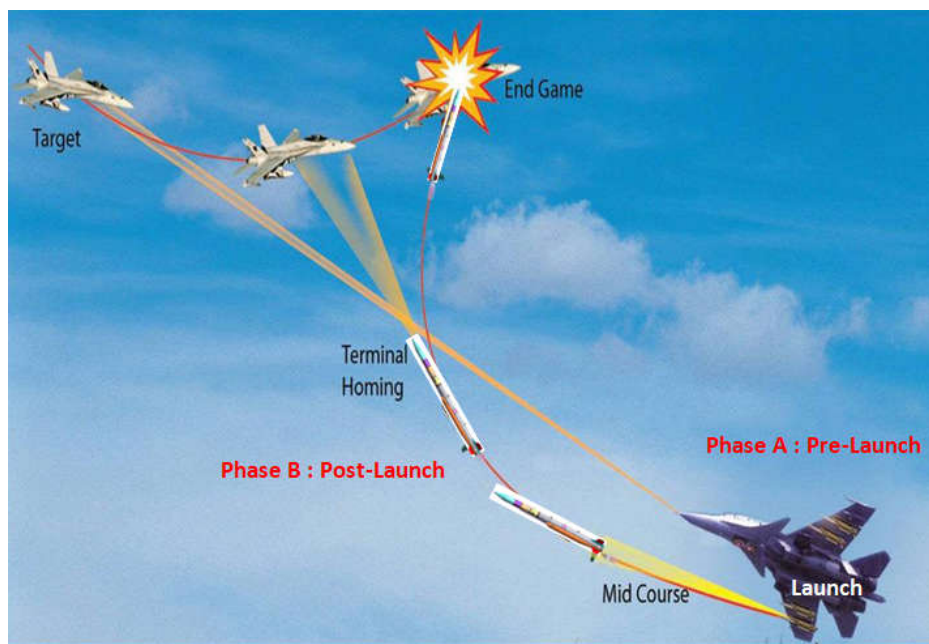


Figure-6.2: Operational requirements and different phases of Air-to-Air missile engagement scenario

3. Terminal phase: In this phase, the requirement of angle of attack is more and rate of angle of attack varies based on altitude and Mach number, So Fuel flow controller dynamically

computes the required area and speed to set the position of throttle valve. It is the most critical phase of air-to-air missile trajectory for fuel flow controller operation and any deviation can lead to higher miss-distance between the missile and target. While getting more thrust from ramjet engine and fast changing of missile operating condition, the role of third loop is also critical in this phase of trajectory. Finally this loop has to maintain the back pressure margin under intake disturbance for stable operation of ramjet engine.

6.4 Description of 6-DOF Model and its Interaction with Fuel Flow Controller for Air-to-Air Missile

The mathematical model of ramjet engine including intake model, 6-DOF equation based air-to-air missile configuration and point mass model of aerial target is presented in chapter 3. The complete six-degrees-of-freedom (6-DOF) model of air-to-air missile along with its different sub-systems including guidance, autopilot and fuel flow controller, aerodynamics model, pressure sensor model, missile actuator model and Inertial navigation sensor (INS) is simulated as shown in figure 6.3.

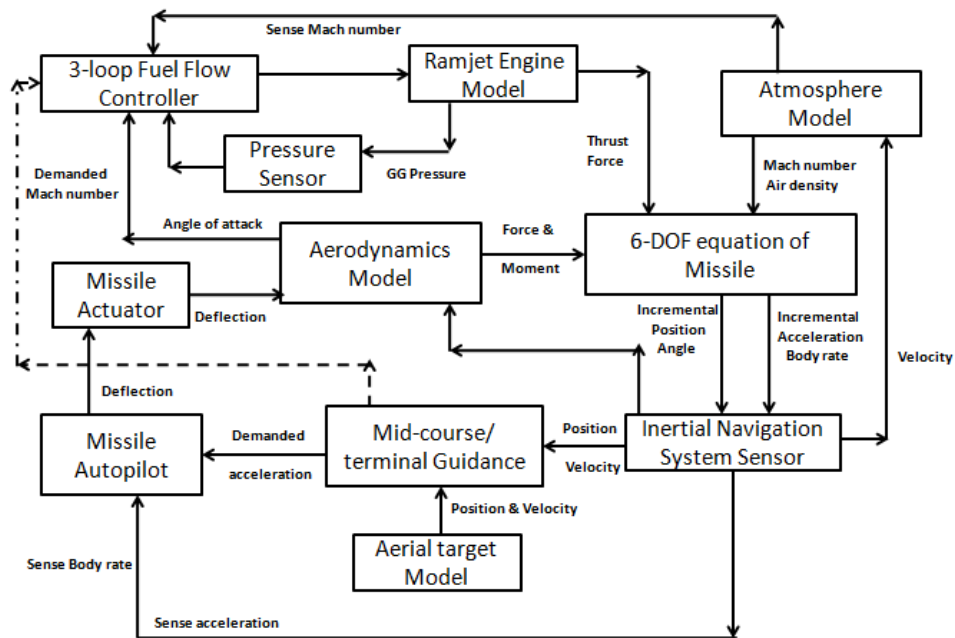


Figure-6.3: Block diagram of complete 6-DOF model

This simulation platform is used to evaluate fuel flow controller design for different engagement scenario. The description of inputs required and design details of ramjet control have been presented in chapter 4 and chapter 5 and brief description of guidance, autopilot and aerodynamics model has been presented below.

1. **Missile Guidance:** Guidance algorithm requires missile position and velocity information from inertial navigation sensor (INS) and target position and velocity from radar or seeker to compute lateral acceleration in elevation and horizontal plane for missile to follow the path towards the target. Proportional navigation based guidance design is considered here, which optimally generates demand to nullify the line-of-sight rate between missile to target for a constant velocity of the missile as shown in figure 6.4. Details of guidance algorithm are provided in Appendix.

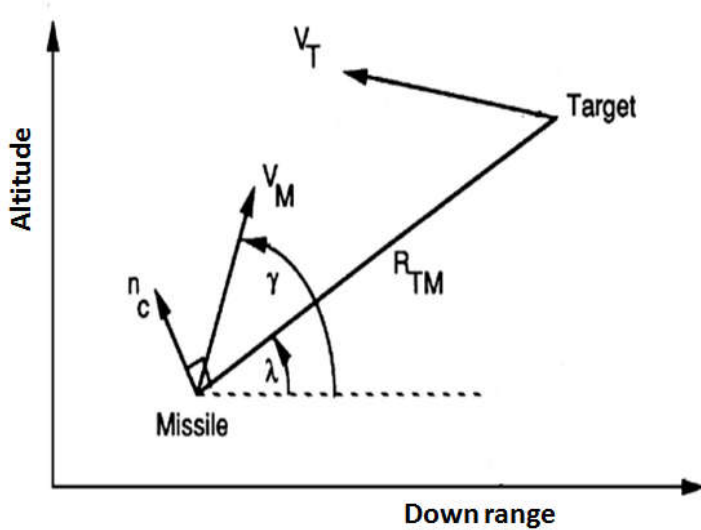


Figure-6.4: Representation of missile-target engagement

So, acceleration demand (n_c) of missile can be written as:

$$n_c = N' V_c \lambda$$

Where, N' is navigation constant, V_c is closing velocity and λ is LOS rate.

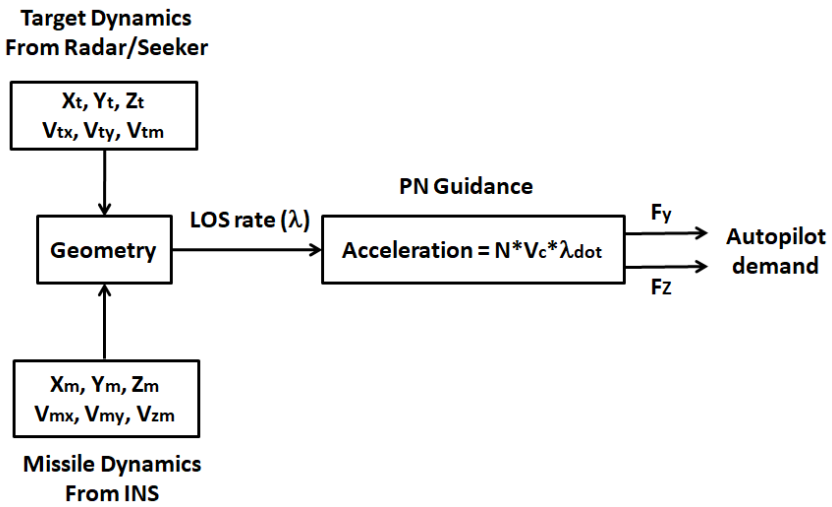


Figure-6.5: Block diagram representation of Proportional Navigation guidance representation

2. **Missile Autopilot:** Missile autopilot algorithm generates deflection command for actuator based on lateral acceleration in elevation and horizontal plane from the guidance demand to change the new dynamic position of missile. This algorithm needs the body rate and acceleration information of gyro and accelerometer sensor to execute the deflection while tracking the guidance demand when maintaining stability, shown in figure 6.5. The generated fin deflection is provided to the actuator while deflection achieved is fed into the 6-DOF equation through aerodynamic model. Details of autopilot algorithm are provided in Appendix.

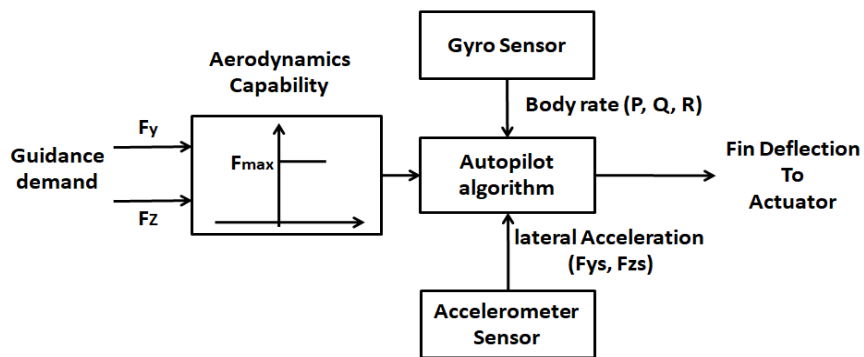


Figure-6.6: Block diagram of missile autopilot representation

3. Aerodynamics Model: Wind tunnel or CFD test of air-to-air missile was conducted to characterize the missile force and moment behaviour as a function of altitude and Mach number, angle of attack and deflection. These complete sets of force coefficient and moment coefficient data have been stored to compute the missile force and moment in 6-DOF equation to update the missile position and velocity with respect to time.

6.5 Air-to-Air Missile Performance with Fuel Flow Controller at Different Engagement Scenario

Long range capability and manoeuvrability ability of missile defines the dominance over target in air-to-air engagement. Solid fuel ramjet propulsion system provides the impact on both of these capabilities. So, in effect the use of solid fuel ramjet energy through fuel flow controller makes the missile more efficient. In this section, the miss-distance of air-to-air missile was evaluated for different engagement scenarios from 0.5km altitude to 15.0km altitude. For a given missile configuration and subsystem design, the velocity of missile is an important variable to decide miss-distance performance for all the engagement. Hence, missile velocity requirement from solid ramjet propulsion must be fulfilled through three loop fuel flow controller.

6.5.1 Missile-Target Engagement at 0.5km Altitude

At this altitude, the dynamic pressure is higher compared to other altitudes and the aerodynamic capability of lift force is high for both missile and target. So, the target can perform high manoeuvring at low altitude for escaping. Missile guidance is needed to generate lateral acceleration to hit the aerial target and the autopilot executes lateral acceleration while generating angle of attack. So, this high angle of attack directly impact drag force of the missile. However, maintaining the same missile velocity, the rates of increasing drag force need to be compensated through ramjet engine. So, fuel flow controller generates additional requirement of fuel mass rate. The performances of missile and fuel flow controller are given below.

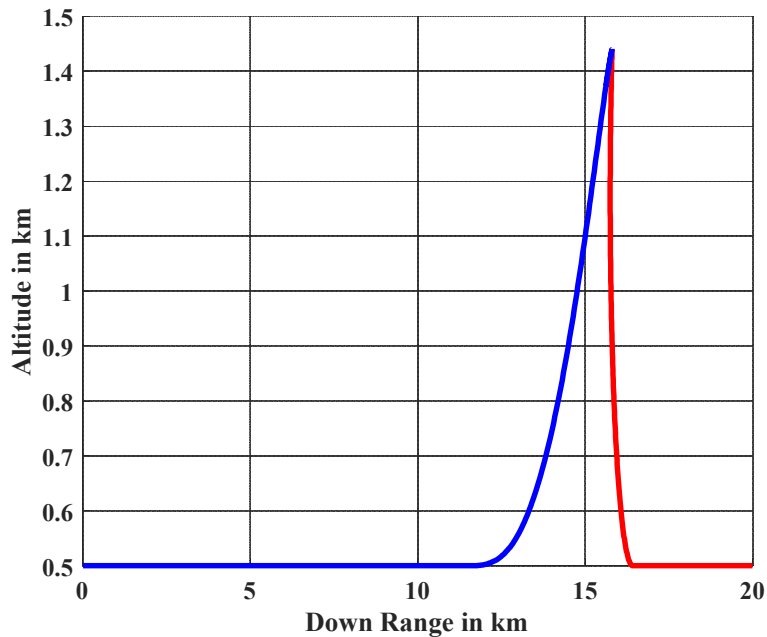


Figure-6.7: 6-DOF simulation result of missile-target engagement scenario at 0.5km altitude with manoeuvring target in pitch up plane

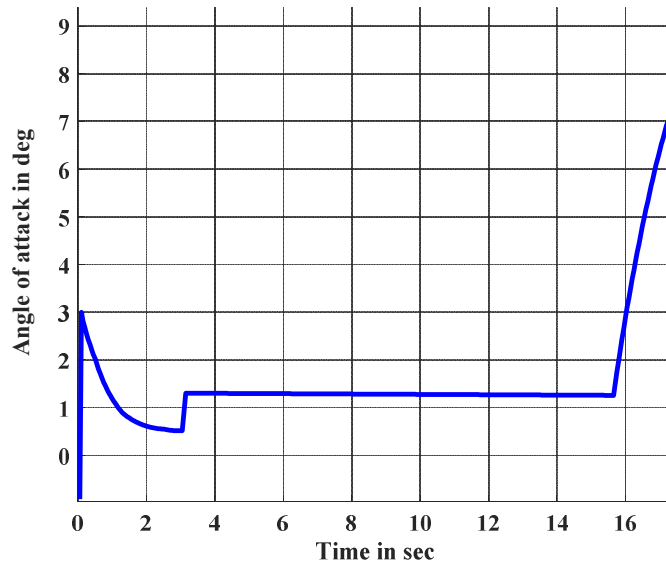


Figure-6.8: Requirement of angle of attack in different phases of trajectory at 0.5km engagement scenario

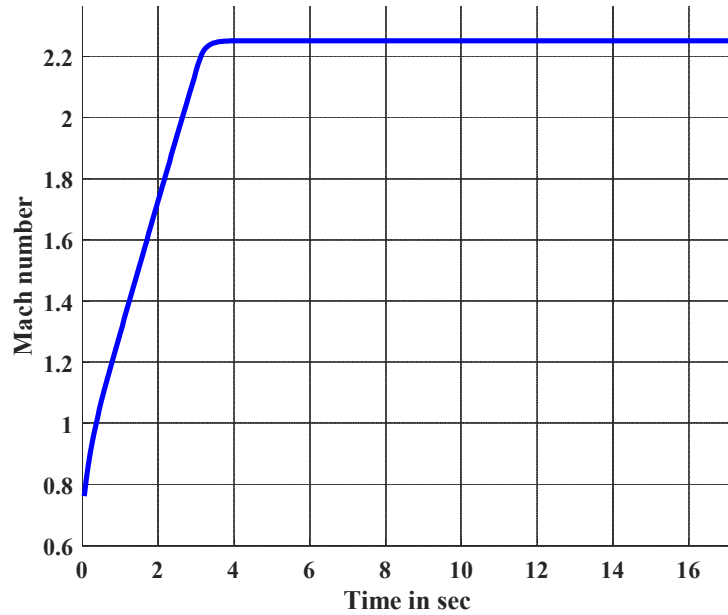


Figure-6.9: Missile Mach number (velocity) at different phases of trajectory at 0.5km altitude engagement by solid ramjet engine propulsion through fuel flow controller

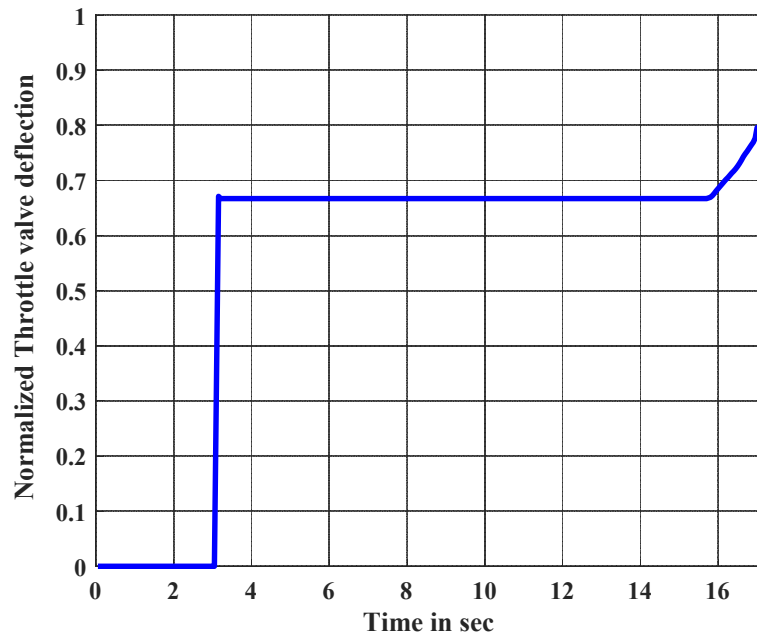


Figure-6.10: Requirement of throttle valve deflection generated by fuel flow controller for different phases of trajectory at 0.5km engagement scenario

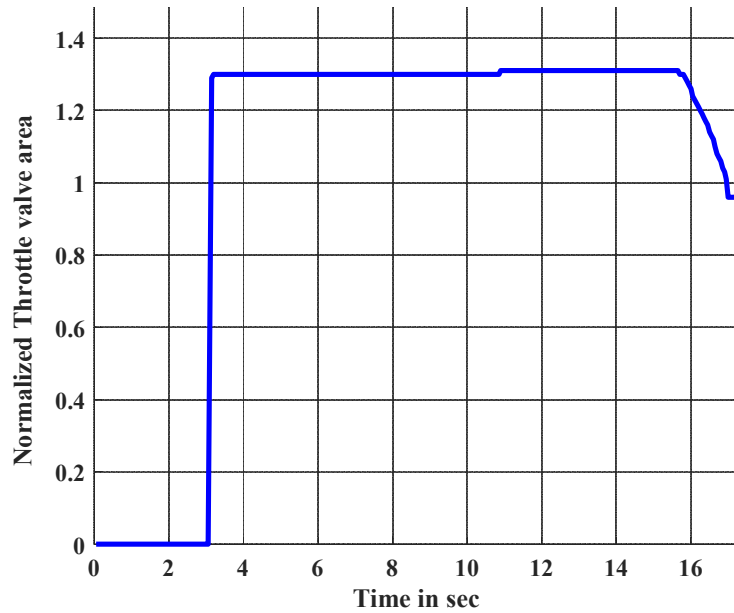


Figure-6.11: Throttle valve area profile of solid ramjet engine by changing deflection angle through fuel flow actuator for different phases of trajectory at 0.5km engagement scenario

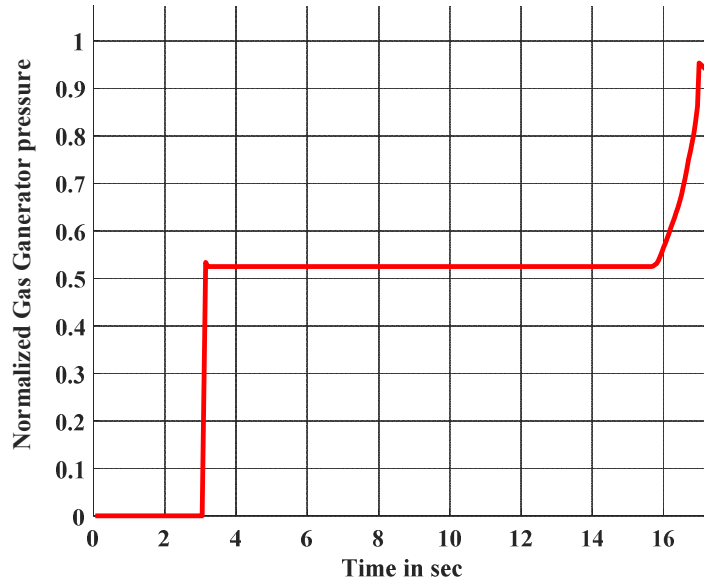


Figure-6.12: Gas generator pressure profile of solid ramjet engine by changing throttle valve area for different phases of trajectory at 0.5km engagement scenario

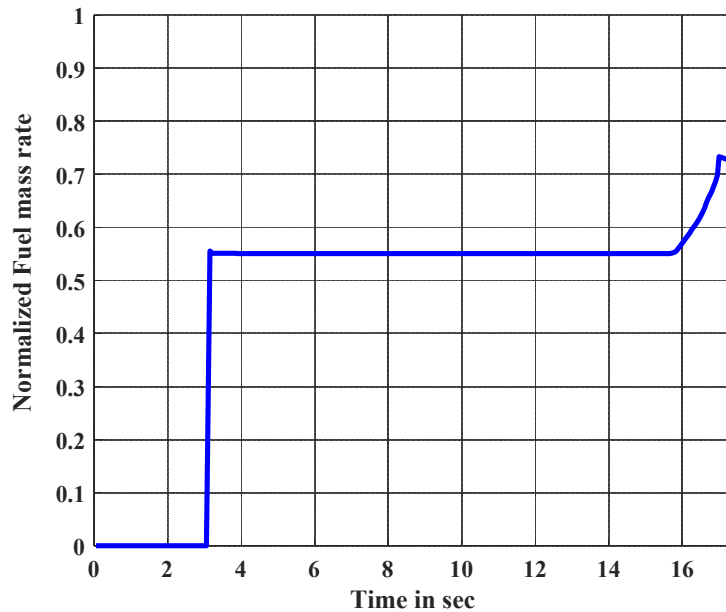


Figure-6.13: Achieved fuel mass rate profile of solid ramjet engine by changing gas generator pressure to produce thrust meeting missile velocity for different phases of trajectory at 0.5km engagement scenario

Discussion of Simulation Results:

Figure 6.7 shows that the air-to-air missile is launched from an aircraft at 0.5km altitude against the target which is also flying at the same altitude. A target starts manoeuvring in the pitch-up plane to escape from the missile. The missile autopilot generated corresponding angle of attack as shown in figure 6.8. With a high angle of attack, Mach number does not change at the end phase of trajectory due to efficient action taken by fuel flow controller as shown in figure 6.9. The miss-distance of this engagement is within warhead vicinity. Internal parameters of throttle deflection, throttle area, gas generator and fuel mass rate are shown in figure 6.10, 6.11, 6.12 and 6.13.

6.5.2 Missile-Target Engagement at 5.0km Altitude

At this altitude a similar type of engagement is simulated to validate fuel flow controller performance with the dynamic pressure comparably lower than 0.5km altitude. So, here again the target can manoeuvre to the best of its capability for escaping. Missile guidance generates lateral acceleration while autopilot executes lateral acceleration when generating angle of attack. However, to maintain the same missile velocity, fuel flow controller generates additional fuel mass rate. The performances of the missile and fuel flow controller are given below.

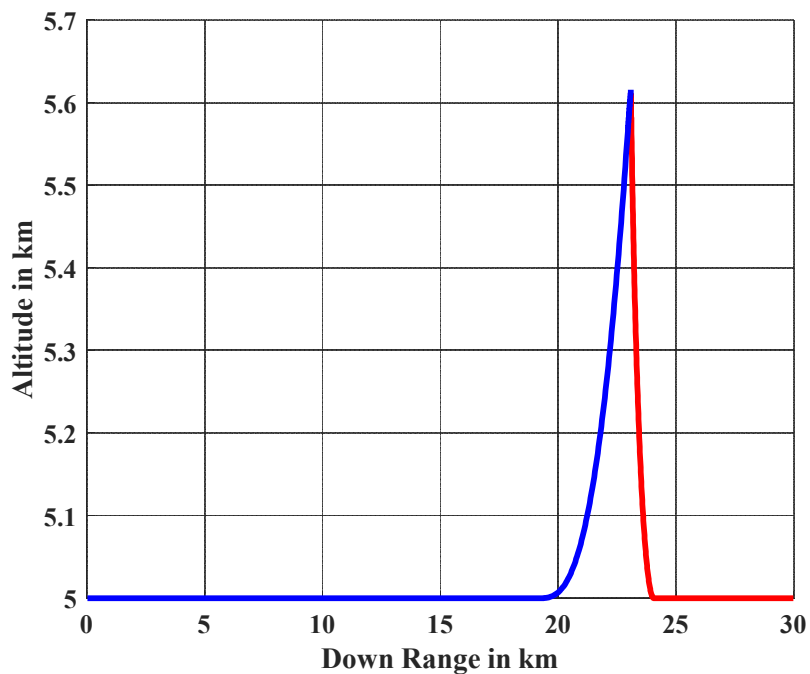


Figure-6.14: 6-DOF simulation result of missile-target engagement scenario at 5.0km altitude with manoeuvring target in pitch up plane

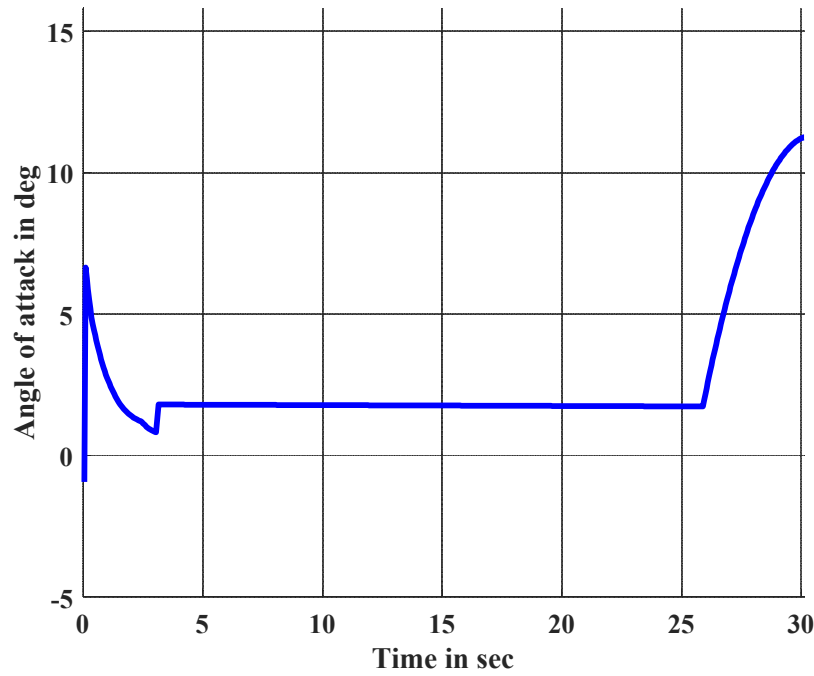


Figure-6.15: Requirement of angle of attack in different phases of trajectory at 5.0km engagement scenario

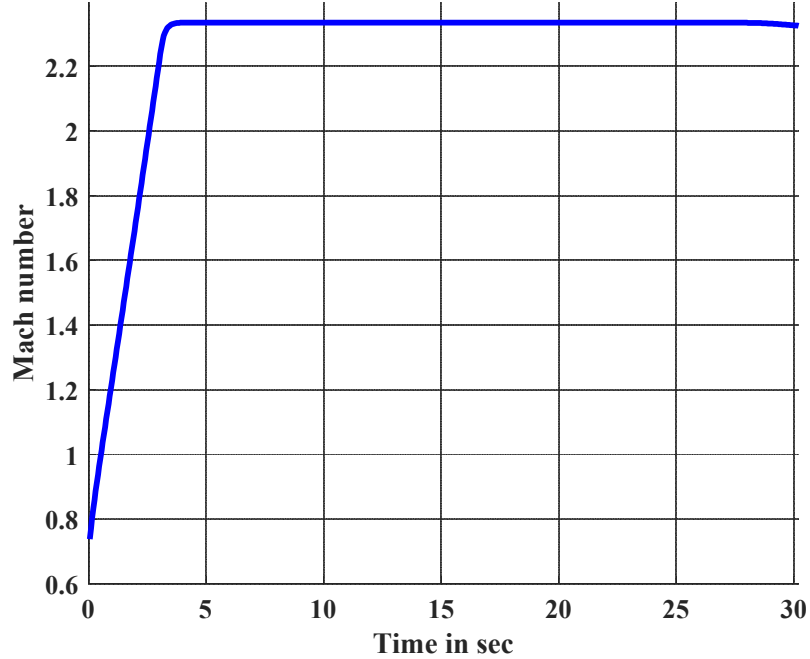


Figure-6.16: Missile Mach number (velocity) at different phases of trajectory at 5.0km altitude engagement by solid ramjet engine propulsion through fuel flow controller

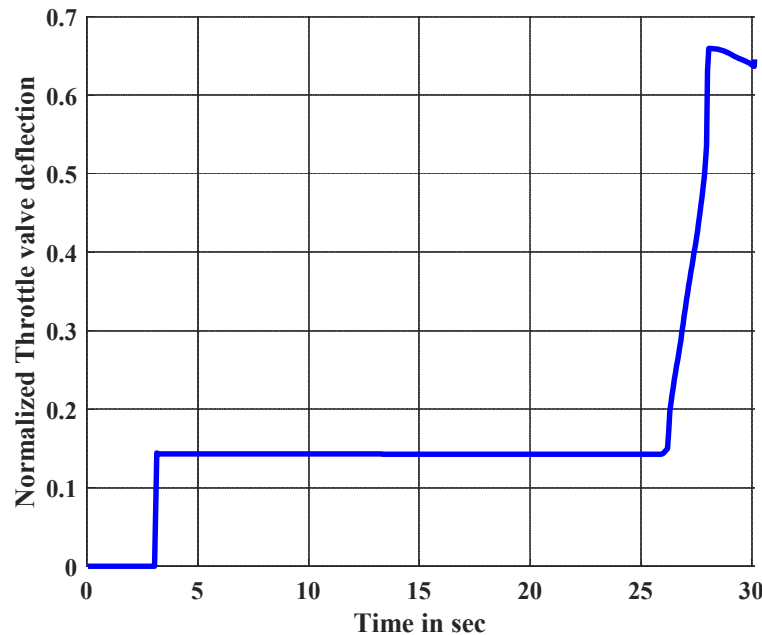


Figure-6.17: Requirement of throttle valve deflection generated by fuel flow controller for different phases of trajectory at 5.0km engagement scenario

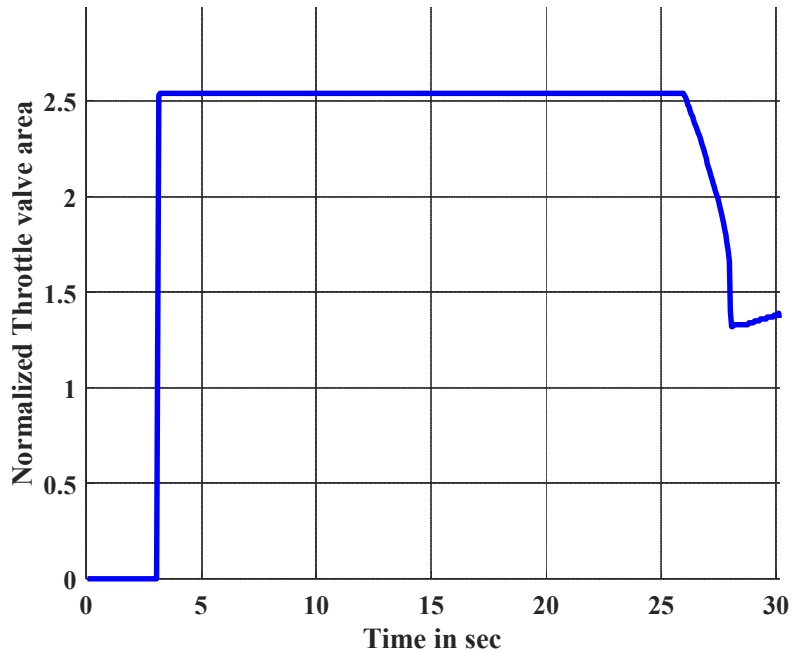


Figure-6.18: Throttle valve area profile of solid ramjet engine by changing deflection angle through fuel flow actuator for different phases of trajectory at 5.0km engagement scenario

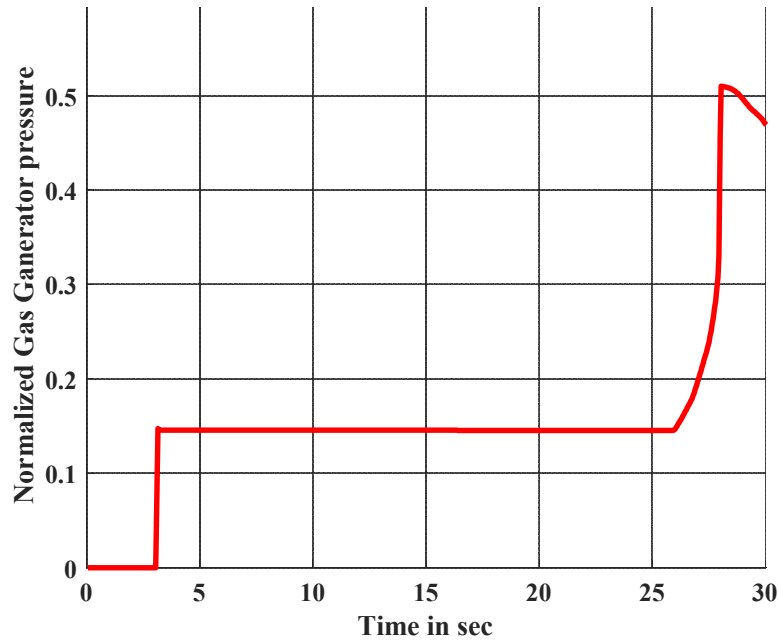


Figure-6.19: Gas generator pressure profile of solid ramjet engine by changing throttle valve area for different phases of trajectory at 5.0km engagement scenario

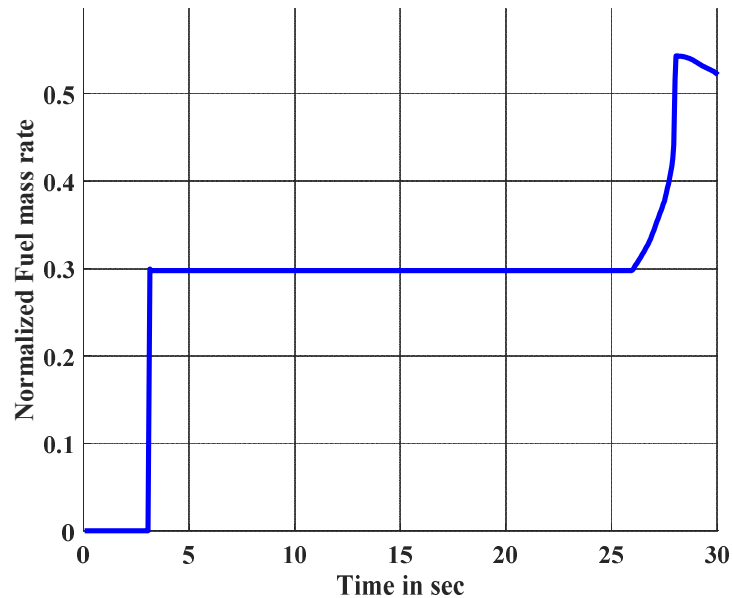


Figure-6.20: Achieved fuel mass rate profile of solid ramjet engine by changing gas generator pressure to produce thrust meeting missile velocity for different phases of trajectory at 5.0km engagement scenario

Discussion of Simulation Results:

Figure 6.14 shows that the air-to-air missile is launched from aircraft at 5.0km altitude against the target which is also flying at the same altitude. The target starts manoeuvring in pitch up plane to escape from the missile. The missile autopilot generated corresponding angle of attack as shown in figure 6.15. With this high angle of attack, Mach number does not change at the end phase of the trajectory due to prompt action taken by fuel flow controller as shown in figure 6.16. The miss-distance of this engagement is also within warhead vicinity. Internal parameters of throttle deflection, throttle area, gas generator and fuel mass rate are shown in figure 6.17, 6.18, 6.19 and 6.20.

6.5.3 Missile-Target Engagement at 10.0km Altitude

In this altitude, non-manoeuvring and manoeuvring target engagement case was evaluated to validate fuel flow controller performance. It is clearly be seen that to maintain missile velocity with and without angle of attack, prompt action is taken by the fuel flow controller. The performances of missile and fuel flow controller are given below.

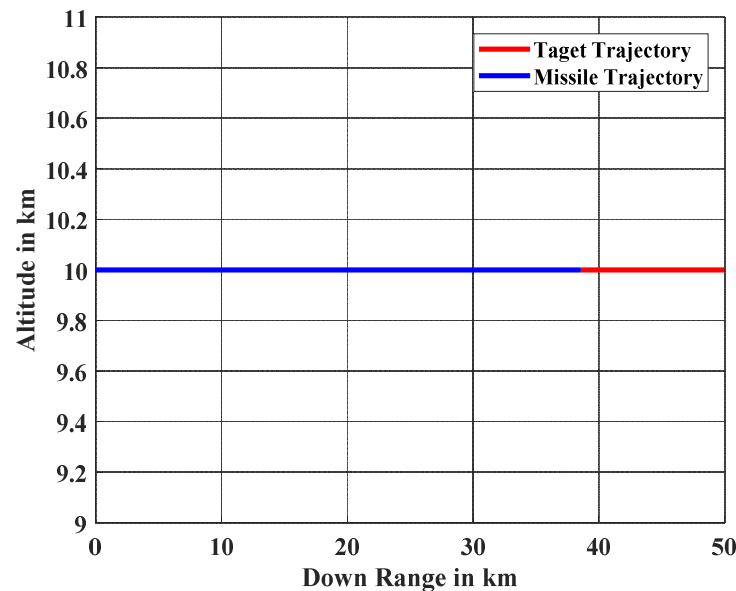


Figure-6.21: 6-DOF simulation result of missile-target engagement scenario at 10.0km altitude with non-manoeuvring target

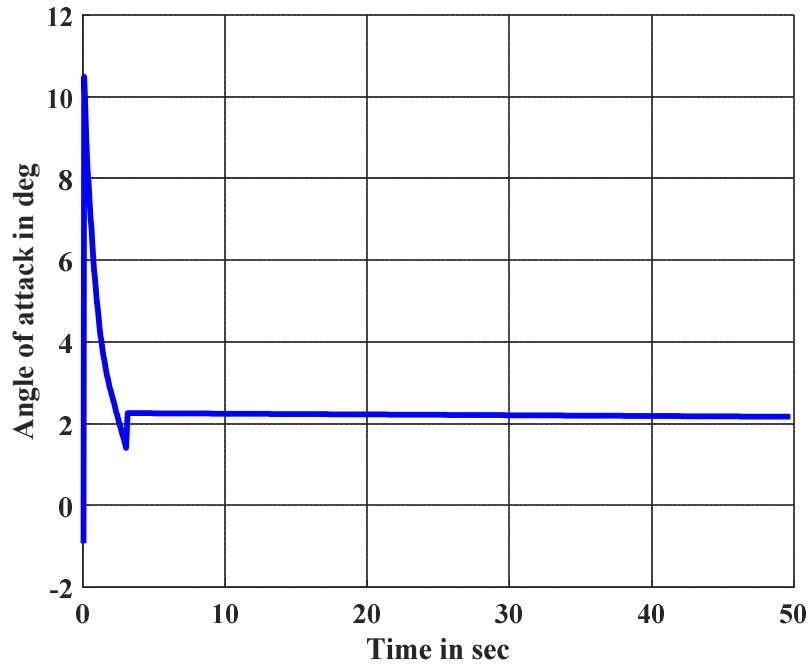


Figure-6.22: Requirement of angle of attack in different phases of trajectory at 10.0km engagement scenario

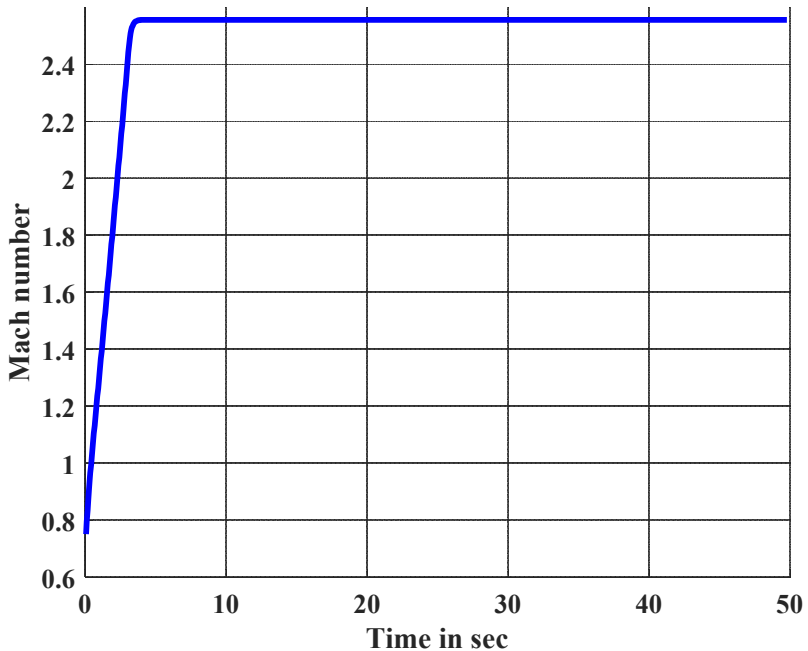


Figure-6.23: Missile Mach number (velocity) at different phases of trajectory at 10.0km altitude engagement by solid ramjet engine propulsion through fuel flow controller

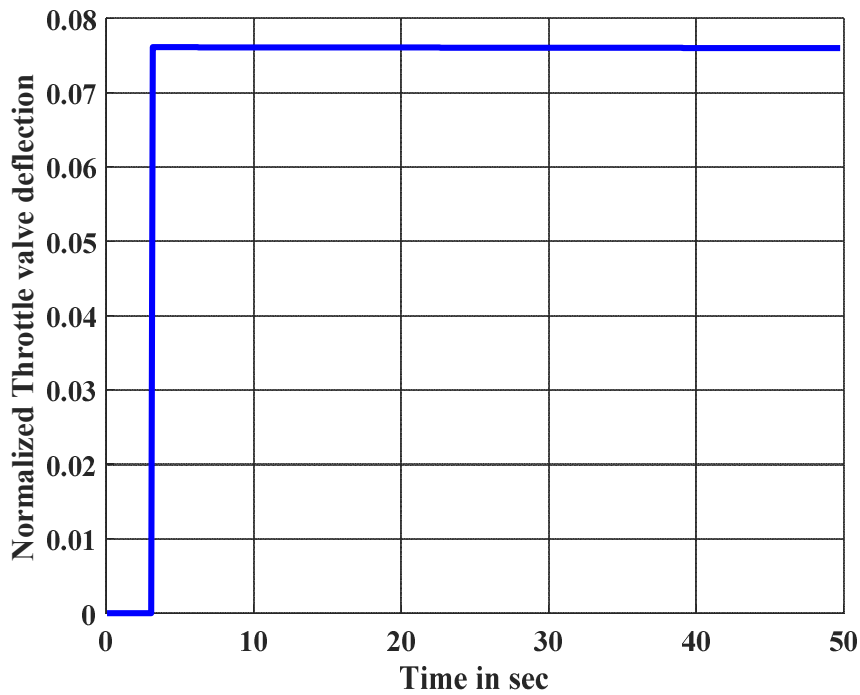


Figure-6.24: Requirement of throttle valve deflection generated by fuel flow controller for different phases of trajectory at 10.0km engagement scenario

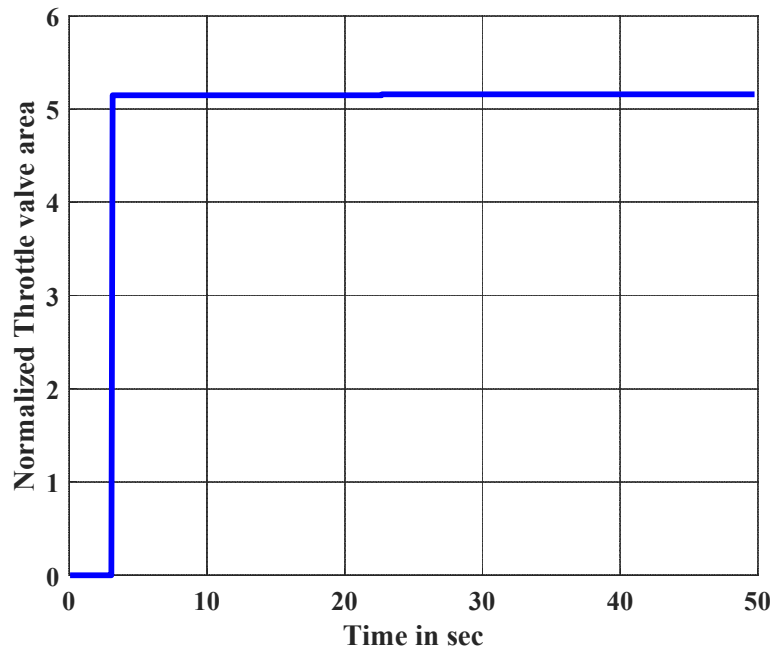


Figure-6.25: Throttle valve area profile of solid ramjet engine by changing deflection angle through fuel flow actuator for different phases of trajectory at 10.0km engagement scenario

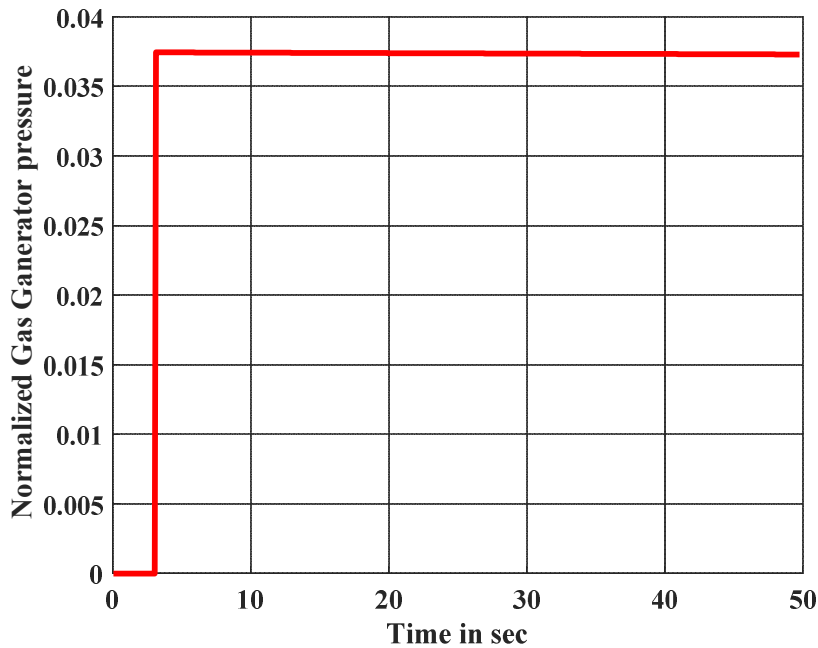


Figure-6.26: Gas generator pressure profile of solid ramjet engine by changing throttle valve area for different phases of trajectory at 10.0km engagement scenario

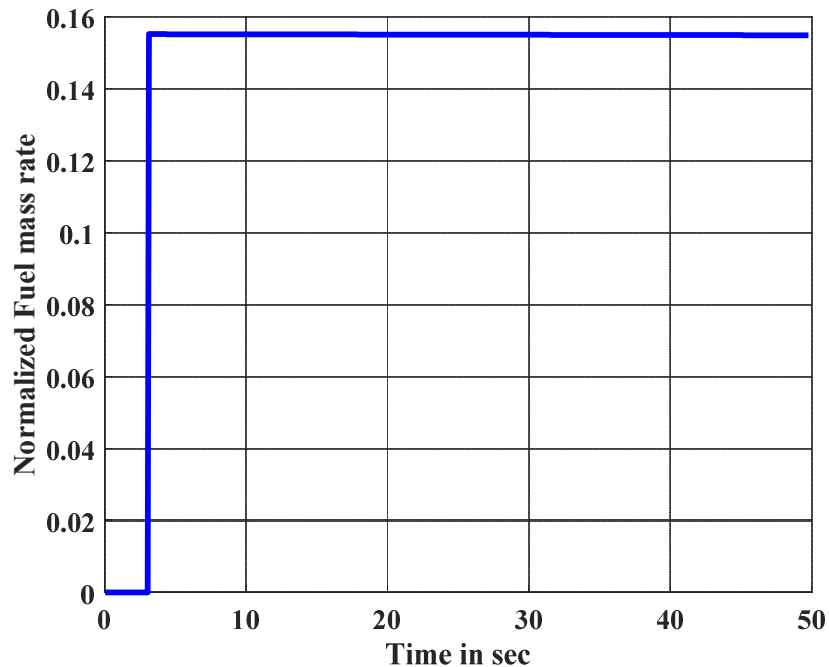


Figure-6.27: Achieved fuel mass rate profile of solid ramjet engine by changing gas generator pressure to produce thrust meeting missile velocity for different phases of trajectory at 10.0km engagement scenario

Manoeuvring case

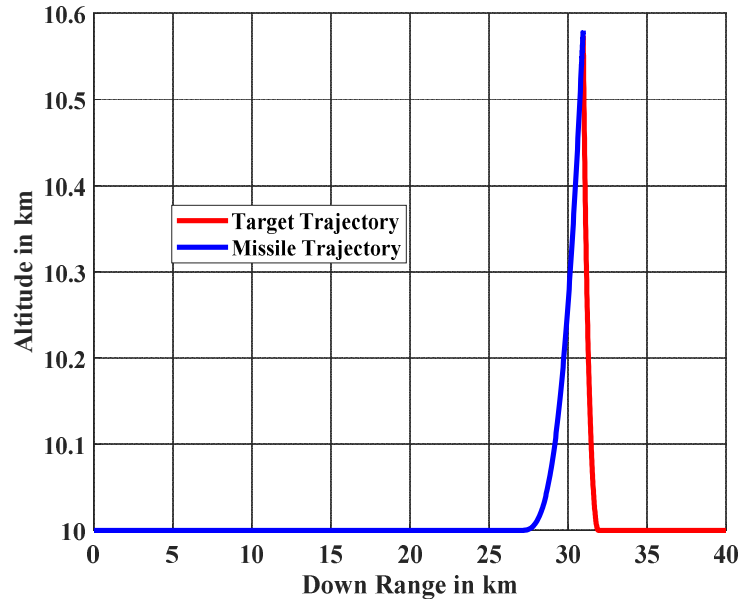


Figure-6.28: 6-DOF simulation result of missile-target engagement scenario at 10.0km altitude with manoeuvring target in pitch up plane

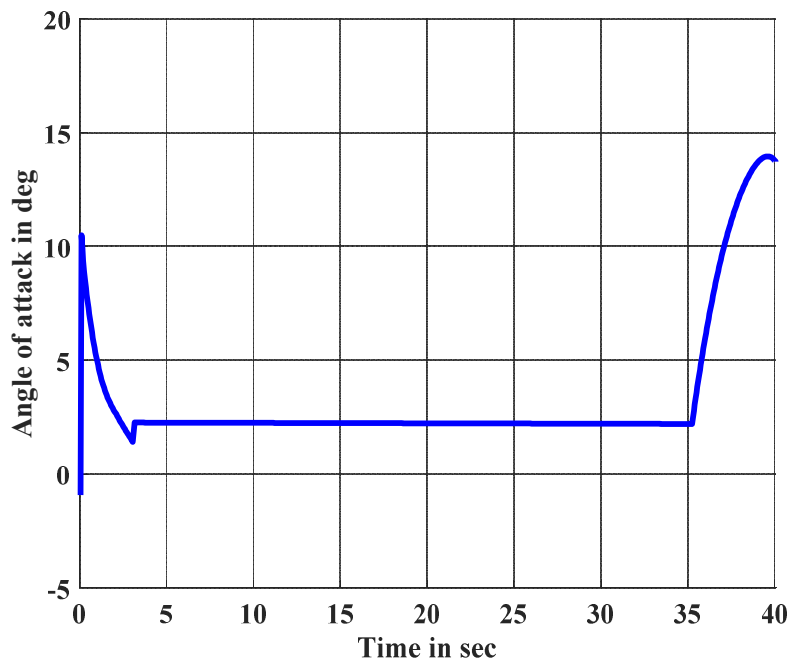


Figure-6.29: Requirement of angle of attack in different phase of trajectory at 10.0km engagement scenario

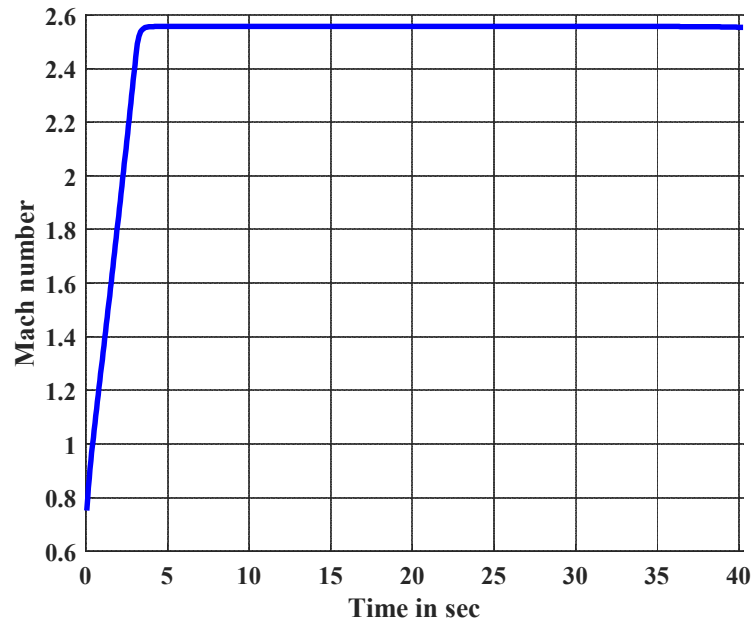


Figure-6.30: Missile Mach number (velocity) at different phases of trajectory at 10.0km altitude engagement by solid ramjet engine propulsion through fuel flow controller

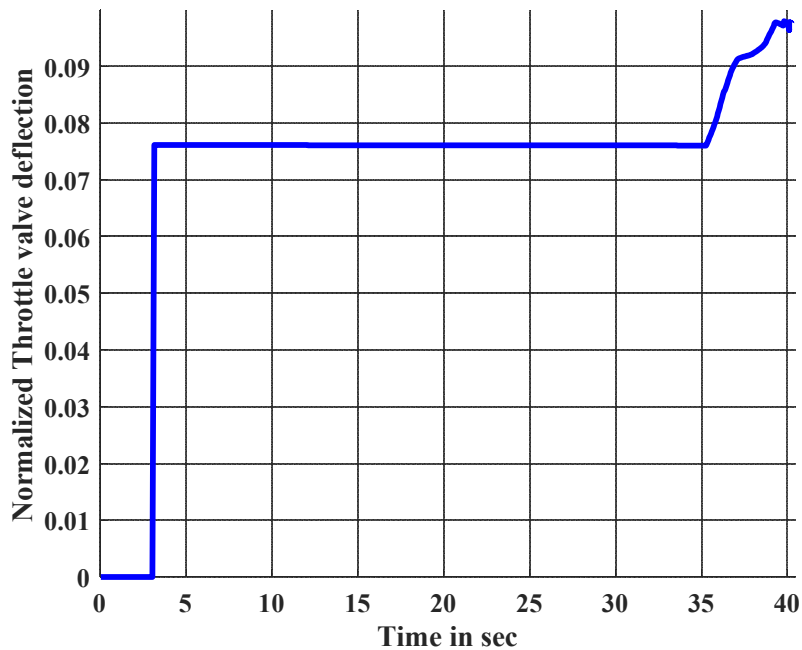


Figure-6.31: Requirement of throttle valve deflection generated by fuel flow controller for different phases of trajectory at 10.0km engagement scenario

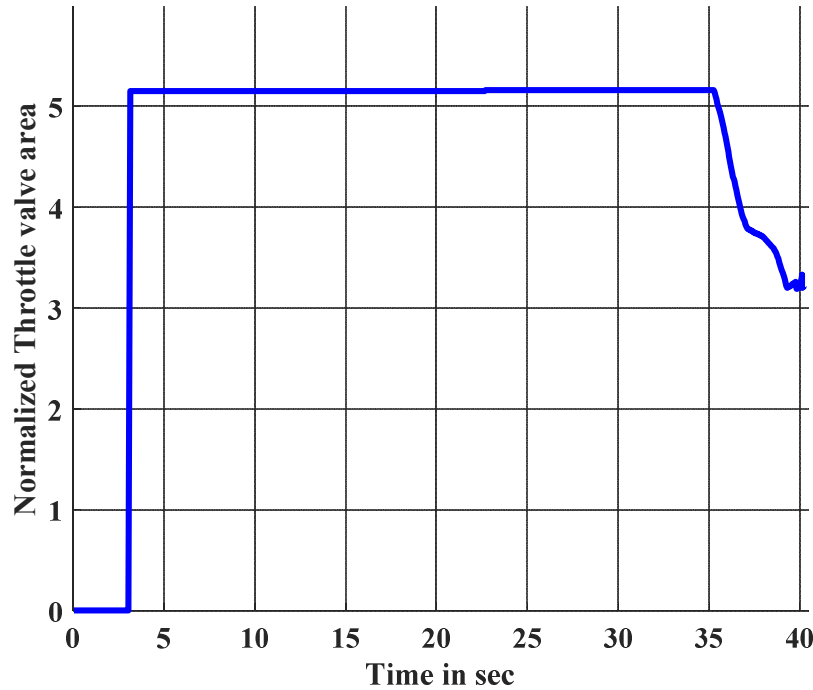


Figure-6.32: Throttle valve area profile of solid ramjet engine by changing deflection angle through fuel flow actuator for different phases of trajectory at 10.0km engagement scenario

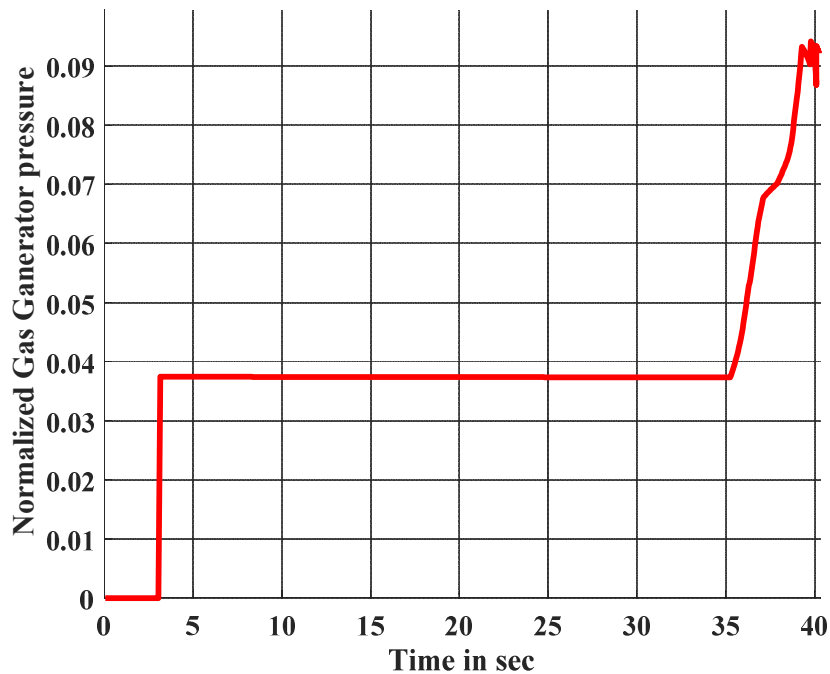


Figure-6.33: Gas generator pressure profile of solid ramjet engine by changing throttle valve area for different phase of trajectory at 10.0km engagement scenario

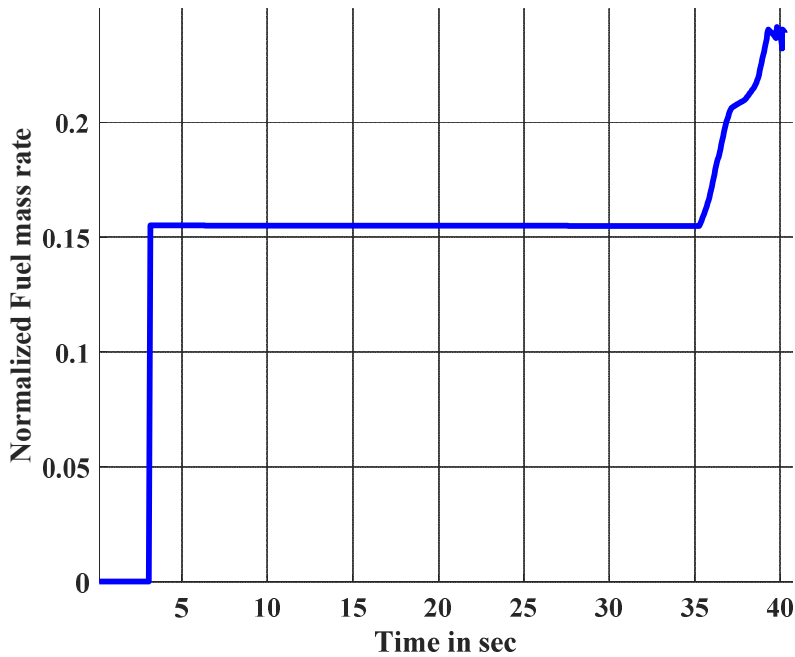


Figure-6.34: Achieved fuel mass rate profile of solid ramjet engine by changing gas generator pressure to produce thrust meeting missile velocity for different phases of trajectory at 10.0km engagement scenario

Discussion of Simulation Results:

Figure 6.21 and 6.28 show that the air-to-air missile was launched from an aircraft at an altitude of 10.0km against non-manoeuvring and manoeuvring target which was also flying at the same altitude. The missile autopilot generated the corresponding angle of attack for both trajectories as shown in figure 6.22 and 6.29. Mach number did not change at the end phase of both trajectories due to prompt action taken by fuel flow controller as shown in figure 6.23 and figure 6.30. The miss-distance of these engagements was also within the required range. Internal parameters of throttle deflection, throttle area, gas generator and fuel mass rate are shown in figure 6.24 to 6.27 and figure 6.31 to 6.34 of ramjet engine for both the trajectories. The fluctuation in ramjet engine parameters at the end also show that the performance of the third loop to maintain back pressure margin for stable operation of intake was adequate.

6.5.4 Missile-Target Engagement at 15.0km Altitude

At this altitude, a similar type of engagement was simulated to validate fuel flow controller performance. The dynamic pressure was comparatively lower at this altitude; the speed of response of fuel flow controller was higher. The dynamic behaviour of missile was also slower at this altitude. Fuel flow controller needs to generate additional fuel mass rate for meeting the above changes accordingly. The performances of the missile and fuel flow controller is given below.

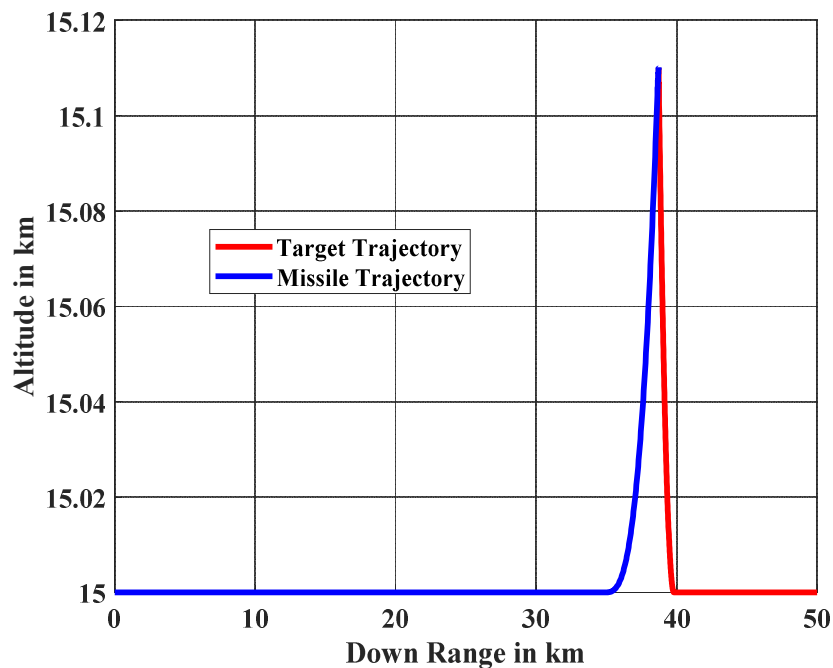


Figure-6.35: 6-DOF simulation result of missile-target engagement scenario at 15.0km altitude with manoeuvring target in pitch up plane

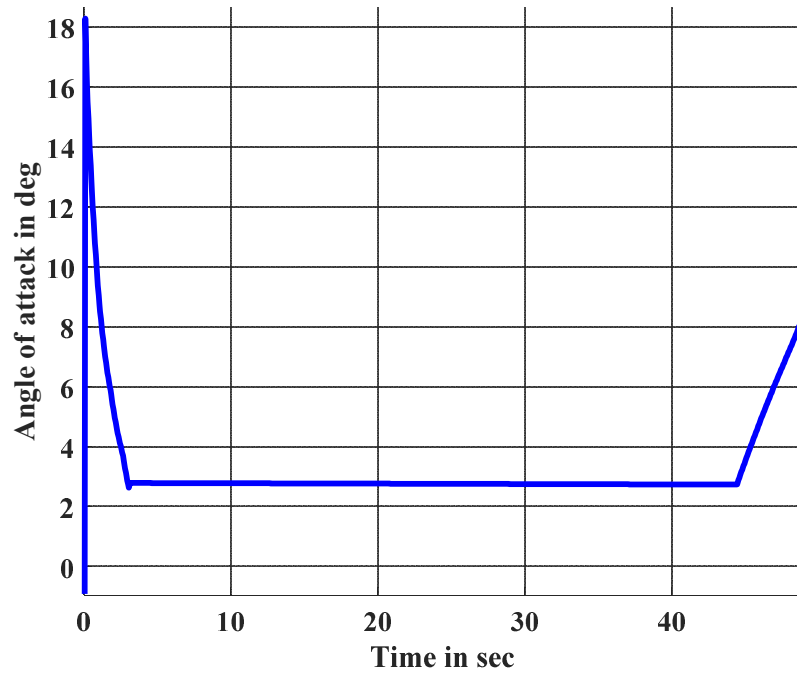


Figure-6.36: Requirement of angle of attack in different phases of trajectory at 15.0km engagement scenario

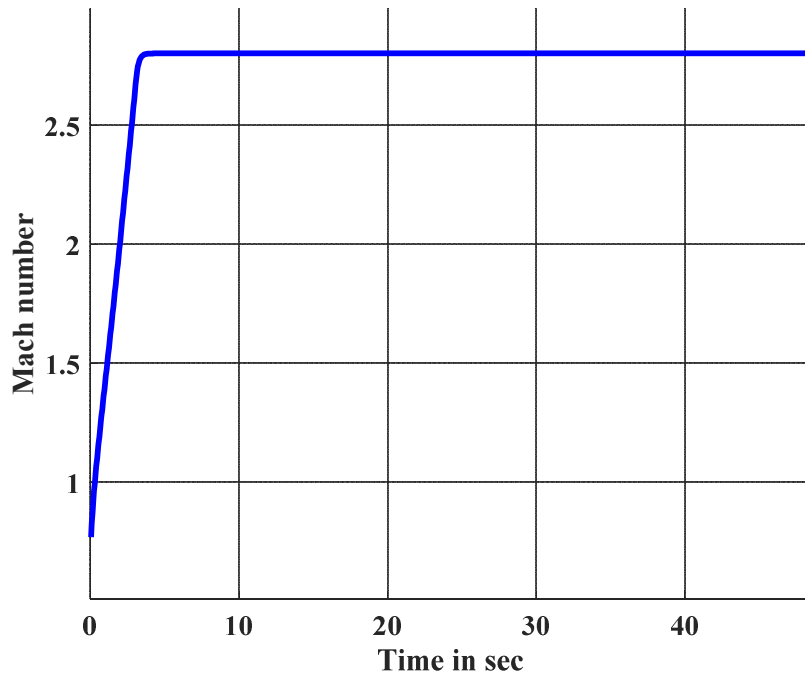


Figure-6.37: Missile Mach number (velocity) at different phases of trajectory at 15.0km altitude engagement by solid ramjet engine propulsion through fuel flow controller

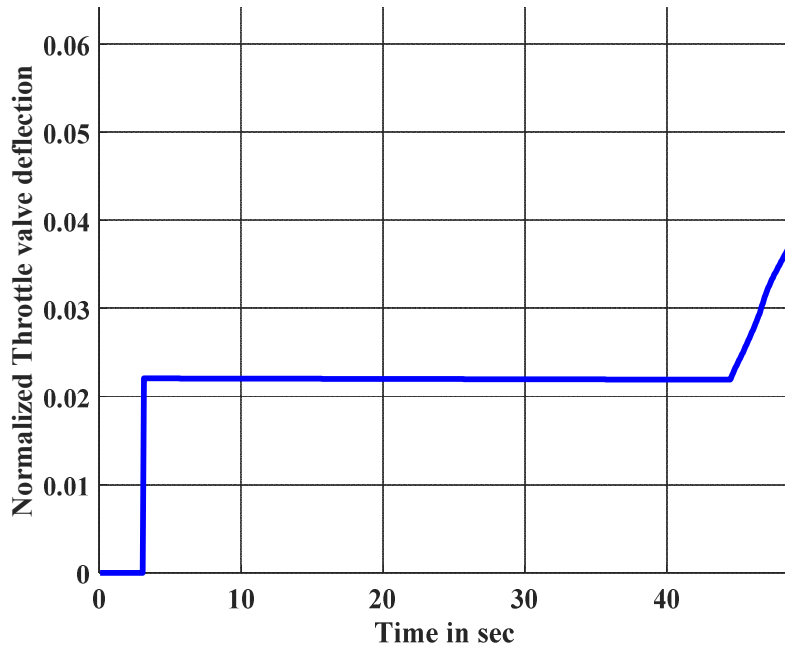


Figure-6.38: Requirement of throttle valve deflection generated by fuel flow controller for different phases of trajectory at 15.0km engagement scenario

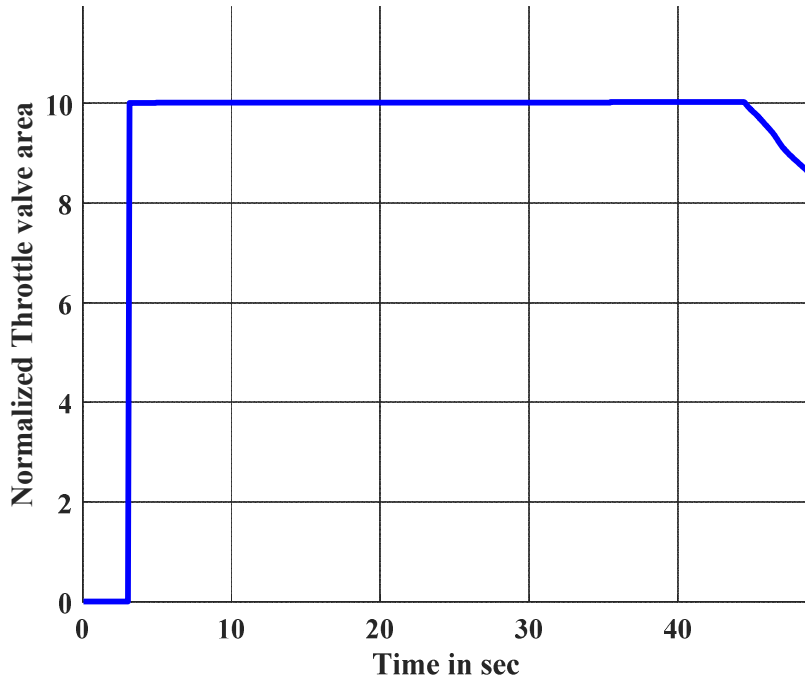


Figure-6.39: Throttle valve area profile of solid ramjet engine by changing deflection angle through fuel flow actuator for different phases of trajectory at 15.0km engagement scenario

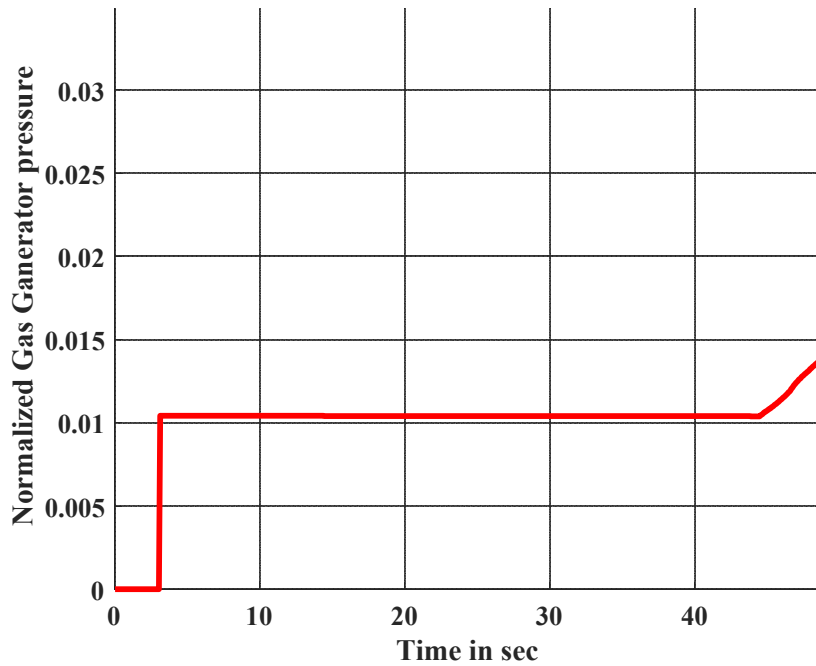


Figure-6.40: Gas generator pressure profile of solid ramjet engine by changing throttle valve area for different phases of trajectory at 15.0km engagement scenario

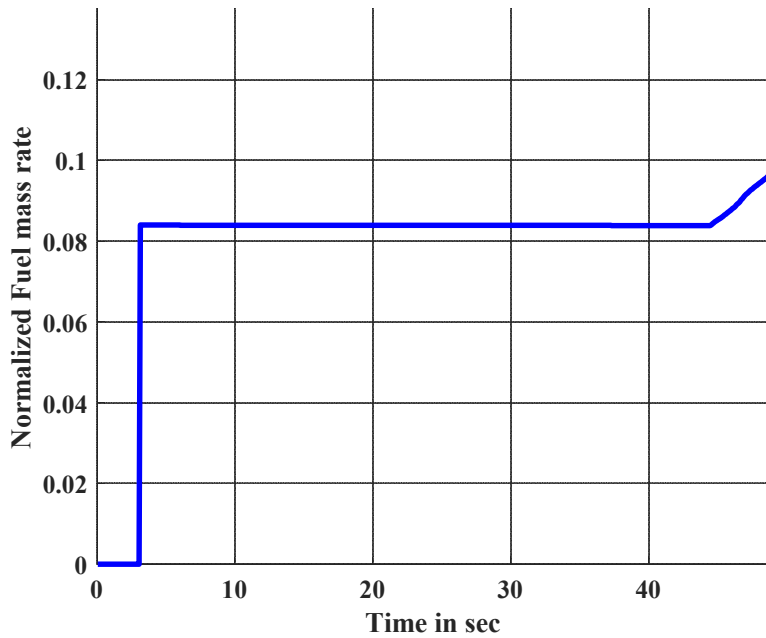


Figure-6.41: Achieved fuel mass rate profile of solid ramjet engine by changing gas generator pressure to produce thrust meeting missile velocity for different phases of trajectory at 15.0km engagement scenario

Discussion of Simulation Results:

Figure 6.35 shows that the air-to-air missile was launched from aircraft at 15.0km altitude against the target which was also flying in same altitude. A target starts manoeuvring in pitch up plane to escape from the missile. The missile autopilot generated corresponding angle of attack as shown in figure 6.36. With this high angle of attack, Mach number was not changed at the end phase of trajectory due to action taken by fuel flow controller as shown in figure 6.37. The miss-distance of this engagement was also within requirement. Internal parameters of throttle deflection, throttle area, gas generator and fuel mass rate are shown in figure 6.38, 6.39, 6.40 and 6.41.

6.5.5 Missile-Target Engagement at Varying Altitude (Snap Down condition)

In this engagement scenario, varying altitude trajectory was simulated to validate fuel flow controller requirements that were dynamically changing with respect to altitude and dynamic pressure. The performances of missile and fuel flow controller are given below.

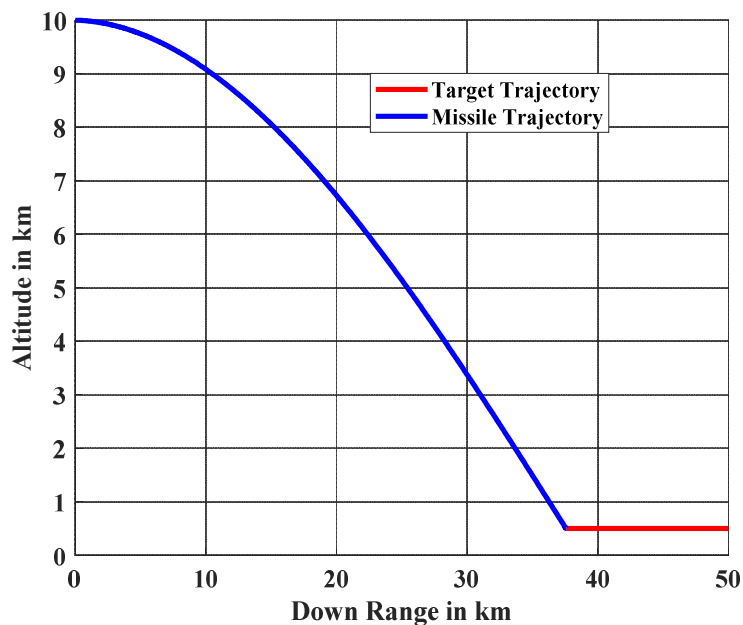


Figure-6.42: 6-DOF simulation result of missile-target varying altitude engagement scenario (Snap down condition) from 10.0km to 0.5km altitude with non-manoeuvring target

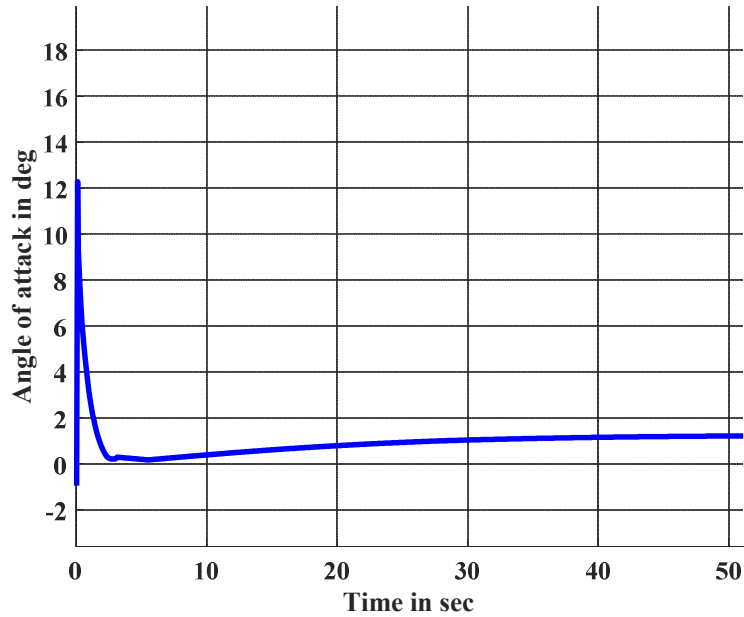


Figure-6.43: Requirement of angle of attack in different phases of trajectory at varying altitude engagement scenario (Snap down condition) from 10.0km to 0.5km altitude

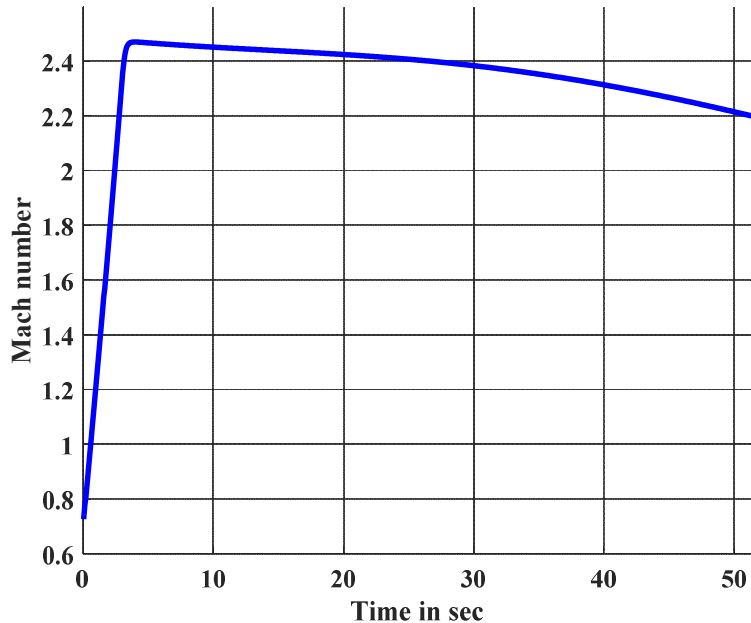


Figure-6.44: Missile Mach number (velocity) at different phases of trajectory at varying altitude engagement scenario (Snap down condition) from 10.0km to 0.5km altitude by solid ramjet engine propulsion through fuel flow controller

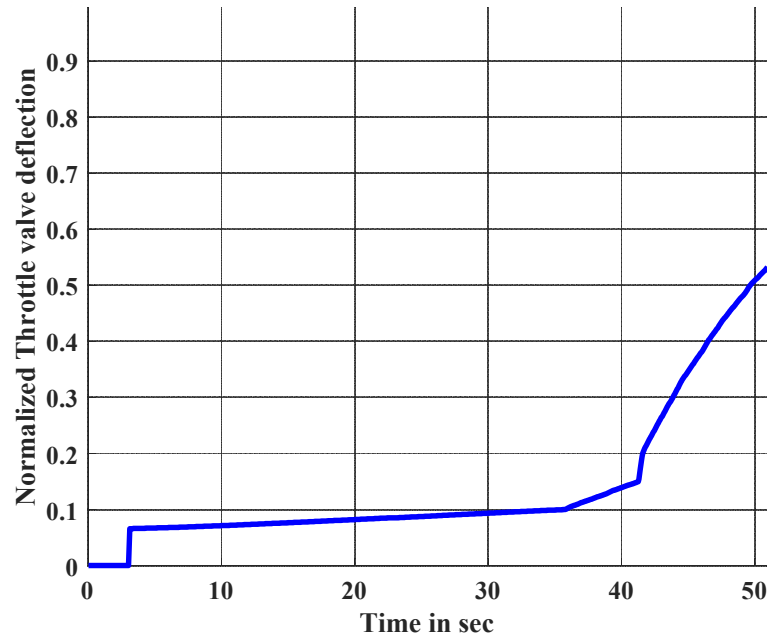


Figure-6.45: Requirement of throttle valve deflection generated by fuel flow controller for different phases of trajectory at varying altitude engagement scenario (Snap down condition) from 10.0km to 0.5km altitude

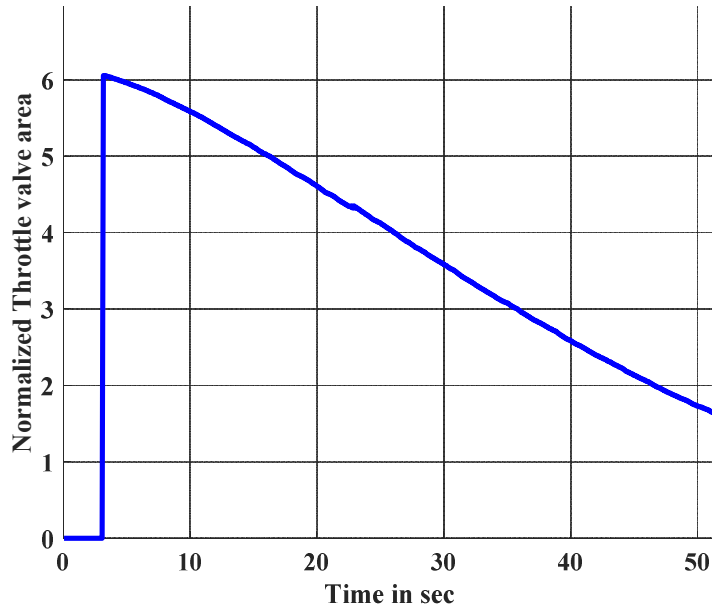


Figure-6.46: Throttle valve area profile of solid ramjet engine by changing deflection angle through fuel flow actuator for different phases of trajectory at varying altitude engagement scenario (Snap down condition) from 10.0km to 0.5km altitude

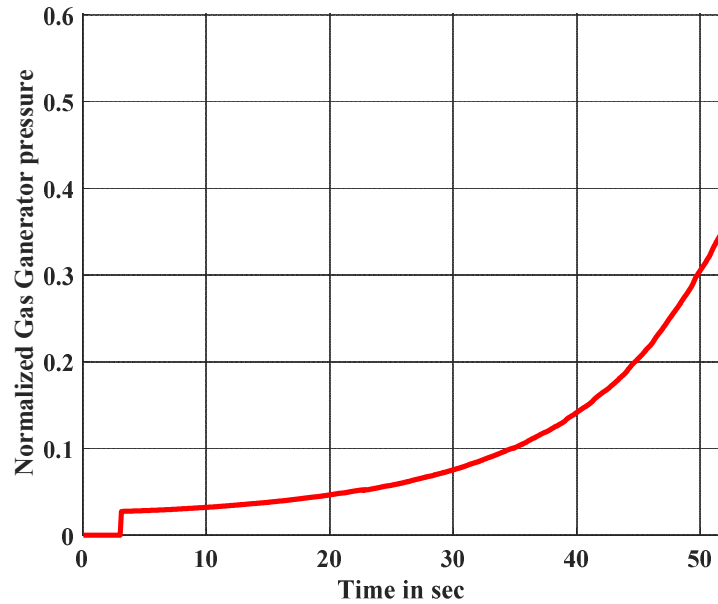


Figure-6.47: Gas generator pressure profile of solid ramjet engine by changing throttle valve area for different phases of trajectory at varying altitude engagement scenario (Snap down condition) from 10.0km to 0.5km altitude

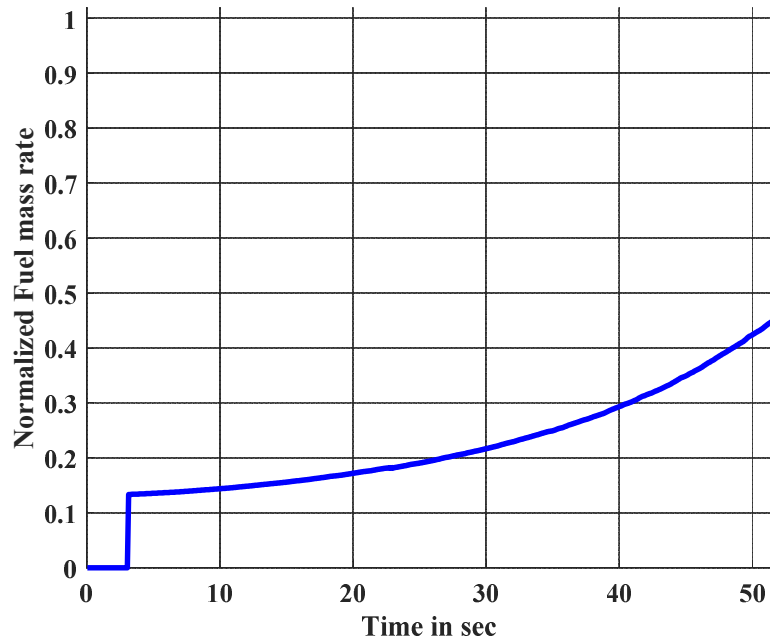


Figure-6.48: Achieved fuel mass rate profile of solid ramjet engine by changing gas generator pressure to produce thrust meeting missile velocity for different phases of trajectory at varying altitude engagement scenario (Snap down condition) from 10.0km to 0.5km altitude

Discussion of Simulation Results:

Figure 6.42 shows that the air-to-air missile was launched from an aircraft at 10.0km altitude against the target which was also flying at 0.5km altitude. Angle of attack requirement kept changing throughout the trajectory as shown in figure 6.43. Mach number did not change throughout the trajectory due to dynamic action taken by fuel flow controller as shown in figure 6.44. The miss-distance of this engagement was low and within limits. Internal parameters of throttle deflection, throttle area, gas generator and fuel mass rate are shown in figure 6.45, 6.46, 6.47 and 6.48.

6.6 Fuel Flow Controller Robustness (Stability) studied in Closed Loop

In classical linear controller, different gains are scheduled for different operating conditions to get the desired response at different Mach number and angle of attack. In nonlinear controller, desired dynamics were imposed on all loops based on operating conditions like angle of attack, Mach number and altitude. The same dynamics is not possible at every operating condition because the response of gas generator is different at different operating conditions. So, the fuel flow controller design of the outer loop dynamics was chosen as a function of above mentioned parameters and the desired dynamics for gas generator loop was chosen for second order dynamics, which is defined by bandwidth ω and damping ζ . Stability of fuel flow controller was checked inserting $Ke^{-j\omega\tau}$ gain-phase offset criteria at fuel flow actuator input point and at gas generator pressure feedback point. Typically, gain offset Vs phase offset curve looks like the one shown in figure 6.49, where gain offset is obtained by perturbing computed deflection of fuel flow actuator by introducing gain variation and phase.

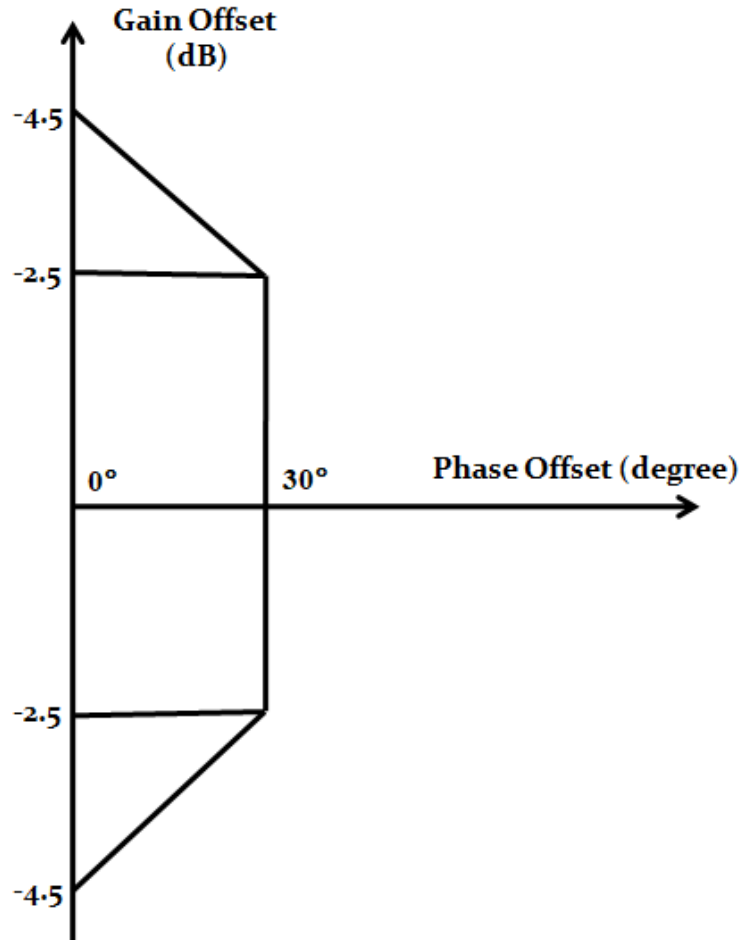


Figure-6.49: Gain-phase offset for loop criteria with plant perturbation

So, the above points A, B, C, D as shown in figure 6.49, gain offset are:

$$A \equiv 1.666(4.5dB)$$

$$B \equiv 1.33(2.5dB)$$

$$C \equiv 0.75(-2.5dB)$$

$$D \equiv 0.60(-4.5dB)$$

It is found that the fuel flow controller minimum phase margin in closed simulation in 6-DOF is always more than 30° for all above trajectories from 0.5km to 15km with aerodynamics parameter perturbation of ($\pm 10.0\%$), inertial perturbation of ($\pm 1.0\%$) and gas generator propellant perturbation of ($\pm 0.5\%$).

6.7 Monte-Carlo simulation results and analysis

Monte-Carlo simulation was carried out to evaluate the performance of fuel flow controller in overall performance of air-to-air missile considering aerodynamics perturbation and inertial parameters uncertainty. It was observed that each sub-system take inputs from other sub-systems and provides output to other sub-systems too. So, in Monte-Carlo simulation when the parameters are perturbed, missile dynamic behaviour affects the basic input parameter to fuel flow controller for ramjet engine performance. Under this one typical air-to-air missile engagement scenario has been simulation with a manoeuvring target. The outcome of ramjet engine with fuel flow controller impact the performance of guidance demand and angle of attack of missile as shown in figure 6.50. So miss-distance as end result is shown in figure 6.51 to show how air-to-air missile with the designed controller are able to satisfy the trajectory requirement..

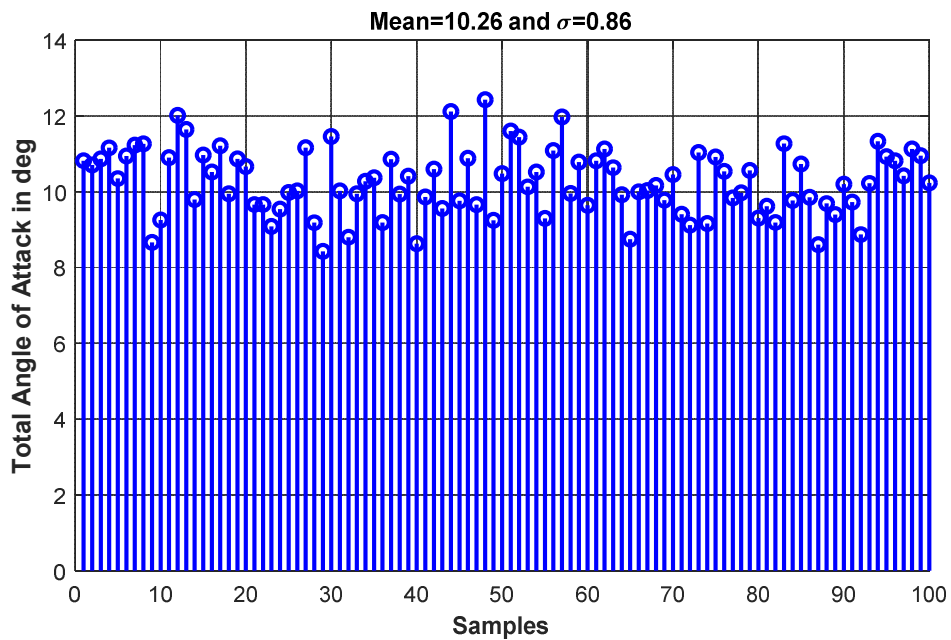


Figure-6.50: Angle-of-attack at each runs of 6-DOF simulation for different missile perturbations and parameters uncertainties in Monte-Carlo simulation with manoeuvring aerial target

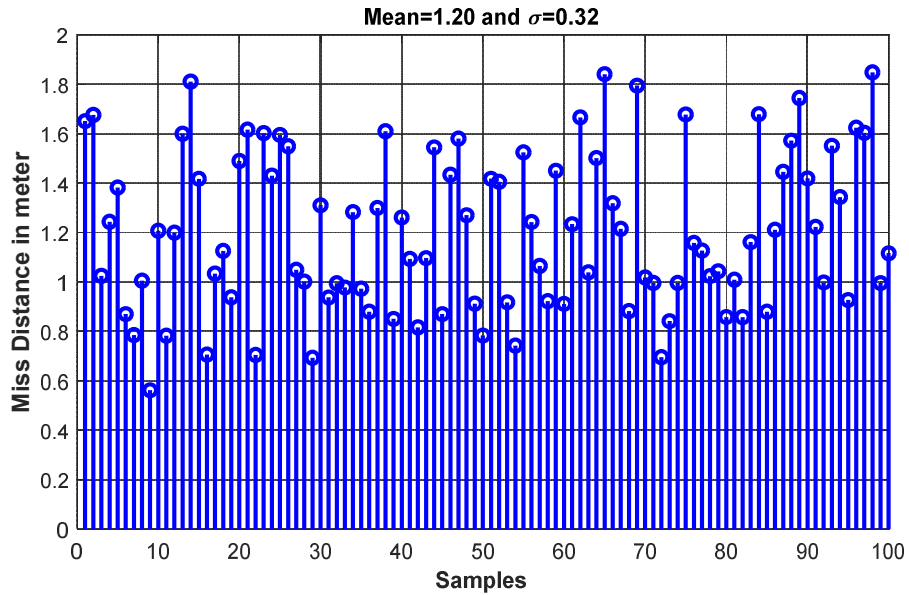


Figure-6.51: Miss-Distance performance at each runs of 6-DOF simulation along with fuel flow controller for different missile perturbations and parameters uncertainties in Monte-Carlo simulation with manoeuvring aerial target

6.8 Summary

In this chapter, air-to-air missile engagement scenario and operational mission sequence requirements have been brought out against the target. The operation and role of fuel flow controller for different mission phase are presented. Furthermore, the six-degrees-of-freedom (6-DOF) model where all sub-systems including guidance, autopilot and its interaction along with fuel flow controlled for trajectory has been also presented. The performance of fuel flow controller was tested at 0.5km, 5km, 10km, 15km engagement and a snap down condition in which altitude and Mach number was varying in trajectory. In all the above engagements, the performance of air-to-air missile was satisfactory and miss-distance was within the stipulated limits. It was also found that the miss-distance is within the requirement under missile perturbations and uncertainties in Monte-Carlo simulation. Hence, the proposed three loop structure based fuel flow controller can be used for any type of air-to-air missile against an aerial target which is based on solid fuel ramjet propulsion system.

Chapter 7

Conclusions

Chapter 7

Conclusions

7.1 Introduction

In this thesis, a nonlinear dynamic inversion based fuel flow controller has been designed for solid fuel ramjet propulsion for air-to-air tactical missile applications. An efficient performance of ramjet propulsion was ensured through two loop fuel flow controller meeting the missile guidance and autopilot requirement to ensure desirable miss-distance performance with aerial target. Furthermore, stable performance of ramjet propulsion was investigated through three loop structure based fuel flow controller ensuring air intake performance for ramjet operation in the presence of disturbances. This chapter presents in brief the significance of the design proposed in this thesis while also discussing future extension of the proposed work.

7.2 Conclusion

The following conclusions have been arrived at from research carried out and reported in previous chapters.

1. The study developed a mathematical model of the ramjet engine keeping in mind angle of attack for more efficient design of fuel flow controller.
 - Ramjet system is a dynamic system and its performance depends on aerodynamic configuration and operating conditions of missile like altitude, Mach number and angle of attack.
 - Without considering angle of attack for ramjet model, the design of fuel flow controller to produce thrust force, is not adequate to meet velocity requirements in the presence of missile manoeuvring. This design may be important for testing and stabilising the ramjet technology on ground.

- When considering angle of attack in ramjet model, the design of fuel flow controller provided the required thrust which have been presented and shown in various engagement scenarios from sea-level to 15km altitude with missile manoeuvring.
- 2. The design specifications of fuel flow controller have been brought out as a function of altitude and Mach number to meet the guidance loop requirement of air-to-air missile flight trajectory at different altitudes.
 - The rate of generating angle of attack, while the missile do manoeuvres, is a function of altitude and Mach number. This affects the missile velocity and deteriorates overall performance.
 - Missile proportional navigation guidance and autopilot generate and execute lateral acceleration demand as a function of altitude and Mach number to ensure meeting the miss-distance requirement. So, fuel flow controller speed of response was evaluated to meet the guidance loop design requirement of missile as a function of altitude and Mach number.
 - Modelling of guidance loop was carried out for different time constant as a function of altitude to bring out the specifications of fuel flow controller.
 - To meet the fuel flow controller speed of response (Bandwidth), the fuel flow actuator specification was generated based on loop separation theory.
- 3. Two loop fuel flow controller based on nonlinear dynamic inversion technique were designed to meet the specification as a function of altitude, Mach number and angle of attack.
 - To meet the guidance loop time constant specification, two loop formulations were carried out, Mach number as outer loop and gas generator pressure as inner loop. Outer loop design relation generates the requirement of inner loop while meeting the guidance loop specification as a function of altitude. Further, the inner loop design relation generates the requirement of throttle area.
 - The dynamic of gas generator along with aerodynamics is nonlinear in nature. Gas generator dynamic (Inner loop) is faster than Mach number dynamic (Outer loop). So, time scale separation exists in the dynamic system.
 - To obtain the desired fastness and accuracy, nonlinear dynamic inversion technique was adopted. It can be achieved by inverting the governing equations of individual dynamics based on measured state and input command.

- Operation of air-to-air missile can vary from low altitude to high altitude. So, step by step relation of outer and inner loop has ensured control gain of fuel flow controller as a function of altitude, Mach number and missile parameters to meet the design requirement.
- Performance of fuel flow controller was presented at different Mach number condition to show design efficiency.

4. Three loop structure based fuel flow controller designed for stable operation of ramjet engine.

- The performance of air intake play a crucial role to provide adequate air mass flow rate in combustion chamber for producing the thrust. The compression of atmospheric air happens due to terminal shock formation inside the air intake duct. Terminal shock location is stable if back pressure (combustion chamber pressure) margin is within the band. Any disturbance beyond the band creates intake instability like un-start and buzz.
- Buzz modeling was carried out to find oscillatory behavior as a function of altitude and Mach number.
- An innovative three loop structure based fuel flow controller was proposed using feed forward dynamic inversion to protect pressure margin of intake in the presence of disturbance.
- Performance of third loop presented with intake buzz and its impact on other parameters were brought out.

5. Design of fuel flow controller has been validated in six-degrees-of-freedom simulation platform of missile with guidance and autopilot. Air-to-Air missile performance has been presented at different engagement scenarios from sea-level (0.5km), 5.0km, 10km, 15km altitude and snap down condition (varying altitude) along with non-manoeuvring and manoeuvring aerial targets and overall missile performance like miss-distance was ensured within the desired limit. Stability margin of fuel flow controller was evaluated in closed loop while introducing gain and delay. Monte-Carlo simulation was carried out under different types of perturbation to bring out miss-distance performance of missile with fuel flow controller. It shows that the fuel flow controller design is efficient and stable.

6. Hence, the proposed fuel flow controller design can be used for all types of air-to-air missile or surface-to-air missile against an aerial target which is based on solid ramjet propulsion system.

7.3 Scope for Future Research

In gas generator, the Solid fuel get burnt and converts into gaseous form. The fuel gases needs to be flown from gas generator to combustion chamber through the throat valve produce thrust. Due to high temperature and pressure, the gases fuel can ablate the throat or deposition on throat which makes it very hard to control the required fuel flow rate due to change in throat area characteristics. So, this type of problem can be solved by conducting a huge number of ramjet engine tests at different conditions and further this data may be used for improving the ramjet engine characteristics.

References

1. P. Zarchan, "Tactical and Strategic Missile Guidance (Sixth edition)", American Institute of Aeronautics and Astronautics, pp 107-135, 2013.
2. S. S. Chin, "Missile Configuration design", McGraw-Hill Book, pp 107-112, 1961
3. George M. Siouris, "Missile Guidance and Control Systems", Springer-Verlag New York, Inc. pp 53-222, 2004.
4. Eugene L. Fleeman, "Tactical Missile Design", AIAA Education series, pp 17-88, 2001.
5. George P. Sutton, "Rocket Propulsion Elements", Seventh edition, 2001, John Wiley & Sons,
6. S.F. Ronald, "A century of ramjet propulsion technology evolution", Journal of Propulsion and Power, Vol. 20 (1), pp 27-58, 2004.
7. H. L. Besser, "History of ducted rocket development at Bayern Chemie", 44th AIAA/ASME/SAE/ASEE, Joint Propulsion Conference & Exhibit, July, 2008. DOI: 10.2514/6.2008-5261
8. R. Wilson, C. Limage, P. Hewitt, "The evolution of ramjet missile propulsion in the U.S. and where we are headed". AIAA, Paper 1996-3148, 1996.
9. J. L. Moerel, R. F. Calzone, W. H. C. Halswijk, R. M. Van Der Horst, R. Stowe and M. Lauzon, "Performance simulation of a rocket and a ramjet air-to-air missile", AIAA-2001-4412, AIAA Modelling and Simulation Technologies Conference and Exhibit, Montreal, Canada, Aug. 6-9, 2001.
10. A. E. H. J. Mayaer, W. H. C. Halswijk, H. J. Komduur, R. Stowe and M., Lauzon, "A Modular ducted rocket missile for threat and performance assessment", AIAA Modelling and Simulation Technologies Conference and Exhibit, San Francisco, California, AIAA 2005-6013, 15-18 Aug. 2005.
11. T. Miyamoto and H. Matsumoto, "An Experimental Study on an Air Intake Performance for a Rocket/Ramjet Engine", in Proc. AIAA/SAE/ASME 17th Joint Propulsion Conference, Colorado Springs, Colorado, July 27-29, 1981.
12. C. Hirschen, D. Hermann and A. Gulhan, "A Expermintal investigation of the performance and unsteady behaviour of a supersonic intake", J Propulsion Power, 23(3), pp.566-574, 2007.

13. M. S. Y. Ebaid and K. J. M. Al-Khishali, “ The effect of multiple conical shock waves at the engine intake on the performance of a single-mode ramjet”, Proc Institution of Mechanical Engineers Part G: Journal of Aerospace Engineering 2014, Vol 228(7), pp. 1183-1194, 2013.
14. J. L. Moerel, R. G. Veraar and W. H. C. Halswijk. “ Internal Flow Characteristics of a Rectangular Ramjet Air Intake”, AIAA/ASME/SAE/ASEE 45th Joint Propulsion Conference & Exhibit, Denver, Colorado, 2-5 August, 2009. DOI: 10.2514/6.2009-5076
15. J., Seddon and E. L. Goldsmith, “*Intake Aerodynamics*”, AIAA Education Series, AIAA, New York, Chap.13, 1985
16. J. Seddon and E. L. Goldsmith, “*Practical Intake Aerodynamics Design*”, AIAA Education Series, AIAA, New York, Chap.5, 1998.
17. Dirk Herrmann and Ali Gulhan, “Influence of intake Orientation on Ramjet Peformance”, Journal of Propulsion and Power, Vol. 26, No. 4, July-August 2010.
18. W. Miller, S. McClendon and W. Burkes, “Design approaches for variable flow ducted rockets,” in Proc. AIAA/SAE/ASME 17th Joint Propulsion Conference, (Colorado Springs, Colorado), 1981.
19. B. Naton, A. Gany and H. Wolff, “ Thrust Modulation of solid Propellant Rocket by Means of a Fluidic Vortex Valve with Secondary Chamber”, Acta Astronautica, 9(12), pp. 703-711, 1982.
20. A. Gany and B. Natan, “ Optimal Fluidic Voortex Valve and solid Propellant Combination for Variable Thrust Solid and Ducted Rocket”, Collection of papers, 24th Isrel Conf. on Aviation and Astronautics, pp. 238-240, Feb. 17-18, 1982.
21. C. Goldman and A. Gany, “Thrust modulation of ram-rockets by a vortex valve,” in AIAA, ASME, SAE, and ASEE, Joint Propulsion Conference and Exhibit, (Lake Buena Vista, FL), 1996.
22. H. L. Besser and G. Kurth, “Meteor - european air dominance missile powered by high energy throttleable ducted rocket,” in Proc. RTO-MP-AVT-208, pp. 1-17, 2012.
23. S. Burroughs, “Status of army pintle technology for controllable thrust propulsion,” in 37th AIAA/ASME/SAE/ASEE Joint Propulsion Conference and Exhibit, (Salt Lake City, Utah), 2001.
24. K. Xie, Y. Liu, L. Qin, X. Chen, Z. Lin and S. Liang, “Experimental and numerical studies on combustion character of solid-liquid rocket ramjet,” in 45th

AIAA/ASME/SAE/ASEE Joint Propulsion Conference, no. AIAA2009-5124, (Denver, Colorado), 2009.

25. C. Bauer, F. Davenne, N. Hopfe and G. Kurthy, "Modeling of a throttleable ducted rocket propulsion system," in Proc. AIAA/ASME/ASEE Joint Propulsion Conference & Exhibit, (San Diego, California), pp. 1–15, 2011. DOI: 10.2514/6.2011-5610
26. C. Bauer, N. Hopfe, P. Caldas-Pinto, F. Davenne and G. Kurth, "Advanced flight performance evaluation methods of supersonic air-breathing propulsion system by a highly integrated model based approach," in Proc. RTOMP-AVT-208, pp. 1–14, 2012.
27. A. Atwood, T. Boggs, T. P. P.O. Curran, and D. Hanson-Parr, "Burning rate of solid propellant ingredients, part 1: Pressure and initial temperature effects," *Journal of Propulsion and Power*, vol. 15, pp. 740–747, Nov-Dec, 1999.
28. J. Chang, B. Li, W. Bao, W. Niu and D. Yu, "Thrust control system design of ducted rockets," *Acta Astronautica*, vol. 69, no. 1, pp. 86–95, 2011.
29. W. Bao, B. Li, J. Chang, W. Niu and D. Yu, "Switching control of thrust regulation and inlet buzz protection for ducted rocket," *ACTA Astronautica*, vol. 67, no. 7, pp. 764–773, 2010.
30. W. Bao, Y. Qi and J. Chang, "Multi-objective regulating and protecting control for ducted rocket using a bumpless transfer scheme," *Proceedings of the IMechE, Part G: Journal of Aerospace Engineering*, pp. 311–325, 2012.
31. Y. Qi, W. Bao, J. Zhao and J. Chang, "Coordinated control for regulation/protection mode-switching of ducted rockets," *ACTA Astronautica*, vol. 98, pp. 138–146, 2014.
32. W. Bao, W. Niu, C. J.T., T. Cui and D. Yu, "Control system design and experiment of needle-type gas regulating system for ducted rocket," *Proceedings of the Institution of Mechanical Engineers, Part G, Journal of Aerospace Engineering*, vol. 224, no. 5, pp. 563–573, 2010.
33. Y. Qi, W. Bao, J. Chang, and J. Cui, "Fast limit protection design: A terminal sliding mode control method," in *Proceedings of the 33rd Chinese Control Conference*, (Nanjing, China), 2014.
34. M. Ostrander and M. Thomas, "Air turbo-rocket solid propellant development and testing," in Proc. AIAA/ASME/SAE/ASEE 33th Joint Propulsion Conference and Exhibit, 1997.

35. J. L. Bergmans and R. D. Salvo, “Solid rocket motor control: theoretical motivation and experimental demonstration,” in Proc. AIAA/ASME/SAE/ASEE 39th Joint Propulsion Conference and Exhibit, pp. 20–23, 2003.
36. D. Thomaier, “Speed control of a missile with throttleable ducted rocket propulsion,” in Proc. Advances in Air-Launched Weapon Guidance and Control, pp. 12-15, 1987.
37. A. G. Sreeriatha and N. Bhardwaj, “Mach number controller for a flight vehicle with ramjet propulsion,” in Proc. AIAA/ASME/SAE/ASEE 35th Joint Propulsion Conference and Exhibit, no. AIAA 99-294, (Los Angeles, CA), 1999.
38. P. Pinto and G. Kurth, “Robust propulsion control in all flight stages of a throttleable ducted rocket,” in Proc. AIAA/ASME/ASEE Joint Propulsion Conference & Exhibit, no. AIAA-2011-5611, (San Diego, California), pp. 1– 12, 2011.
39. S. Joner and I. Quinquis, “Control of an exoatmospheric kill vehicle with a solid propulsion attitude control system,” in AIAA Guidance, Navigation, and Control Conference and Exhibit, no. AIAA 2006-6572, (Keystone, Colorado), 2006.
40. A. Ilchmann, E. P. Ryan, and C. J. Sangwin, “Tracking with prescribed transient behaviour,” ESAIM: Control, Optimisation and Calculus of Variations, vol. 7, pp. 471–493, 2002.
41. J. L. Bergmans and R. I. Myers, “Throttle valves for air turbo rocket engine control,” in Proc. AIAA/ASME/SAE/ASEE 33th Joint Propulsion Conference and Exhibit, 1997.
42. C. A. Davis and A. B. Gerards, “Variable thrust solid propulsion control using labview,” in Proc. AIAA/ASME/SAE/ASEE 39th Joint Propulsion Conference and Exhibit, no. AIAA 2003-5241, (Huntsville, Alabama), 2003.
43. J. L. Bergmans and R., D, Salvo, “Solid Rocket motor control : theoretical motivation and experimental demonstration,” in Proc. AIAA/ASME/SAE/ASEE 39th Joint Propulsion Conference and Exhibit, pp. 20-23, 2003.
44. W. Lee, Y. Eun, H. Bang and H. Lee, “Efficient thrust disturbance with adaptive pressure control for multi-nozzle solid propulsion system,” Journal of Propulsion and Power, vol. 29, no. 06, pp. 1410–1419, 2013.
45. Y. Yildiz, A. Annaswamy, D. Yanakiev, and I. Kolmanovsky, “Spark ignition engine fuel-to-air ratio control: An adaptive control approach,” Control Engineering Practice, vol. 18, no. 12, pp. 1369–1378, 2010.

46. Y. Yildiz, A. Annaswamy, D. Yanakiev, and I. Kolmanovsky, "Adaptive idle speed control for internal combustion engines," in Proc. Amer. Control Conf., (New York City), pp. 3700–3705, July 2007.

47. Y. Yildiz, A. Annaswamy, D. Yanakiev, and I. Kolmanovsky, "Automotive powertrain control problems involving time delay: An adaptive control approach," in Proc. ASME Dynamic Systems and Control Conference, (Ann Arbor, Michigan), Oct. 2008.

48. Y. Yildiz, A. Annaswamy, D. Yanakiev, and I. Kolmanovsky, "Adaptive air fuel ratio control for internal combustion engines," in Proc. Amer. Control Conf., (Seattle, Washington), pp. 2058–2063, June 2008.

49. H. Shekhar, "Mathematical formulation and validation of muraours linear burning rate law for solid rocket propellants," Central European Journal of Energetic Materials, vol. 9, no. 4, pp. 353–364, 2012.

50. T. Ohshima, K. Kanbe, H. Kimura, K. Fujiwara, K. Suzuki and R. Yanagi "Control of the Intake Shock Position in the Test Rig for Ramjet Engine". AIAA Paper 1997-2885, AIAA/ASME/SAE/ASEE 33rd Joint Propulsion Conference and Exhibit, Seattle, Jul 6-9, 1997

51. N. K. Gupta, B. K. Gupta, N. Ananthkrishnan, G. R. Shevare, I. S. Park and H. G. Yoon, "Integrated Modeling and Simulation of an Air-breathing Combustion System Dynamics." AIAA Paper 2007-6374, AIAA Modeling and Simulation Technologies Conference and Exhibit, Hilton Head, South Carolina, 20-23 August 2007.

52. P. B. Chandra Kumar, Nitin K. Gupta, N. Ananthkrishnan and V. S. Renganathan. "Modeling, Dynamic Simulation and Controller Design For an Air-breathing Combustion System". 47th AIAA Aerospace Sciences meeting, 5-8 January 2009, Orlando, Florida. DOI: 10.2514/1.42368

53. Anil Alan, Yildiray Yildiz, U Poyraz and Utku Olgun, "Gas Generator Pressure Control in Throttleable Ducted rockets : A Classical and adaptive control approach". 1st AIAA/SAE/ASEE Joint propulsion conference, Orland, FL, July 27-29, 2015. DOI: 10.2514/6.2015-4236

54. E. M. Gretzer, "Surge and Rotating Stall in Axial Flow Compressors- Part 1: Theoretical Compression System Model",. Journal of Engineering for Power, vol-98, pp 190-198,, April 1976.

55. Takayuki Kojima, Tetsuya Sato, Shujiro S. Nobuhiro and Tanantsuyu, "Experimental study on restart control of a supersonic Air-breathing engine". Journal of propulsion and power, vol-20, No-2, March-April 2004.

56. G. Douglas MacMartin, "Dynamics and control of shock motion in a Near isentropic inlet". Journal of Aircraft, Vol-41, No-4, July-August 2004.

57. Simon Trapier; Sebastien Deck, Philippe Duveau and Pierre Sagant, "Time-Frequency Analysis and Detection of Supersonic Inlet Buzz". AIAA Journal, Vol-45, No-9, September 2007.

58. IK-Soo Park, N. Ananthkrishnan, Min-Jea Tahk, C. R. Vineeh and Nitin, K. Gupta. "Low-order model for Buzz oscillation in the intake of a ramjet engine". Journal of Propulsion and Power, Vol-27, No-2, March-April 2011.

59. IK-Soo Park, Sun-Kyoung Kim, Hyo-Won Yeon, Hong-Gye Sung, Jung-Woo Park and Min-Jea Tahk, "Control-oriented model for Intake shock position Dynamics in ramjet Engine". Journal of Propulsion and Power, Vol-27, No-2, March-April 2011.

60. Tao Cui, Young Wang, Kai Liu, and Jin. Jianren, "Classification of Combustion-Inlet Interaction for Air-breathing ramjet Propulsion". AIAA Journal, Vol-53, No-8, August 2015.

61. K. Oswatitsch, "Pressure Recovery for Missiles with Reaction Propulsion at High Supersonic Speeds (The Efficiency of shock Diffusers)," NACA TM 1140, 1947.

62. R. Trimp, "A Theory for Stability and Buzz Pulsation Amplitude in Ram Jets and an Experimental Investigation Including Scale Effects." NACA Rept, 1265, 1956.

63. D. M. Mayer and G. C. Paynter, "Prediction of Supersonic Inlet Unstart Caused by Freestream Disturbances." AIAA Jounal, Vol. 33, No.2, 1995, pp. 266-275.

64. A. S. Boksenbaum and D. Novik, "Control Requirements and Control Parameters for a Ram Jet with Varable-Area Exhaoust Nozzle," NACA RM E8H24, Nov. 1948.

65. A. Ferr and L. M. Nucci, "The Origin of Aerodynamic Instaility of Supersonic Inlets at Subcritical Conditions," NACA RM L50K30, 1951.

66. C. L. Dailey, "Supersonic Diffuser Instability," Ph.D Thesis, California Inst. Of Technology, Pasadena, CA, 1954.

67. S. Trapier, P. Duveau and S. Deck, " Experimental Study of Supersonic Inlet Buzz," AIAA Journal, Vol. 44, No. 10, pp. 2354-2365, 2006. DOI:10.2514/1.20451

68. C. Hirschen, D. Herrmann and A. Gulhan, "Experimental Investigations of the Performance and Unsteady Behavior of a Supersonic Intake," *Journal of Performance and Power*, Vol. 23, No. 3, pp. 566-574, 2007. DOI:10.2514/1.25103

69. P. J. Lu, and L. T. Jain, "Numerical Investigation of Inlet Buzz Flow," *Journal of Propulsion and Power*, Vol. 14, No. 1, pp. 99-100, Jan. – Feb. 1998. DOI: 10.2514/2.5254

70. S. Trapier, S. Deck, P. Duveau and P. Sagaut, "Time-Frequency Analysis and Detection of Supersonic Inlet Buzz," *AIAA Journal*, Vol. 45, No. 9, pp. 2273-2284, Sept. 2007. DOI: 10.2514/1.29196

71. R. G. Willoh, "A Mathematics Analysis of Supersonic Inlet Dynamic," *NASA TND-4969*, Aug. 1968.

72. H. G. Hurrell, "Analysis of Shock Motion in Ducts During Disturbances in Downstream Pressure," *NACA TN 4090*, Sept. 1957.

73. J. Y. Oh, F. Ma, S. Y. Hsieh and V. Yang, "Interaction Between Shock and Acoustic Waves in a Supersonic Inlet Diffuser," *Journal of Propulsion and Power*, Vol. 21, No. 3, pp. 486-495, May-june 2005. DOI:10.2514/1.9671

74. J. F. Connors, "Some Aspects of Supersonic Inlet Stability," *NACA RM E55116a*, 1956

75. A. S. Boksenbaum and D. Novik, "Control Requirements and Control Parameters for a Ram Jet with Variable-Area Exhaust Nozzle," *NACA RM E8H24*, Nov. 1948.

76. G. Kopasakis and J. W. Connolly, "Shock Positioning Controls Design for a Supersonic Inlet," *AIAA/ASME/SAE/ASEE 45th Joint Propulsion Conference and Exhibit*, AIAA Paper 2009-5117, Denver, CO, Aug. 1997.

77. S. K. Kim, H. W. Yeom, J. S. Jeon and H. G. Sung, "An Integrated Dynamic Model to Control Ramjet Propulsion System," *Proceedings of the KSAS-JSASS Joint International Symposium on Aerospace Engineering*, pp. 467-470, 2008.

78. A. Ferri and L.M. Nucci, "The Origin of Aerodynamic Instability of Supersonic Inlets at Subcritical Conditions," *NACA RM L50K30*, 1951.

79. S. A. Fisher, M. C. Neale and A. J. Brooks, "On the Sub-Critical Stability of Variable Ramp Intakes at Mach Numbers Around 2," *National Gas Turbine Establishment, Rept. ARC-R/M-3711*, Fleet, England, U.K., Feb. 1970.

80. T. Nagashima, T. Obokata and T. Asanuma, "Experiment of Supersonic Air Intake Buzz," *Inst. of Space and Aeronautical Science, Rept. 481*, Tokyo, Nov. 1972.

81. W. Sterbentz and J. Evvard, "Criterions for Prediction and Control of Ram-Jet Flow Pulsations," NACA RM E51C27, 1951
82. R. Newsome, "Numerical Simulation of Near-Critical and Unsteady, Subcritical Inlet Flow," AIAA Journal, Vol. 22, No. 10, pp. 1375– 1379, 1984
83. P. J. Lu and L. T. Jain, "Numerical Investigation of Inlet Buzz Flow," Journal of Propulsion and Power, Vol. 14, No. 1, pp. 90–100, Jan.–Feb. 1998.
84. G. L. Cole, G. H. Neiner and R. E. Wallhagen, "Coupled Supersonic Inlet-Engine Control Using Overboard Bypass Doors and Engine Speed to Control Normal Shock Position," NASA TN D-6019, Dec. 1970.
85. Y. Watanabe and A. Murakami., "Control of Supersonic Inlet with Variable Ramp," 25th Congress of the International Council of the Aeronautical Sciences, International Council of the Aeronautical Sciences Paper ICAS-2006-5.2.4, 2006.
86. T. Eggers and P. Novell, "Design Studies of the JAPHAR Experimental Vehicle for Dual Mode Ramjet Demonstration," AIAA Paper 2001-1921, April 2001.
87. J. Park, B. Seo, H. Sung, N. Ananth krishinan, and M. Tahk., "Optimal Terminal Shock Position Under Disturbances for Ramjet Supercritical Operation," Journal of Propulsion and Power, Vol. 29, No. 1, pp. 238–248, 2023. DOI:10.2514/1.B34431
88. I. Park, S. Kim, H. Yeom, H. Sung, J. Park and Tahk, M., "Control Oriented Model for Intake Shock Position Dynamics in Ramjet Engine," Journal of Propulsion and Power, Vol. 27, No. 2, pp. 499–502, 2011. DOI:10.2514/1.B34008
89. X.X. Shi, J.T. Chang, W. Bao, W.D.R. Yu and B. Li, "Supersonic inlet buzz margin control of ducted rocket", Proceedings of the Institution of Mechanical Engineers, Part G, Journal of Aerospace Engineering, in press.
90. W.Y. Niu, W. Bao, T. Cui, J.W. Cao and F.Q. Lan, "Dynamic modeling and model reduction order of controllable flow solid ducted rockets", Journal of Solid Rocket Technology 31 (4), pp. 325–330, 2008.
91. J.T. Chang, D.R. Yu, W. Bao and L. Qu, "Dimensionless analysis of the unstart boundary for 2-D mixed hypersonic inlets", The Aeronautical Journal 112, pp. 547–555, 2008.
92. B. He, J.T. Chang and D.R. Yu, "Analysis of the buzz boundary for ramjet inlets", Journal of Propulsion Technology Vol. 28 (3), pp.269–272, 2007.
93. S. Theodoulis and G. Duc, "Missile Autopilot Design: Gain Scheduling and the Gap Metric", *Journal of Guidance Control and Dynamics*, Vol. 32, pp. 986 - 996, 2009.

94. R. Reiner, G. J. Balas and W. L. Garrard, "Flight Control Design Using Robust Dynamic Inversion and Time-Scale Separation", *Automatica*, Vol. 32, pp. 1493-1504, 1996.
95. H. K. Khalil, "Nonlinear Systems", *Prentice- Hall, Englewood Cliffs*, 3rd edition, NJ, 2002.
96. D. J. Bugajski, D. F. Enns and M. R. Elgersma, "A Dynamic Inversion Based Control Law with Application to the High Angle of Attack Research Vehicle", in *AIAA Guidance, Navigation and Control Conference*, Portland, OR, pp. 826-839, AIAA-1990-3407, Aug. 1990.
97. A. J. Calise, S. Lee and M. Sharma, "Development of a Reconfigurable Flight Control Law for Tailless Aircraft", *Journal of Guidance, Control, and Dynamics*, Vol. 24, pp. 896-902, Sept-Oct. 2001.
98. D. Enns, D. Bugajski, R. Hendrick and G. Stein, "Dynamic Inversion: An Evolving Methodology for Flight Control Design", *International Journal of Control*, Vol. 59, No. 1, pp. 71-91, 1994.
99. B. S. Kim and A. J. Calise, "Nonlinear Flight Control Using Neural Networks", *Journal of Guidance, Control and Dynamics*, Vol. 20, pp. 26-33, Jan-Feb. 1997.
100. S. H. Lane and R. F. Stengel, "Flight Control Design Using Nonlinear Inverse Dynamics", *Automatica*, Vol. 24, No. 4, pp. 471-483, 1988.
101. Y. Shin, M. Johnson and A. J. Calise, "Neural Network-Based Adaptive Control for Nonlinear Flight Regimes", in *AIAA Guidance, Navigation and Control Conference*, Austin, TX, AIAA-2003-5717, Aug. 2003.
102. S. A. Snell, D. F. Enns and W. L. Garrard, "Nonlinear Inversion Flight Control for a Super-maneuverable Aircraft", *Journal of Guidance, Control and Dynamics*, Vol. 15, pp. 976-984, July-Aug. 1992.
103. S. Devasia, D. Chen and B. Paden, "Nonlinear Inversion-Based Output Tracking", *IEEE Transactions on Automatic Control*, Vol. 41, No. 7, pp. 930-942, 1996.
104. P. K. Menon, "Nonlinear Command Augmentation System for a High Performance Fighter Aircraft", in *AIAA Guidance, Navigation and Control Conference*, Monterey, CA, pp. 720-730, 1993.
105. J. Reiner, G. J. Balas and W. L. Garrard, "Robust Dynamic Inversion for Control of Highly Maneuverable Aircraft", *Journal of Guidance, Control and Dynamics*, Vol. 18, pp. 18-24, Jan.-June 1995.

106. Q. Wang and R. F. Stengel, "Robust Nonlinear Flight Control of a High Performance Aircraft", *IEEE Transactions on Control Systems Technology*, Vol. 13, No.1, pp.15-26, 2005.

107. K. A. Wise, J. S. Brinker, A. J. Calise, D. F. Enns, M. R. Elgersma, and P. Voulgaris, "Direct Adaptive Reconfigurable Flight Control for a Tailless Advanced Fighter Aircraft", *International Journal of Robust and Nonlinear Control*, Vol. 9, pp. 999-1012, 1999.

108. R. J. Adams and S. S. Banda, "Robust Flight Control Design Using Dynamic Inversion and Structured Singular Value Synthesis", *IEEE Transactions on Control Systems Technology*, Vol. 1, pp. 80-92, June 1993.

109. J. S. Brinker and K. A. Wise, "Stability and Flying Qualities Robustness of a Dynamic Inversion Aircraft Control Law", *Journal of Guidance, Control and Dynamics*, Vol. 19, pp. 1270-1277, Nov.-Dec. 1996.

110. J. M. Bungton, R. J. Adams and S. S. Banda, "Robust, Nonlinear, High Angle of Attack Control Design for a Supermaneuverable Vehicle", in *AIAA Guidance, Navigation and Control Conference*, pp. 690-700, Aug. 1993.

111. P. K. Menon, G. B. Chatterji and V. H. L. Cheng, "Two-Time-Scale Autopilot for High Performance Aircraft", in *AIAA Guidance, Navigation and Control Conference*, New Orleans, LA, AIAA-1991-2674, Aug. 1991.

112. C. Schumacher and P. P. Khargonekar, "Stability Analysis of a Missile Control System With a Dynamic Inversion Controller", *Journal of Guidance, Control and Dynamics*, Vol. 21, pp. 12-19, May-June 2005.

113. Y. Shin, A. J. Calise and M. A. Motter, "Application of Adaptive Autopilot Designs for an Unmanned Aerial Vehicle", in *AIAA Guidance, Navigation and Control Conference*, San Francisco, CA, AIAA-2005-6166, An invited paper, Aug. 2005.

114. Naira Hovakimyan, "Adaptive Dynamic Inversion via Time-Scale Separation", *IEEE Transactions on Neural Networks*, Vol. 19, No. 10, Oct., 2008, pp 1702-1711.

115. H. Nijmeijer and A. J. Van Der Schaft, "Nonlinear Dynamical Control Systems", *Springer*, 1990.

116. Isidori, A., "Nonlinear Control Systems", *Springer*, 1995.

117. M. Krstic, I. Kanellakopoulos and P. Kokotovic, "Nonlinear and Adaptive Control Design", *John Wiley*, New York, 1995.

118. E. Lavretsky and N. Hovakimyan, "Adaptive Dynamic Inversion for Nona-ne-inControl Systems via Time-Scale Separation: Part II", *In Proceedings of American Control Conference*, Portland, OR, 2005.

119. N. Hovakimyan, E. Lavretsky and A. J. Sasane, "Dynamic Inversion for NonaffineinControl Systems via Time-Scale Separation: Part I", *2005 American Control Conference* Portland, OR, USA, June 8-10, 2005.

120. W. H. Chen, "Nonlinear Disturbance Observer-Enhanced Dynamic Inversion Control of Missiles", *Journal of Guidance Control and Dynamics*, Vol. 26, pp. 161-166, 2003.

121. D. G. Choe and J. H. Kim, "Pitch Autopilot Design Using Model-Following Adaptive Sliding Mode Control", *Journal of Guidance Control and Dynamics*, Vol. 25, pp. 826-829, 2002.

122. D. S. Naidu and A. J. Calise, "Singular Perturbations and Time Scales in Guidance and Control of Aerospace Systems: A Survey", *Journal of Guidance Control and Dynamics*, Vol. 24, pp. 1057-1078, 2001.

123. Van Oort, "Modular Adaptive Input-to-State Stable Back-stepping of a Nonlinear Missile Model", *AIAA Guidance Navigation and Control Conference*, Hilton Head, South Carolina. AIAA 2007-6676, Aug. 20-23, 2007.

124. M. U. Salamci, M. K. Ozgoren and S. P. Banks, "Sliding Mode Control With Optimal Sliding Surfaces for Missile Autopilot Design", *Journal of Guidance Control and Dynamics*, Vol. 23, pp. 719-727, 2000.

125. Z. J. Yang, "A Novel Robust Nonlinear Motion Controller With Disturbance Observer", *IEEE transactions on Control Systems Technology*, Vol. 16, pp. 137-147, 2008.

126. Z. Zhao and H. Jun, "A High Gain Integral Dynamic Compensation Method for Nonlinear Missile Control", *18th IFAC World Congress Milano*, Italy, August 28 - September 2, 2011.

127. S. Sieberling, Q. P. Chu and J. A. Mulder, "Robust Flight Control Using Incremental Nonlinear Dynamic Inversion and Angular Acceleration Prediction", *Journal of Guidance, Control and Dynamics* Vol. 33, No. 6, 1732-1742, Nov-Dec. 2010, pp.

128. J. Monaco, D. Ward and R. Bird, "Implementation and Flight Test Assessment of an Adaptive, Re-configurable Flight Control System", *Proc. AIAA Guidance, Navigation, and Control Conference*, New Orleans, LA, AIAA-97-3738, Aug. 1997.

129. B. J. Bacon and A. J. Ostrofi, "Reconfigurable Flight Control Using Nonlinear Dynamic Inversion With a Special Accelerometer Implementation", *Proc. AIAA Guidance, Navigation, and Control Conference*, AIAA-2000-4565.

130. M. D. Tandale and J. Valasek, "Fault-Tolerant Structured Adaptive Model Inversion Control", *Journal of Guidance, Control and Dynamics* Vol. 29, No. 3, pp.635-642, May-June 2006.

131. R. Colgren and D. Enns, "Dynamic Inversion Applied to the F-117A", *Proceedings of the AIAA Modeling and Simulation Technologies Conference*, AIAA, Reston,VA, pp.275-284, 1997

132. P. Smith and A. Berry, "Flight Test Experience of a Non-Linear Dynamic Inversion Control Law on the VAAC Harrier", *Proc. AIAA Guidance, Navigation, and Control Conference*, AIAA Paper 2000- 3914, Aug. 2000.

133. A. J. Ostrofi. and B. J. Bacon, "Force and Moment Approach for Achievable Dynamics Using Nonlinear Dynamic Inversion", *Proceedings of the AIAA Guidance, Navigation and Control Conference and Exhibit*, AIAA, Reston, VA, pp. 424-434, 1999.

134. H. Fer and D. F. Enns, "An Approach to Select Desired Dynamics Gains for Dynamic Inversion Control Laws", *Proceedings of the AIAA Guidance, Navigation and Control Conference*, AIAA, Reston, VA, pp. 755-769, 1997.

135. J. Georgie and J. Valasek, "Evaluation of Longitudinal Desired Dynamics for Dynamic-Inversion Controlled Generic Re-entry Vehicles", *Journal of Guidance and Control Dynamics* Vol. 26, No. 5, pp. 811-819, Sept-Oct 2003.

136. U. Korte, "Tasks and Needs of the Industrial Clearance Process", *Advanced Techniques for Clearance of Flight Control Laws edited by C.Fielding, A.Varga, S. Bennani and S.Selier, Lecture Notes in Control and Information Sciences, No. 283, Springer-Verlag, Berlin, Chap.2*, pp. 13-33, 2002.

137. J. F. Magni, S. Bennani and J. Terlouw, "Robust Flight Control: A Design Challenge", *GARTEUR, Springer-Verlag*, 1997.

138. W. Hahn, "Stability of Motion", *Springer-Verlag* New York Inc., pp. 102-115,271-278, 1967

139. H. K. Khalil, "Nonlinear Systems", *Macmillan Publishing Company*, pp. 97-122, 136-151, 1992

140. P. V. Kokotovic and H. K. Khalil, "Singular Perturbations in Systems and Control", *IEEE Press*, New York, 1986.
141. P. V. Kokotovic, H. K. Khalil and J. O'Reilly, "Singular Perturbation Methods in Control: Analysis and Design", *Academic Press*, New York, 1986.
142. M. B. McFarland and C. N. D'Souza, "Missile Flight Control With Dynamic Inversion and Structured Singular Value Synthesis", *Proceedings of the AIAA Guidance, Navigation and Control Conference*, Scottsdale, AZ, pp. 544-550, 1994
143. D. S. Naidu, A. J. Calise, "Singular Perturbations and Time Scales in Guidance, Navigation, and Control of Aerospace Systems: Survey", *Proceedings of the AIAA Guidance, Navigation and Control Conference*, Baltimore, MD, pp. 1338-1362, 1995.
144. C. Schumacher, "Tactical Missile Autopilots: Gain-Scheduled HOO Control and Dynamic Inversion", Ph.D. Thesis, Univ. of Michigan, Ann Arbor, MI, 1997.
145. C. Schumacher, P. P. Khargonekax, "A Comparison of Missile Autopilot Designs Using T-L Control with Gain Scheduling and Nonlinear Dynamic Inversion", *Proceedings of the American Controls Conference*, Albuquerque, NM, pp. 2759-2763, 1997.
146. C. Schumacher, P. P. Khargonekar, "Missile Autopilot Designs Using H-infinity Control with Gain Scheduling and Nonlinear Dynamic Inversion", *Journal of Guidance, Control and Dynamics*, Vol. 21, No. 2, pp. 234-243, 1998.
147. A. Bhattacharya, P. N. Dwivedi, P. Kumar, P. G. Bhale and R. N. Bhattacharjee, "A Practical Approach for Robust Scheduling of Nonlinear Time-Scale Separated Autopilot", *Proceedings of International Conference on Advances in Control and Optimisation of Dynamical Systems*, Bangalore, India, 2007.

Appendix

1- Proportional Navigation (PN) Guidance of Missile

In PN guidance, the acceleration command can be written as:

$$F_D = N' V_C \lambda \quad (A.1.1)$$

where N' is navigation constant, V_C is closing velocity and λ is line of sight (LOS) rate. These commands are perpendicular to the instantaneous line of sight (LOS) vector. But usually the control action is present in body frame or any of the body fixed frame. So one practical way is to resolve this demand into the body fixed frame, and subsequently use it for control deflection calculation by autopilot. But the axial component of the demand cannot be achieved as control action is not present in missile longitudinal direction. The missile has only lateral correction mechanism, but not longitudinal. Hence the guidance demand in LOS frame cannot be achieved fully.

The other way to handle this situation is formulating an implicit way of achieving the guidance demand. Going back to the guidance objective, the lateral acceleration demand perpendicular to line of sight (LOS) needs to be achieved for successful interception of the target. Any lateral acceleration pulled in the direction of LOS will only make the interception delayed or quicker. Proportional navigation guidance scheme exploits this feature. In Proportional navigation guidance compensation, the axial acceleration of the missile is considered and a lateral acceleration demand along LOS is introduced.

Let $T_{LOS2Body}$ be the transformation matrix from LOS frame to Body frame and

$A_{LOS} = [0 \ A_Y \ A_Z]^T$ the lateral demand computed by Proportional navigation guidance law.

Then:

$$T_{LOS2body} = \begin{bmatrix} T_{11} & T_{12} & T_{13} \\ T_{21} & T_{22} & T_{23} \\ T_{31} & T_{32} & T_{33} \end{bmatrix} \quad (A.1.2)$$

Let A_x be an extra demand in the direction of LOS and the resultant demand in body frame be

$$a_{body} = \begin{bmatrix} a_x & a_y & a_z \end{bmatrix}^T, \text{ we have;}$$

$$a_{dBody} = T_{LOS2Body} \times A_{dLOS} \quad (A.1.3)$$

$$a_x = T_{11}A_x + T_{12}A_y + T_{13}A_z \quad (A.1.4)$$

a_x is the missile forward acceleration and is measured using the onboard INS. So from the above equation, A_x is computed.

$$A_x = \frac{a_x - T_{12}A_y - T_{13}A_z}{T_{11}} \quad (A.1.5)$$

Now this new combination of lateral acceleration demand $A_{dLOS} = [A_x \ A_y \ A_z]^T$ in LOS frame will attribute to exact realization of demand perpendicular to LOS. Further mathematics can be done to prove that the new combination of lateral acceleration demand in LOS frame when realized in body frame will attribute to two of the perpendicular to LOS components of the lateral acceleration demand achieved exactly.

2-Nonlinear Dynamic Inversion based Missile Autopilot

Nonlinear Dynamic Inversion (NDI) based missile autopilot has been presented in this section. There is a need for realizing the lateral acceleration demands in pitch and yaw plane from the guidance loop for autopilot design. For this purpose, nonlinear dynamic inversion technique is used, the details of which are discussed. The dynamic inversion control design approach presented here exploits the time scale separation that inherently exists in missile dynamics in body rate and acceleration. Thus, each time scale separated dynamic can be controlled by the feedback liberalization technique. That is, the outer loop inversion controller uses the states of the fast dynamics (body rate) to control those of slow dynamics (acceleration), and the inner loop inversion controller uses the control fin deflections to control the states of fast dynamics. In this

approach, body rate states p , q , r are identified as fast dynamic responses while α , β and ζ are characterized as slow state variables as shown in figure A.1.

The body rates p , q , r strongly depend on the fin deflections movement. Thus to start with a fast state controller, p , q , r were designed. Having designed a fast-state controller, a separate, approximate inversion procedure was carried out to design the slow state controller α , β and ζ . It may be noted that, such a model reduction was possible as there was significant difference in the time scale between the fast and slow state in the open loop dynamic of the tactical air-to-air missile.

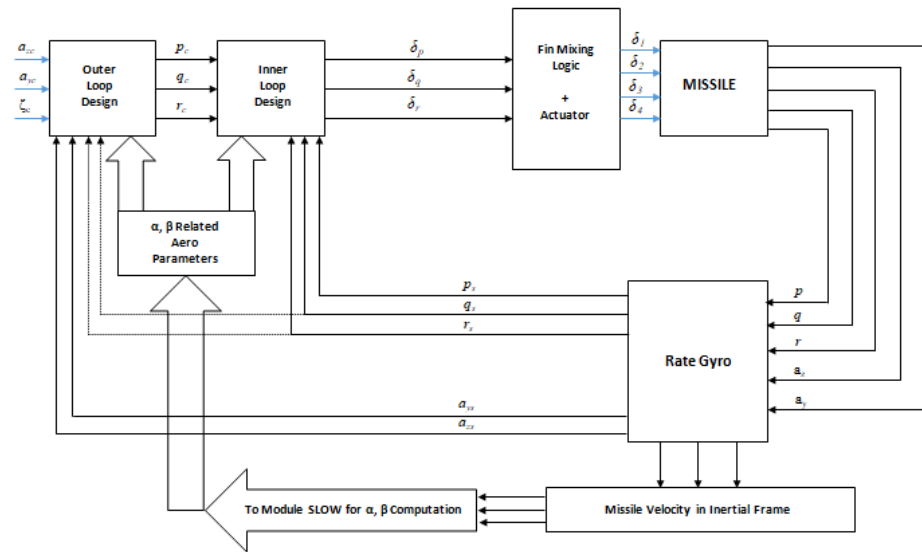


Figure-A.1: Representation of Missile Autopilot Block diagram

Outer Loop Design (Lateral Acceleration)

The outer loop (lateral acceleration) generates the pitch and yaw plane body rates, which are inputs to the inner loop to generate fin deflection. Towards this objective, first the commanded rate of the lateral acceleration in pitch a_z and yaw a_v directions are written as:

$$\begin{bmatrix} \cdot \\ a_{z_c} \\ \cdot \\ a_{y_c} \end{bmatrix} = \begin{bmatrix} \omega_\alpha (a_{z_c} - a_z) \\ \omega_\beta (a_{y_c} - a_y) \end{bmatrix} \quad (A.2.1)$$

Where, $\omega_\alpha > 0$ and $\omega_\beta > 0$ are the outer loop gains in pitch and yaw plane. Next, assuming a_z and a_y to be primary functions of α and β respectively, a_z and a_y be written as:

$$\begin{bmatrix} a_z \\ a_y \end{bmatrix} = \begin{bmatrix} \frac{\partial a_z}{\partial \alpha} \alpha \\ \frac{\partial a_y}{\partial \beta} \beta \end{bmatrix} \quad (A.2.2)$$

Hence, once a_{z_c} and a_{y_c} are known, these can be converted to α_c and β_c as follows:

$$\begin{bmatrix} \alpha_c \\ \beta_c \end{bmatrix} = \begin{bmatrix} a_{z_c} \frac{\partial \alpha}{\partial a_z} \\ a_{y_c} \frac{\partial \beta}{\partial a_y} \end{bmatrix} \quad (A.2.3)$$

Where, $\frac{\partial \alpha}{\partial a_z}$ and $\frac{\partial \beta}{\partial a_y}$ are defined by

$$\begin{bmatrix} \frac{\partial \alpha}{\partial a_z} \\ \frac{\partial \beta}{\partial a_y} \end{bmatrix} = \begin{bmatrix} \frac{m}{QSC_{N_\alpha}} \\ \frac{m}{QSC_{y_\beta}} \end{bmatrix} \quad (A.2.4)$$

Once α_c and β_c are known, α_c and β_c above equations can be inverted to obtain the demanded body rates q_c and r_c respectively. Simultaneously, to stabilize the roll dynamics, defining gain $\omega_{p_c} > 0$, an appropriate p_c is also generated. The results are then combined to obtain commanded body rates as

$$\begin{bmatrix} p_c \\ q_c \\ r_c \end{bmatrix} = \begin{bmatrix} -\omega_{p_c} \int_{t_0}^t pdt \\ \alpha_c + \frac{1}{\cos \alpha} \left[(p \times \cos \alpha + r \times \sin \alpha) \sin \beta + \frac{1}{mv_s M} (-0.5 \rho V^2 SC_L - mg_\alpha) \right] \\ -\frac{1}{\cos \alpha} \left[\beta_c - p \times \sin \alpha - \frac{1}{mv_s M} (0.5 \rho V^2 SC_Y + mg_\beta) \right] \end{bmatrix} \quad (A.2.5)$$

Inner Loop Design

This loop generates the necessary fin deflections to track the desired body rates. Here a second order dynamics is considered for the desired dynamics, which is given by:

$$\begin{bmatrix} \dot{p}_c \\ \dot{q}_c \\ \dot{r}_c \end{bmatrix} = \begin{bmatrix} -2\xi_p\omega_p p + \omega_p^2 \int (p - p_c) \\ -2\xi_q\omega_q q + \omega_q^2 \int (q - q_c) \\ -2\xi_r\omega_r r + \omega_r^2 \int (r - r_c) \end{bmatrix} \quad (A.2.6)$$

Where, ω_p , ω_q and ω_r are the desired natural frequencies for the roll, pitch and yaw channels respectively. Similarly, ξ_p , ξ_q and ξ_r are the desired damping ratios of roll, pitch and yaw channels respectively.

Once, p_c , q_c and r_c are known, the rate equations in Eq. can be inverted to obtain fin deflections in roll (δ_p), pitch (δ_q) and yaw (δ_r), which can be written as:

$$\begin{bmatrix} \delta_p \\ \delta_q \\ \delta_r \end{bmatrix} = \begin{bmatrix} C_{l_c} - \frac{C_{l_p} dp}{2V} \\ \frac{C_{l_{\delta_p}}}{C_{l_{\delta_p}}} \\ \frac{C_{m_c} - C_{m_q} q - C_{m_\alpha} \alpha}{C_{m_{\delta_q}}} \\ \frac{C_{n_c} - C_{n_r} r - C_{n_\beta} \beta}{C_{n_{\delta_r}}} \end{bmatrix} \quad (A.2.7)$$

Where, C_{l_c} , C_{m_c} and C_{n_c} are the necessary aerodynamic coefficients, which can be written as:

$$\begin{bmatrix} C_{l_c} \\ C_{m_c} \\ C_{n_c} \end{bmatrix} = \begin{bmatrix} \frac{\left(p_c - \frac{(I_y - I_z)rq}{I_x} \right) I_x}{0.5\rho V^2 S d} \\ \frac{\left(q_c - \frac{(I_z - I_x)rp}{I_y} \right) I_y}{0.5\rho V^2 S d} \\ \frac{\left(r_c - \frac{(I_x - I_y)qp}{I_z} \right) I_z}{0.5\rho V^2 S d} \end{bmatrix} \quad (A.2.8)$$

List of Publications

Journal Publications

- [1] Srikant Srivastava, P. N. Dwivedi and D. M. Vinod Kumar, “2-Loop Nonlinear Dynamic Inversion Fuel flow Controller Design for Air-to-Air Ducted Ramjet Rocket”, *Defense Science Journal*, Vol. 71, No. 2, pp. 265-270, March 2021. DOI:10.14429/dsj.71.15155 (SCI)
- [2] Srikant Srivastava, P. N. Dwivedi and D. M. Vinod Kumar, “3-Loop Structure based Fuel Flow Controller Design for Robust Operation of Ducted Ramjet Rocket”, *Defense Science Journal*, Vol. 71, No. 4, pp. 572-578, July 2021. DOI:10.14429/dsj.71.16397 (SCI)

Curriculum-Vitae

Name : Srikant Srivastava
Date of Birth : 16th June 1979
Gender : Male
Contact number : +919912732288/ 9912059035
Email Id : srikant.srivat@gmail.com
Working : Scientist 'E', DRDL (DRDO), Hyderabad.

Academic Qualification:

Program	Institution	Grade/Percentage	Year of Completion
M.Tech	IIT-Kharagpur, INDIA	7.8 (CGPA)	2003
B.Tech	G.B.P.E.C Uttrakhand, INDIA	89%	2001